

RG 2002-08

GEOLOGY OF THE LAC DU PELICAN AREA (34P)

Documents complémentaires

Additional Files



Licence



License

Cette première page a été ajoutée
au document et ne fait pas partie du
rapport tel que soumis par les auteurs.

Énergie et Ressources
naturelles

Québec 

RG 2002-08

Geology of the
Lac du Pélican area
(34P)

Anne-Marie Cadieux
Alain Berclaz
Jean-Yves Labbé
Pierre Lacoste
Jean David
Kamal N. M. Sharma



Deformed rhyodacite lobe and envelope (Faribault-Thury Complex).

Geology of the Lac du Pélican area (34P)

Anne-Marie Cadieux

Alain Berclaz

Jean-Yves Labbé

Pierre Lacoste

Jean David

Kamal N.M. Sharma

RG 2002-08

Abstract

The rocks in the Lac du Pélican area (NTS 34P), mapped at 1:250,000 scale during the summer of 2000, were subdivided into two lithodemic complexes and six intrusive suites, which formed between 2.77 and 2.69 Ga. The Faribault-Thury Complex and the Pélican-Nantais Complex contain a variety of mafic, intermediate to felsic metavolcanic rocks and metasedimentary rocks that form volcano-sedimentary belts within the different granitoid suites. From the oldest to the youngest, these suites are: the Rochefort Suite (tonalite), the Bottequin Suite (tonalite, trondhjemite, quartz diorite), the Châtelain Suite (granodiorite), the La Chevrotière Suite (porphyritic monzogranite to quartz monzonite, granodiorite, granite), the MacMahon Suite (enderbite, opdalite, gabbro, orthopyroxene diorite, pyroxenite), and the Lepelle Suite (tonalite to granodiorite). All these Archean units are cut by two sets of Paleoproterozoic dykes: the Klotz gabbro dykes (2209 Ma), and the Payne River diabase dykes (1875-1790 Ma).

All lithologies in the Lac du Pélican area underwent several phases of deformation. Primary volcanic or sedimentary structures in supracrustal rocks were deformed in a penetrative fashion, transposed by a series of deformational events and considerably modified by metamorphic recrystallization. The central and southwesternmost parts of the area are characterized by a weak aeromagnetic gradient. The latter is oriented NW-SE and cut by a prominent set of N-S-trending positive aeromagnetic anomalies. These two patterns are characterized by ductile structures (D_1 to D_3), and are transected by various networks of lineaments oriented N-S (D_4) and WNW-ESE (D_5) to NW-SE (D_6), which outline brittle structures at the brittle-ductile transition.

Our work has outlined three types of settings which yielded anomalous analytical results: 1) iron formations with Cu \pm Au \pm Ag \pm Zn mineralization, 2) ultramafic and mafic intrusions with Cu \pm Zn mineralization, and 3) fault zones and quartz veins with Cu \pm Zn \pm Au \pm Ag \pm Mo \pm U mineralization. Two showings discovered in fault zones respectively yielded concentrations of 0.75% Cu and 0.3% Mo.

DOCUMENT PUBLISHED BY “GÉOLOGIE QUÉBEC”

Director

Alain Simard

Head of the Service géologique de Québec

Pierre Verpaelst

Supervisor of Geoscience Inventories

Robert Marquis

Critical review

Michel Hocq

Translation

Michelle Mainville

Editing and page layout

Jean-Pierre Lalonde

Kamal N.M. Sharma

Computer-assisted drawing

Alain Berclaz

Anne-Marie Cadieux

Paul Brouillette

Nathalie Drolet

Technical supervision

Charlotte Grenier

Document accepted for publication on the 2002/03/01

TABLE OF CONTENTS

INTRODUCTION	5
Location, Access and Topography	5
Methodology	5
Previous Work	5
Acknowledgements	6
REGIONAL GEOLOGY	7
LITHOSTRATIGRAPHY	8
Volcano-Sedimentary Complexes	8
Faribault-Thury Complex (Afh)	8
Iron Formation (Afh1)	8
Paragneiss (Afh2) and Biotite-Garnet Diatexite (Afh2a)	8
Volcanic Rocks (Afh3)	9
Tonalite (Afh4), Trondhemite (Afh4a) and Diorite (Afh4b)	9
Pélican-Nantais Complex (Apna)	12
Migmatitic Quartzofeldspathic Paragneiss (Apna1)	12
Metavolcanic Rocks (Apna2)	13
Tonalite and Trondhemite (Apna3)	13
Granitoid Intrusive Suites	13
Rochefort Suite (Arot)	14
Bottequin Suite (Abtq)	14
Châtelain Suite (Achl)	14
La Chevrotière Suite (Alcv)	14
Porphyritic Monzogranite, Granodiorite to Quartz Monzonite (Alcv1)	15
Granite (Alcv2)	15
Granodiorite (Alcv3)	15
Hornblende-Biotite Diatexite (Alcv4)	15
MacMahon Suite (Acmm)	16
Ultramafic Plutonic Rocks (Acmm1)	16
Gabbro to Leuconorite (Acmm2)	16
Orthopyroxene Diorite to Monzodiorite (Acmm3)	16
Orthopyroxene-Rich Enderbite (Acmm4)	17
Clinopyroxene-Rich Enderbite (Acmm5)	17
Opdalite, Mangerite and Charnockite (Acmm6)	17
Orthopyroxene Diatexite (Acmm7)	18
Lepelle Suite (Alep)	18
Diorite, Gabbro to Leucogabbro (Alep1)	18
Tonalite to Granodiorite (Alep2)	18
Late Dykes (Paleoproterozoic)	18
Klotz dykes (pPktz)	18
Payne River dykes (pPpay)	19
STRUCTURAL ANALYSIS	19
Phases of Ductile Deformation D1 to D3	19

(continues on the following page)

(Table of Contents continued...)

Phase of Deformation D4	21
Phases of Deformation D5 and D6	21
LITHOGEOCHEMISTRY	23
Volcano-Sedimentary Complexes	23
Mafic volcanic rocks	23
Intermediate volcanic rocks	23
Felsic volcanic rocks	23
Ultramafic volcanic rocks of the Faribault-Thury Complex	27
Granitoid Suites	28
Diorites and tonalites	28
Granodiorites and Granites	30
Enderbitic to charnockitic rocks and associated ultramafic to mafic rocks	30
Proterozoic Gabbro and Diabase Dykes	31
ECONOMIC GEOLOGY	31
Mineralization Associated with Iron Formations	33
Mineralization Associated with Ultramafic to Mafic Intrusions	33
Mineralization Associated with Fault Zones and Quartz Veins	33
Mineral Potential of the Pélican Belt	34
CONCLUSIONS	34
REFERENCES	36
APPENDIX 1 : TABLES	38
APPENDIX 2 : PHOTOGRAPHS	45

INTRODUCTION

Mapping in the Lac du Pélican area was conducted under the geological mapping program launched by the Ministère des Ressources naturelles du Québec in 1997 in the Far North region of Québec (north of the 55th parallel). The objectives of the Far North Program are to establish a regional geological framework at 1:250,000 scale, in order to open this vast, geologically little-known territory covering more than 350,000 km² to mineral exploration. The area covered by this survey corresponds to NTS sheet 34P, which lies along the extension of surveys conducted by Madore *et al.* (1999) in map sheet 24M to the east, by Madore *et al.* (2001) to the north (NTS 35A) and by Leclair *et al.* (2001) in map sheet 34I to the south (Figure 1).

This report contains the results and interpretations derived from a geological survey conducted during the summer 2000 in the Lac du Pélican area. The objectives of the Pélican project were to increase the level of geological knowledge, define the lithostratigraphic nature and specify the metallogenic setting of the area. It incorporates mapping carried out by Percival *et al.* (1997a and b) in the northwestern part of the map area (Figure 1).

Location, Access and Topography

The Lac du Pélican area is located in an isolated part of Québec's Far North, in the heart of Nunavik. Important water bodies includes Lac Payne in the southwest, Lac du Pélican in the northwest and the Rivière Arnaud in the east (see Figure 2). The centre of the area lies 235 km east of Puvirnituk, located on the eastern shore of Hudson Bay. The map area is delimited by latitudes 59°00' and 60°00' and longitudes 72°00' and 74°00'. It covers a surface area of about 12,500 km² (112 x 110 km, see Figure 2). It is accessible by floatplane, short takeoff aircraft (Twin Otter) or by helicopter from Puvirnituk. Water bodies in the area are completely free of ice for water landings in mid-July. A landing strip near Lac Payne, located in the southwestern part of the area, immediately north of the mouth of Lac Payne (59°15'36"N - 73°15'36"W) is suitable for short takeoff aircraft.

The Lac du Pélican area lies in the Arctic tundra, and is completely free of forest cover. Topographic relief is weak to moderate, with altitude variations ranging from 30 to 300 m. Altitude variations between riverbeds and hilltops may reach 300 m, and constitute the main topographic features. Outcrops are numerous and generally large-scale. They are lichen-covered, which gives them a dark uniform colour, occasionally making geological observations difficult. The southwestern part of the area (south of Lac Payne) contains vast swampy areas where outcrops are scarce and restricted in size.

Methodology

Fieldwork conducted in the Lac du Pélican area took place over a period of 10 weeks. Mapping was performed by six geologists and six assistants, who were transported in the field by a *Long Ranger 206-L* helicopter from the base camp, located on an island in the Lacs Kangiitsaviit (59°30'43"N - 73°12'44"W). Geological mapping was carried out along traverses ranging from 8 to 12 km, spaced every 5 km on average. Certain areas were the focus of more detailed work given their mineral potential, and isolated checks conducted on nearly 100 sites by helicopter completed the mapping coverage. Geological interpretation was done on 1:125,000 topographic base maps, incorporating aeromagnetic and remote sensing data, then later compiled to 1:250,000 scale. The geological map of the Lac du Pélican area (34P) as well as all field data are available in the digital databases of the SIGÉOM system of the Ministère des Ressources naturelles du Québec.

During the field program, about 1,500 rock samples were collected and systematically cut. Among the most representative samples, 76 were selected for whole rock analyses, and 111 for assays. Analytical results are available in the SIGÉOM database. Three hundred samples were used to prepare thin sections. Six samples were collected for geochronological purposes, for U-Pb and Pb-Pb isotopic analyses. The Far North geochronology program is overseen by Jean David (MRN) at the GÉOTOP laboratory at the Université du Québec à Montréal.

Previous Work

The first geological survey of the area consisted of a 1:1,000,000 scale reconnaissance survey conducted by Stevenson (1968). This survey is based solely on information collected along pre-determined flight lines with observation sites spaced every 10 km. Later on, Percival *et al.* (1997a and b) mapped at 1:250,000 scale an area that incorporates the northwestern part of map sheet 34P and the western part of map sheet 35A (Figure 1).

Within the scope of the Far North Program, the Lac du Pélican area (34P) was covered by a lake sediment geochemistry survey (MRN, 1998) conducted by SIAL in the summer 1997. During this survey funded by the MRN and five industry partners, samples were collected along an average grid spacing of 3.5 km. The results outline several anomalies potentially considered as exploration targets.

Since 1998, Géologie Québec has conducted four geological mapping projects per year (Figure 1). In 1998, three projects were carried out in the northeastern Superior Province (Madore *et al.*, 1999; Gosselin and Simard, 2000; Parent *et al.*, 2000) and one project was conducted in the Rae Province (as defined by Hoffman, 1988 and 1989) by Verpaelst *et al.* (2000). In 1999, the four projects were conducted in the NE Superior Province (Madore and Larbi,

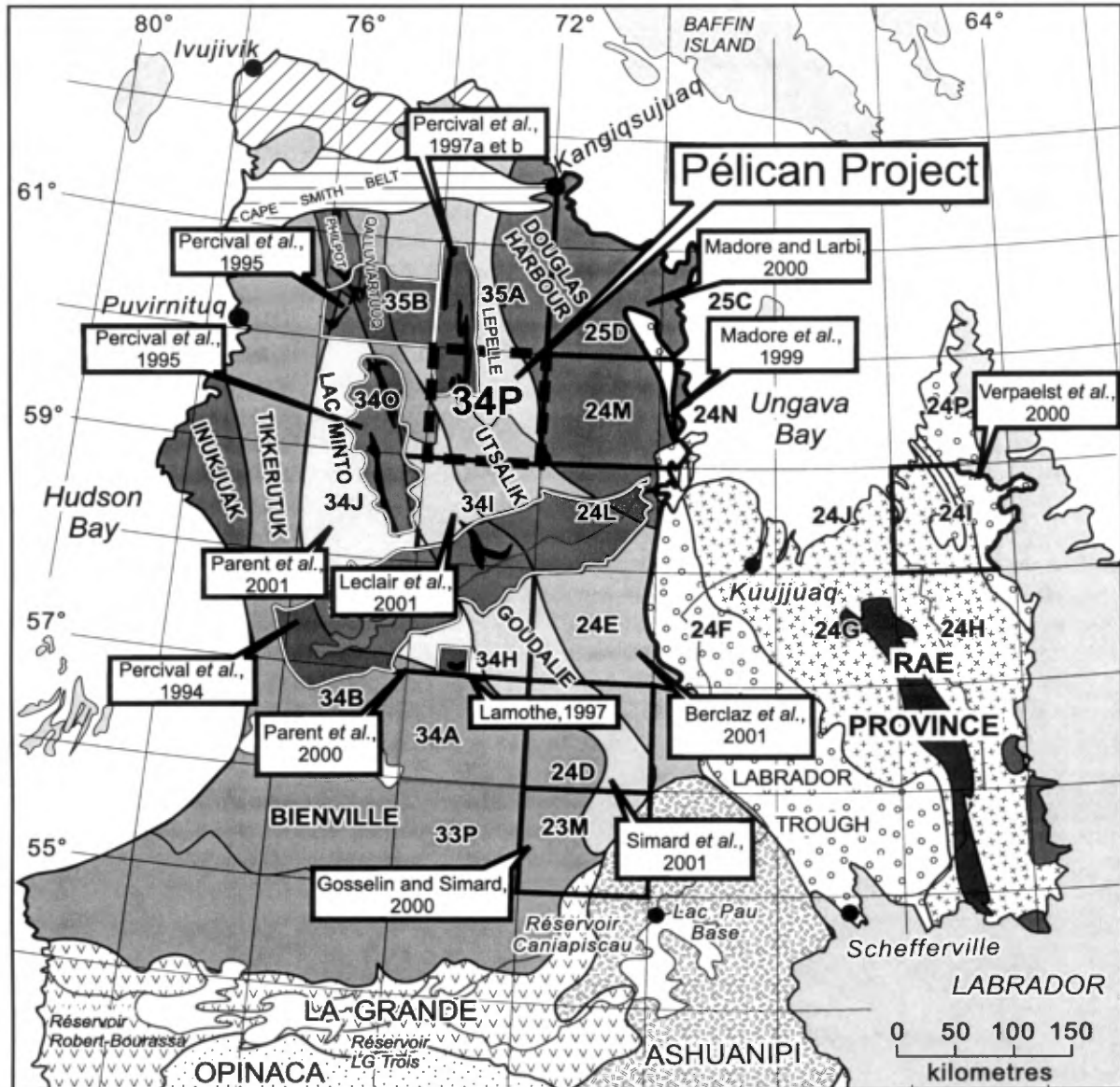


FIGURE 1 – Locations of the Lac du Pélican area (34P), of recent geological mapping projects in the Far North and the lithotectonic subdivisions of the northeastern Superior Province (modified after Percival *et al.*, 1997a).

2000; Berclaz *et al.*, 2001; Parent *et al.*, 2001; Simard *et al.*, 2001).

Since 1997, two exploration permits were acquired in the Lac du Pélican area, one of which was abandoned without any work (PEM 1354). The active permit (PEM 1340), held by SOQUEM and Cambior, encompasses the southern part of the Pélican belt, and was covered by a heliborne geophysical survey and explored for base metals and gold in 1999. Adjacent areas were investigated for gold, base metals and uranium by SOQUEM, Cambior, Virginia Gold Mines and Falconbridge.

Acknowledgements

Our thanks go to all the following persons for their contribution to the 2000 geological survey: geologists in our

mapping crew, Gabrièle Lemieux, Gabriel Machado, Joanne Nadeau and Robert Thériault; geological assistants, Frédéric Blondeau, Maude Boucher, Serge Hébert, Marielle Murray, Maryse Robidas and Philippe Tremblay. We would also like to thank Annie Johannes (from Kuujuaq) for her efficient assistance in the field. We would also like to express our gratitude to our cook, André Bourget, who demonstrated remarkable culinary talents, and also our successive camp managers, Nil Tardif and Yvan Caron. Our thanks go out to helicopter pilots Luc Gauthier and Jacques Galichon, and mechanics Barry Hesketh and Sylvain Ouellet of *Canadian Helicopters*, who transported our crews in a safe and efficient manner. Government air services were responsible for the logistics involved in transporting our crew and equipment between Québec and Puvirnituq. Then, *Air Inuit Airlines* provided transportation of our equipment

and supplies to the base camp. Supply logistics were efficiently carried out by Aliva Tulugak, to whom we extend our heartfelt gratitude. The cooperation of Denis-Jacques Dion and Marc Beaumier was very much appreciated for the preparation of aeromagnetic maps and lake sediment geochemistry maps. The Service des Technologies à Référence Spatiale produced regional spatiomaps from Landsat images. Digital geological maps were produced in SIGÉOM thanks to the indispensable technical assistance of Patrick Olivier and Nelson Leblond. Finally, we would like to thank Michel Hocq for petrographic descriptions and a critical review of this report. To all these persons, we extend our deepest gratitude.

REGIONAL GEOLOGY

The Lac du Pélican area (34P) is located in the northeastern part of the Superior Province, initially described as the Minto Subprovince (Card and Ciesielski, 1986), then later as the Minto Block (Percival *et al.*, 1992). This part of the Archean craton in the Superior Province is described as being mainly composed of high-grade (granulitic) granitoid rocks, outlined by a NW-SE-trending structural pattern and strongly positive magnetic anomalies (Percival *et al.*, 1992; Card and Poulsen, 1998).

The northeastern Superior Province was subdivided into a number of domains based on lithological, structural and aeromagnetic criteria (Percival *et al.*, 1997a and b; Figure 1). During a "transect" along the Rivière aux Feuilles, the Tikkerutuk, Lac Minto, Goudalie and Utsalik lithotectonic domains were introduced by Percival *et al.* (1991 and 1992). The Inukjuak, Philpot, Qalluviartuuq, Lepelle and Douglas Harbour domains were introduced later on (Percival and Card, 1994; Percival *et al.*, 1995, 1996, 1997a and b). According to these authors' descriptions, the various domains consist of plutonic assemblages of variable compositions and ages, in which are enclosed numerous volcano-sedimentary sequences. Plutonic assemblages characterized by vast negative and positive aeromagnetic anomalies are essentially composed of tonalite, granodiorite, diatexite and granite, with enclaves and intrusions of diorite, gabbro, pyroxenite and peridotite. Volcano-sedimentary sequences are mainly enclosed in tonalites characterized by negative aeromagnetic anomalies. They occur as narrow (1-5 km) troughs extending in length for 10 to 20 km, and are mainly composed of metamorphosed basalt, greywacke, iron formation, tuff, and minor amounts of rhyodacite, dacite, andesite, sandstone, conglomerate and ultramafic rock.

Fieldwork conducted over the past few years by Géologie Québec reveals a less radical portrait of the Archean craton in the NE Superior Province. This craton was previously perceived as being the product of the juxtaposition of

amalgamated lithotectonic domains of variable ages and origins, in sharp contrast with the southern part of the Superior Province (Percival *et al.*, 1992; Stern *et al.*, 1994; Percival and Skulski, 2000). North of the 55th parallel, a series of tectono-magmatic events took place over the period from > 3.0 Ga to 2.0 Ga (Machado *et al.*, 1989; Percival *et al.*, 1992; Stern *et al.*, 1994; Buchan *et al.*, 1998; Madore *et al.*, 1999; Gosselin and Simard, 2000; Parent *et al.*, 2000; Madore and Larbi, 2000; Berclaz *et al.*, 2001; Leclair *et al.*, 2001; Simard *et al.*, 2001; David, in preparation). This series of tectono-magmatic events is as follows:

(i) First off, the formation, between *ca.* 3.1 and 2.9 Ga, of a Mesoarchean tonalitic phase, subsequently preserved as remnants of a protocraton and supracrustal sequences.

(ii) Between *ca.* 2.91 and 2.745 Ga, three volcanic cycles, to which are associated essentially tonalitic and trondhjemitic plutonic events, affected the area. During this time, an early phase of deformation (D₁) and a first phase of metamorphism (M₁) are recorded between 2.82 and 2.79 Ga. Between *ca.* 2.79 and 2.745 Ga, magmatic activity occurred in a diachronous fashion, from the northeast towards the southeast of the area, and volcanism evolved from a tholeiitic to a calc-alkaline affinity. This period is characterized by the emplacement of isolated syenite, carbonatite and volcanic rocks related to a phase of rifting.

(iii) The period between *ca.* 2.735 and 2.725 Ga is marked by the onset of potassic magmatism, with the emplacement of granite-granodiorite-diatexite plutons. These units characterize a major episode of intracrustal melting and terrain accretion during a second phase of deformation (D₂) and metamorphism (M₂) (this report).

(iv) An enderbitic to charnockitic event, previously believed to be essentially restricted to the northeastern part of the area, between 2.74 and 2.73 Ga to form granulitic megacomplexes, now appears to extend throughout the entire area between 2.725 and 2.69 Ga. This syntectonic (D₃) magmatic episode is interpreted as being responsible for granulite-facies metamorphism (M₃) recorded during this time.

(v) Between *ca.* 2.69 and 2.675 Ga, the area was the site of a major collisional event (D₄), responsible for substantial recycling of older lithologies, for an upper amphibolite metamorphic episode (M₄), as well as the emplacement of an important volume of granite, diatexite and pegmatite.

(vi) Then, late alkaline magmatism is recorded as nepheline syenite and carbonatite intrusions (*ca.* 2.66 to 2.64 Ga; Skulski *et al.*, 1997), several networks of diabase and gabbro dykes (*ca.* 2.51 to 2.0 Ga; Buchan *et al.*, 1998), as well as ultramafic to mafic lamprophyre and carbonatite dykes (Berclaz *et al.*, 2001). Extensive hydrothermal remobilization is also associated with this period.

(vii) Finally, a Trans-Hudsonian deformation (D₅) is recorded west of the Labrador Trough (Berclaz *et al.*, 2001), and NE of the Douglas Harbour domain [sic] (Madore and Larbi, 2000).

LITHOSTRATIGRAPHY

The Lac du Pélican area (34P) is underlain by Archean rocks of the Superior Province, subdivided into lithodemes and lithostratigraphic units (two complexes and six suites; Figure 2). The stratigraphic sequence presented here was defined based on cross-cutting relationships observed in the field and U/Pb results from age dating analyses performed on six samples collected in the study area, as well as results from various units mapped in adjacent areas (David, in preparation), in addition to four dates derived from the work of Percival *et al.* (1997a).

Volcano-Sedimentary Complexes

In the area covered by this survey, a number of bands of mafic (basalt, amphibolite, mafic gneiss), intermediate (andesite) to felsic (rhyodacite, dacite) metavolcanic rocks and metasedimentary (paragneiss and iron formation) rocks form volcano-sedimentary belts enclosed within the various granitoid suites (since all rocks in the area are metamorphosed, the prefix “meta-” is omitted in order to simplify the text and the legend accompanying the SIGÉOM map). These belts are often composite, and reach several kilometres in size. Dismembered belt segments form lenticular enclaves from hectometric to centimetric in size in the granitoids. Volcano-sedimentary belts in map sheet 34P were grouped into two volcano-sedimentary complexes: the Faribault-Thury Complex (*Afth*) in the east, and the Pélican-Nantais Complex (*Apna*) in the northwestern part of the map area. Note that no magmatic textures or structures were observed in these volcanic rocks.

Faribault-Thury Complex (*Afth*)

The Faribault-Thury Complex (*Afth*) was introduced in the Lac Peters area (NTS 24M, Figure 1) by Madore *et al.* (1999) to designate large zones of intrusive rocks mainly composed of tonalite and trondhjemite. These areas contain numerous volcano-sedimentary belts extending up to 20 km in length by 5 km in width, metamorphosed to the amphibolite facies. This complex also extends northward into NTS sheets 25D, 25C and 25E (Madore and Larbi, 2000), and westward into NTS sheet 35A (Madore *et al.*, 2001). Overall, supracrustal bands in the Faribault-Thury Complex (*Afth*) are dominated by basaltic rocks (mafic gneiss and amphibolite) and are much more extensive than their counterparts in the Pélican-Nantais Complex (*Apna*). In the Lac du Pélican area (34P), all volcano-sedimentary lithologies encountered in the Faribault-Thury Complex (*Afth*) are foliated or gneissic, and metamorphosed to the amphibolite or granulite facies. Several tonalitic rocks were dated between *ca.* 2.69 and 2.87 Ga, and a volcanic rock was dated at 2820 ± 6 Ma (David, in preparation).

Iron Formation (*Afth1*)

Iron formations in the Faribault-Thury Complex (*Afth1*) are intimately associated with paragneisses (*Afth2*). They consist of dismembered horizons from one to ten metres thick, generally composed of banded rocks, belonging either to the oxide or the silicate facies, with an occasional hybrid facies (Appendix 2; Photo 1). Silicate-facies iron formations are more commonly encountered in the Faribault-Thury Complex than oxide-facies rocks.

Silicate-facies iron formations are very siliceous, and contain very little magnetite. They are enclosed in mafic rock sequences. They show a dark grey-green colour in fresh surface, and a rusty brown colour in weathered surface. They are formed of cm-scale beds with alternating felsic and mafic compositions. Felsic horizons are mainly composed of quartz and feldspar, whereas mafic horizons contain garnet, biotite, cordierite, sillimanite, hornblende and grunerite. Cordierite and garnet are often poikilitic. These iron formation horizons host rusty zones, some of which contain anomalous copper, gold, silver, zinc and arsenic (see section entitled “Economic Geology”). Magnetite, pyrite, chalcopyrite and pyrrhotite mineralization is associated with mafic bands. These minerals are disseminated in the rock or occur as mm-scale to cm-scale semi-massive horizons. Secondary epidote, chlorite and hematite alteration is often observed in these silicate-facies rocks.

Oxide-facies iron formations, on the other hand, form massive magnetite bands from decimetric to metric in thickness, occurring within paragneiss units or mafic volcanic rocks. Mineralization occurs as pyrite, chalcopyrite, sphalerite and arsenopyrite, disseminated between magnetite crystals or as mm-scale laminae parallel to banding.

Paragneiss (*Afth2*) and Biotite-Garnet Diatexite (*Afth2a*)

The paragneiss unit of the Faribault-Thury Complex includes quartzofeldspathic gneisses (unsubdivided facies) that contain less than 50% mobilizate (*Afth2*), as well as a sub-unit of biotite-garnet diatexite (*Afth2a*).

Paragneisses (Afth2) occur as m-thick to km-thick bands reaching up to 20 km in length. They are generally intimately associated with basaltic and andesitic rocks and iron formations. These paragneisses also occur as enclaves of centimetric to decimetric in size or bands up to several kilometres long in diatexites, or as metatexites. The grey-brown to rusty brown paragneisses are either melanocratic, fine-grained and homogeneous, or leucocratic to mesocratic, medium to coarse-grained and heterogeneous. They are composed of biotite, quartz, plagioclase and garnet, with variable amounts of staurolite, orthopyroxene, hornblende, cordierite, sillimanite, fibrolite and muscovite, according to the lithology. Garnet is idiomorphic to hypidiomorphic. Staurolite contains very little inclusions, which generally consist of very fine-grained and rectilinear biotite. Staurolite

crystals form penetrative twins. Sillimanite occurs as fine-grained needles, whereas staurolite and garnet form porphyroblasts. Very fine-grained magnetite is disseminated in several locations. In addition to garnet porphyroblasts, the paragneisses also contain 5 to 50% garnet-quartz-feldspar leucosome, with or without orthopyroxene. Rusty zones observed in paragneiss units of the Faribault-Thury Complex are due to the alteration of disseminated sulphides (into limonite and goethite); they did not yield any significant assay results.

Biotite-garnet diatexites (Afth2a) are medium-grained and heterogeneous, both on the scale of the outcrop and in hand sample. Tonalitic to granodioritic material forms up to 60% of the volume of this sub-unit; this material contains fine to medium-grained mafic paragneiss enclaves stretched parallel to the foliation, from 1 cm to 10 m in size.

Volcanic Rocks (Afth3)

Volcanic rocks in the Faribault-Thury Complex are dominated by a basaltic unit (Afth3) interlayered with three minor sub-units: ultramafic volcanic rocks (Afth3a), andesites (Afth3b), and dacites and rhyodacites (Afth3c). Sub-units Afth3a and Afth3b occur as thin discontinuous bands, and are not shown on the geological map.

Basalts (Afth3) occur as bands of commonly migmatized mafic gneiss or amphibolite extending more or less continuously for a few metres to several kilometres in length. The basalts are melanocratic, dark green, fine to medium-grained, and non-magnetic to moderately magnetic. They form homogeneous or heterogeneous horizons of generally foliated, but locally massive or gneissic amphibolite. These horizons are strongly metamorphosed and transposed parallel to the regional foliation (D_1 and D_2). Basalts are mainly composed of variable proportions of olive green to brownish green hornblende, plagioclase, garnet and pyroxene (clinopyroxene and orthopyroxene; Appendix 2, Photo 2). They contain variable amounts of accessory minerals (sphene, leucoxene, apatite) and alteration minerals (sericite, muscovite, clinozoisite, pistacite). Amphibolites observed in thin section are granoblastic and equigranular to heterogranular. Locally, porphyritic plagioclase grains are observed in a fine-grained mafic groundmass.

Ultramafic volcanic rocks (Afth3a; non-mappable bands) in the Faribault-Thury Complex occur in variably deformed units with contacts parallel to the regional foliation. They are dark green to black in fresh surface and exhibit a typical buff brown colour in weathered surface. Ultramafic volcanic rocks are medium-grained, equigranular, saccharoidal, glomeroclastic, weakly foliated and homogeneous. They are mainly composed of amphibole (actinolite, tremolite or cummingtonite), serpentine and chlorite (clinocllore), in addition to leucoxene. The foliation is defined by amphibole which may be strongly nematoblastic, as well as by lepidoblastic chlorite. Magnetite and carbonates are accessory minerals, and occur as small pods parallel to the foliation. Sulphides are scarce and generally fine-grained.

Andesites (Afth3b; non-mappable units) chiefly occur in km-thick bands, but also as thin bands within basaltic units. These volcanic rocks are mesocratic, medium grey with a slightly bluish weathered surface, and fine-grained. They may be differentiated from basalts by the greater proportion of felsic bands, and by the presence of quartz. These rocks form relatively homogeneous and massive horizons (without much compositional variation), that alternate with intermediate to felsic tectonic bands, which may represent metatuffaceous layers.

The *dacite and rhyodacite sub-unit (Afth3c)* of the Faribault-Thury Complex contains leucocratic rocks, white to pale grey and felsic in composition. These rocks are foliated to mylonitic, and generally exhibit an intense lineation. They are homogeneous, fine-grained and contain quartz (rhyodacite) and/or plagioclase (dacite) phenocrysts, suggesting the presence of tuffaceous facies. Their mineral constituents include quartz, plagioclase, biotite, muscovite and sericite. They contain rusty zones with up to 5% disseminated pyrite.

The *tonalite (Afth4), Trondhjemite (Afth4a) and Diorite (Afth4b)*

Tonalite (Afth4), Trondhjemite (Afth4a) and Diorite (Afth4b)

The tonalite unit (Afth4) of the Faribault-Thury Complex includes a trondhjemitic sub-unit (Afth4a) and a dioritic sub-unit (Afth4b).

Two varieties of *tonalite (Afth4)* were identified but are not differentiated on the map. The first is represented by homogeneous, medium-grained, massive to foliated rocks. These tonalites contain rare intermediate to mafic enclaves. The second variety is represented by gneissic or foliated rocks ranging from a tonalitic to trondhjemitic composition, that are commonly migmatized to the point of locally becoming diatexitic. This second variety contains a minor proportion of quartz diorite, diorite, gabbro and granodiorite enclaves, as well as numerous dykes of pink pegmatite. The tonalites (Afth4) are generally homogeneous. They exhibit colours ranging from white to grey to greenish grey. They are non-magnetic to moderately magnetic. The foliation is generally very well developed, and the rocks even exhibit gneissic to mylonitic textures in certain locations. Locally, quartz grains are stretched and form rods. The rock is medium-grained overall, although the grain size locally varies from fine to coarse. The dominant mafic mineral in these rocks is biotite, which may occur with hornblende, magnetite and allanite.

Trondhjemites (Afth4a) are homogeneous and exhibit a moderate to very strong foliation (to the point of becoming gneissic to mylonitic). They are whitish and medium-grained. They contain numerous enclaves of quartz diorite, diorite and gabbro. The proportion of mafic minerals (5 to 10%

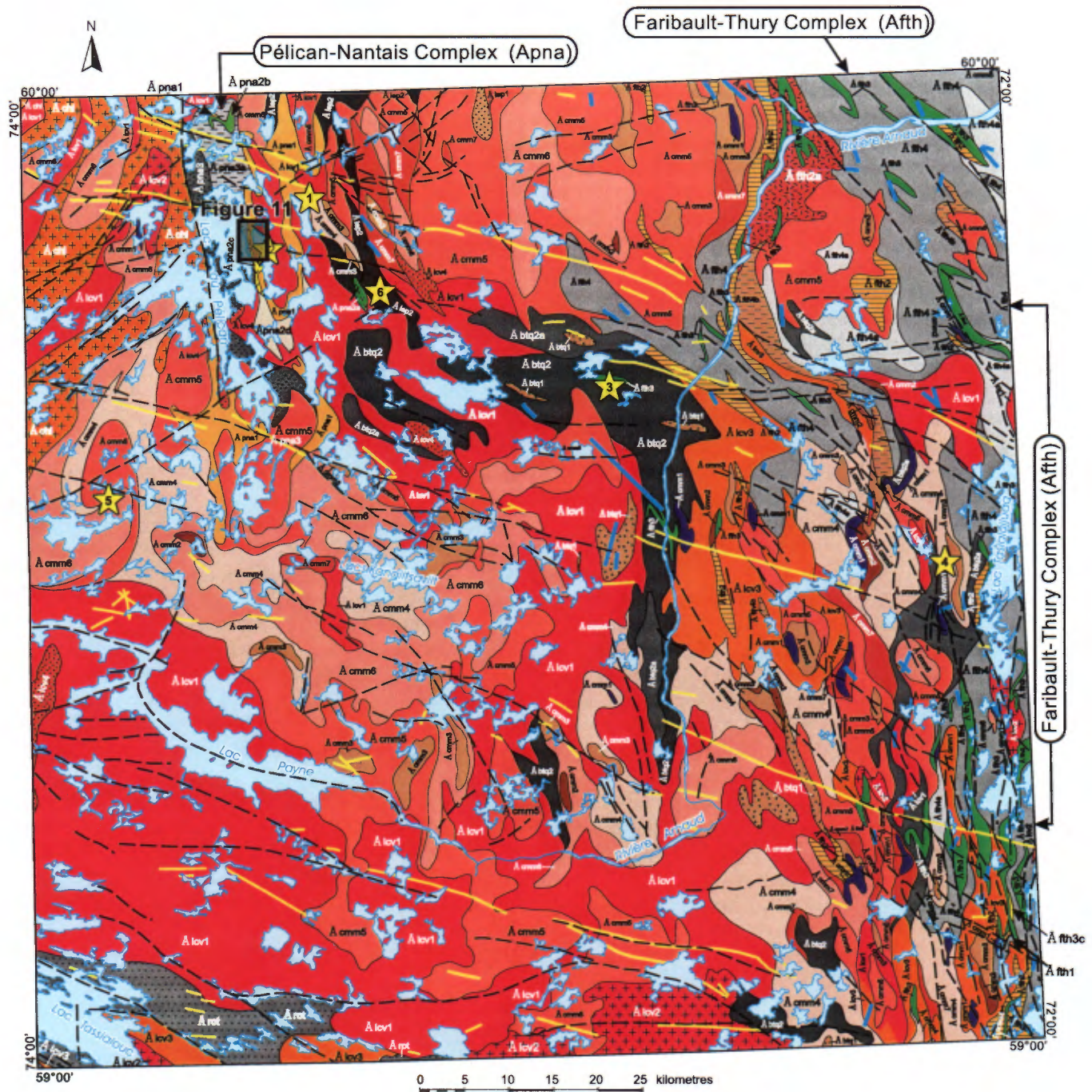


FIGURE 2 – Simplified geological map of the Lac du Pécan area (34P).


STRATIGRAPHIC LEGEND

PALEOPROTEROZOIC

Payne River Dykes (~1800 Ma)

 pPpay Diabase dykes


Klotz Dykes (~2209 Ma)

 pPktz Gabbro dykes

ARCHEAN

Lepelle Suite (Alep)


 Alep2 Tonalite-granodiorite


 Alep1 Diorite-gabbro-leucogabbro


MacMahon Suite (Acmm)


 Acmm7 OX diatexite

 Acmm6 Opdalite, mangerite, charnockite

 Acmm5 CX-rich enderbite


 Acmm4 OX-rich enderbite

 Acmm3 OX diorite to monzodiorite

 Acmm2 Gabbronorite to leuconorite

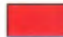
 Acmm1 Ultramafic plutonic rocks

La Chevrotière Suite (Alcv)

 Alcv4 HB-BO diatexite (I1M,I1C,I1D)

 Alcv3 Granodiorite

 Alcv2 Granite


 Alcv1 Porphyritic monzogranite to quartz monzonite

Châtelain Suite (AchI)

 AchI Granodiorite

ARCHEAN

Bottequin Suite (Abtq)

 Abtq2 Tonalite and trondhjemite


 Abtq2a CX tonalite


 Abtq1 Diorite-quartz diorite


Rochefort Suite (Arot)

 Arot Tonalite


Pélican-Nantais Complex (Apna)


 Apna3 Tonalite


 Apna3a Trondhjemite

 Apna2d Felsic schist

 Apna2c Dacite to rhyodacite


 Apna2b Andesite

 Apna2a Basalt (amphibolite, mafic gneiss)

 Apna1 Migmatitic quartzofeldspathic paragneiss

Faribault-Thury Complex (AftH)


 AftH4 Tonalite

 AftH4a Trondhjemite

 AftH4b Diorite-gabbro

 AftH3 Basalt (amphibolite, mafic gneiss)

 AftH3c Dacite-rhyodacite (tuff)

 AftH2 Migmatitic quartzofeldspathic paragneiss

 AftH2a BO±GR diatexite

 AftH1 Banded iron formation



Geochronology sample
(see Table 1, Appendix 2)



Location of Figure 11

FIGURE 2 – Legend

biotite with minor magnetite) is the distinctive feature that separates trondhjemites and tonalites. These trondhjemites are also locally very quartz-rich.

Diorites (Afh4b) are homogeneous, magnetic and massive to weakly foliated. Medium grey and fine-grained, they commonly form schlieren from 1 to 10 cm in size, and more rarely, swarms of intrusive bodies from 100 to 200 m thick. They contain tonalitic bands parallel to the foliation, and may also contain mafic enclaves (amphibolite). Plagioclase typically occurs as prismatic grains. Hornblende, which may be cored by clinopyroxene, and biotite form up to 50% of the rock. Accessory minerals include sphene, apatite, magnetite, ilmenite and locally, interstitial quartz.

Pélican-Nantais Complex (Apna)

The first detailed description of the rocks in the Pélican-Nantais sector was provided by Percival *et al.* (1997a). They identified in this area metavolcanic supracrustal rocks and metasedimentary schists enclosed in two dominant suites of intrusive rocks: a pyroxene-bearing suite and a hornblende-biotite suite. The term “Pélican-Nantais Complex” (Apna) is introduced in this report to describe bands of supracrustal rocks extending for several kilometres, bounded to the west by a shear zone and enclaved to the east by late tectonic intrusions of the La Chevrotière Suite (Alcv) and the MacMahon Suite (Acmm). These two suites respectively correspond to the hornblende-biotite suite and the pyroxene-bearing suite described by Percival *et al.* (1997a and b). Rocks of the Pélican-Nantais Complex (Apna) were subdivided into three units: a paragneiss unit (Apna1), a metavolcanic unit (Apna2) and a tonalite unit (Apna3).

The Pélican-Nantais Complex is represented in map sheet 34P by the Pélican belt (Apna1 and Apna2; observed over 50 km in length and 2 km in width on average), to which is associated a tonalite unit (Apna3). In map sheet 35A, further north, the Pélican-Nantais Complex is represented by the Nantais belt (Madore *et al.*, 2001; their Figure 2). The following sections therefore exclusively describe rocks of the Pélican belt, and associated tonalites observed in map area 34P.

Migmatitic Quartzofeldspathic Paragneiss (Apna1)

The *paragneiss unit (Apna1)* is the dominant unit in the Pélican belt, comprising more than 70% of the supracrustal rocks. It occurs along the eastern margin of the belt, and dominates its southwestern end. It includes all metasedimentary rocks (not subdivided) that contain between 5 and 50% mobilizate (paragneisses and iron formations) as well as a biotite-garnet diatexite.

Paragneisses (Appendix 2; Photo 3) occur as m-thick to km-thick bands reaching up to 50 km in length. They generally occur within volcano-sedimentary belts, intimately associated with basaltic and andesitic rocks and iron formations. These paragneisses also occur as enclaves from cen-

timetric to decimetric in size and bands several kilometres in size associated with diatexites, or as metatexites. The paragneisses are either mesocratic, homogeneous and fine-grained, or leucocratic to mesocratic, heterogeneous and coarse-grained. They are rusty brown and composed of biotite, quartz, plagioclase, garnet, with variable amounts of orthopyroxene or cordierite or sillimanite. Accessory minerals include magnetite, sulphides, zircon (zoned), muscovite, carbonate, chlorite, and rare rutile. Biotite is reddish and lepidoblastic; it most often occurs as a rim around other minerals, and cross-cuts cordierite. Garnet is hypidiomorphic to allotriomorphic, and poikiloblastic; it contains inclusions of globular to vermicular quartz, biotite, plagioclase, cordierite, magnetite and zircon. Garnet and cordierite form porphyroblasts. Orthopyroxene is coarse-grained; it is cross-cut by biotite, and has locally undergone minor replacement by iddingsite. Cordierite is commonly poikilitic, twinned, and is surrounded by a thin pinitite rim. In places, the paragneisses form impressive rusty zones several tens of metres wide, as a result of biotite alteration and alteration of disseminated pyrite and pyrrhotite, which occur in greater proportions near the contact with volcanic rocks. These types of alteration zones did not yield any significant assay results.

Iron formations in the Pélican-Nantais Complex are associated with paragneisses and volcanic rocks. Iron formation horizons contain rusty zones, some of which are anomalous in copper, gold, silver, zinc and arsenic (see section entitled “Economic Geology”). Iron formations occur as dismembered horizons 10 cm to 1 m thick and 1 to 10 m long. They are generally banded, and exhibit both oxide and silicate-facies rocks, and even a hybrid facies in certain locations. The *oxide facies* is dominant, and forms massive magnetite horizons, within paragneiss units or mafic volcanic rocks, or along the contact between mafic and felsic volcanic rocks. Sulphide mineralization consists of pyrite, chalcopyrite, sphalerite and arsenopyrite disseminated between magnetite crystals, or in mm-scale layers parallel to banding. Rare *silicate-facies* rocks, on the other hand, are highly siliceous, and contain very little magnetite. They are enclosed in mafic rock sequences. Silicate-facies rocks, dark grey-green in fresh surface and rusty brown in weathered surface, consist of alternating cm-scale layers composed of variable proportions of the following minerals: garnet, quartz, biotite, cordierite, sillimanite and grunerite. Mineralization, mainly composed of pyrrhotite, pyrite, arsenopyrite and magnetite, occurs disseminated in the rock or as mm-scale to cm-scale semi-massive horizons. In thin section, the two facies of iron formation exhibit a polygonal granoblastic texture. They contain 65 to 80% quartz, less than 5% plagioclase, 10 to 15% dark brown biotite flakes (0.5 mm), up to 5% chloritized hornblende, and 10 to 25% opaque minerals. Biotite and muscovite define the foliation. Sulphides (5-20%), mainly disseminated with the micas, consist of pyrrhotite, pyrite and local chalcopyrite. Magnetite accounts for about 5% of fine-grained opaque mineral phases.

The *biotite-garnet diatexite* is a medium-grained heterogeneous rock. Tonalitic to trondhjemitic mobilizate forms up to 60% of the volume of this sub-unit. This mobilizate contains enclaves of fine to medium-grained melanocratic paragneiss, centimetric to decimetric in size, stretched parallel to the foliation. A quartz-feldspar-garnet mobilizate, sampled northeast of Lac du Pélican (sample 1, Figure 2), yielded an age of crystallization of 2733 ± 3 Ma (Appendix 1, Table 1).

Metavolcanic Rocks (Apna2)

Metavolcanic rocks of the Pélican-Nantais Complex (Apna2) were subdivided into four sub-units: basalts (amphibolite or mafic gneiss; Apna2a), andesites (Apna2b), dacites to rhyodacites (Apna2c) and felsic schists (Apna2d).

Basalts (amphibolites or mafic gneisses; Apna2a) form more or less continuous amphibolite horizons on the order of 10 m to 1 km long, interbedded with paragneisses. They are dark green and fine to medium-grained. They occur as homogeneous bands of foliated amphibolite, and locally contain orthopyroxene-plagioclase mobilizate. These horizons are strongly metamorphosed and transposed parallel to the regional foliation. These basaltic rocks also occur as angular enclaves 10 cm to 1 m in size, elongated parallel to the foliation and occasionally lenticular, within the granitoids. They are strongly recrystallized, with a nematoblastic or granoblastic homogeneous texture. They are composed of 40 to 55% stubby green hornblende grains, and 25 to 60% plagioclase. A few 1 to 2-mm plagioclase grains are riddled with fine quartz inclusions. A twinned, uncoloured amphibole, possibly cummingtonite, was locally observed in trace amounts. The basalts contain 10 to 15% very fine-grained opaque minerals, disseminated and often aligned parallel to the foliation. Epidote is associated with opaque minerals. The latter are quite fresh and consist of disseminated pyrrhotite with fine traces of pyrite and chalcopyrite. The chalcopyrite is associated with pyrrhotite, or occurs as smaller grains in thin fractures. Magnetite (up to 5%) is very fine-grained.

Andesites (Apna2b) form km-scale homogeneous bands of foliated to gneissic rocks, or thin bands within mafic volcanic rocks. They are mesocratic, medium to dark grey with a slightly bluish weathered surface, and fine-grained. They contain plagioclase phenocrysts (crystal tuffs), blocks (lapilli and block tuffs) and locally, hornblende porphyroblasts. These rocks contain the same mafic mineral assemblages (hornblende, cummingtonite, epidote) and opaque minerals (pyrrhotite, pyrite, chalcopyrite, magnetite) as the basaltic rocks, albeit in lesser amounts (< 40% mafic minerals, < 10% opaque minerals), and with more quartz.

The *dacite to rhyodacite sub-unit (Apna2c)* encompasses leucocratic, white to pale grey rocks, with a very siliceous felsic composition. These felsic volcanic rocks form km-thick bands, most frequently in contact with paragneisses. They are fine-grained and contain quartz (rhyodacite) and/or plagioclase (dacite) phenocrysts, suggesting the

presence of tuffaceous facies. In addition to crystal tuff facies, block tuffs and lapilli tuffs (Appendix 2; Photo 4) are frequently observed in the Pélican belt. These rocks are foliated and generally exhibit a well-developed lineation. These volcanic rocks contain quartz, plagioclase, microcline (rarely), biotite and muscovite. Whitish plagioclase (5 to 15%) occurs as phenocrysts, microcline has a granoblastic texture, and biotite is dark brown-red or greenish and is very fine-grained. Up to 25% sillimanite-fibrolite was observed in small stretched pods near strongly epidotized polycrystalline phenocrysts. Accessory minerals include epidote (pistacite), tourmaline, zircon, allanite, apatite and very fine-grained disseminated opaque minerals. Rhyodacites and dacites host a few rusty zones that contain up to 5% disseminated pyrite.

The *felsic schist sub-unit (Apna2d)* designates schistose rocks composed of biotite, plagioclase and quartz, with variable amounts of hornblende and garnet. These brownish grey schists, intensely foliated and medium-grained, mark the contact between porphyritic monzogranites to quartz monzonites of the La Chevrotière Suite (Alcv1) and paragneisses or felsic volcanic rocks of the Pélican-Nantais Complex (Apna). They form a 10-cm to 1-m-thick zone at the contact with tonalite (Apna3) in the western part of the Pélican belt, as well as km-thick zones in the south-central part of the belt, in contact with a porphyritic monzogranite. Near the tonalites, these schists (Apna2d) enclose large monolithic blocks of deformed tonalite. The tonalite/schist contact is strongly deformed, and certain tonalite fragments show gradual contacts with the schistose matrix. The contact between the felsic volcanic rocks and the schists is fairly sharp, and no felsic volcanic fragment was encountered within the schists.

Tonalite and Trondhjemitite (Apna3)

The tonalite unit (Apna3) of the Pélican-Nantais Complex includes a trondhjemitic sub-unit (Apna3a).

Tonalites (Apna3) are medium grey, homogeneous to locally heterogeneous, massive to foliated and medium-grained. They generally contain biotite and magnetite with variable amounts of hornblende. Rare enclaves of paragneiss and intermediate to mafic igneous rock are enclosed in these rocks. A biotite leucotonalite that outcrops east of Lac du Pélican (sample 2, Figure 2) yielded an age of crystallization of 2691 ± 6 Ma, and a secondary age of 2659 ± 9 Ma (Appendix 1, Table 1).

Trondhjemitites (Apna3a) are whitish, homogeneous and foliated. They contain 5 to 10% mafic minerals (biotite and magnetite) and host enclaves of intermediate to felsic igneous rock and paragneiss.

Granitoid Intrusive Suites

In the Lac du Pélican area, granitoid assemblages are very heterogeneous in terms of magnetic signature (ranging

from negative to strongly positive), lithologies (grouped into six different suites) and structure. Mapping conducted in 2000 helped define new units, which were grouped in: the Rochefort Suite (Arot) composed of tonalite, the Bottequin Suite (Abtq) composed of tonalite, trondhjemite and quartz diorite, the Châtelain Suite (Achl) composed of granodiorite, the La Chevrotière Suite (Alcv) composed of porphyritic monzogranite and porphyritic granodiorite to quartz monzonite, as well as granite, granodiorite and hornblende-biotite diatexite, the MacMahon Suite (Acmm) mainly composed of enderbite and opdalite with minor amounts of charnockite, mangerite, orthopyroxene diorite, gabbro and pyroxenite, and finally, the Lepelle Suite (Alep), composed of tonalite to granodiorite with enclaves of intermediate and mafic igneous rocks (diorite, gabbro, leucogabbro).

Rochefort Suite (Arot)

The Rochefort Suite (Arot) was defined by Leclair *et al.* (2001) to identify tonalitic intrusive rocks that cover nearly 40% of the Lac La Potherie area (NTS 34I), south of our study area, and where a sample yielded an age of crystallization of $2768 \pm 9/-6$ Ma (David, in preparation). In the Lac du Pélican area (NTS 34P), tonalites related to the Rochefort Suite (Arot1) are concentrated in the southwestern corner of the map area, south of Lac Payne.

Tonalites (Arot) are homogeneous, with both foliated and banded (tectonically) facies, medium grey, and host intermediate to mafic enclaves ranging from sub-rounded to stretched parallel to the foliation. They are generally medium-grained and porphyroclastic, and are composed of quartz, plagioclase, green hornblende, biotite and epidote. Allanite, apatite, zircon, sphene, leucoxene and sericite are accessory phases.

Bottequin Suite (Abtq)

The Bottequin Suite (Abtq) is introduced in this report to describe tonalitic and dioritic rocks concentrated along the N-S segment of the Rivière Arnaud. Rocks of this suite, associated with a magnetic low, are dominated by a tonalite and trondhjemite unit (Abtq2), locally clinopyroxene-bearing (Abtq2a), with a minor unit of diorite and quartz diorite (Abtq1).

The *diorites and quartz diorites (Abtq1)* commonly form decametric size lenses within the tonalitic unit. They contain biotite, are homogeneous, foliated to banded, medium-grained, strongly magnetic and occasionally strongly epidotized. They may contain highly stretched enclaves of amphibolite.

Tonalites (Abtq2) are homogeneous, massive to foliated, medium grey and medium-grained. They rarely contain intermediate to mafic enclaves. They are weakly to moderately magnetic. *Trondhjemites* may be differentiated from tonalites by their low mafic mineral content (mainly biotite), which

ranges from 5 to 10%. They are homogeneous, massive to gneissic, whitish and medium-grained. They commonly contain numerous rounded to stretched enclaves of diorite, gabbro, amphibolite, paragneiss and ultramafic rock. The trondhjemites and tonalites are quartz-rich, with coarse-grained porphyroclastic plagioclase surrounded by coarse-grained polycrystalline quartz lenses or ribbons that define the foliation in deformed rocks. Biotite, often associated with muscovite, is altered to chlorite. Green hornblende is observed in tonalites, but is absent in trondhjemites. Accessory minerals are allanite, which locally contains epidote cores, apatite, sphene and zircon (zoned or not). *Clinopyroxene tonalites (Abtq2a)* are characterized by the presence of clinopyroxene relics in the core of hornblende grains. These tonalites are easily identified in the field, due to their typical greenish weathered surface. Compositional banding is occasionally observed between mafic and felsic minerals. An early tonalitic gneiss (Abtq2), sampled near the western shore of the Rivière Arnaud (in its northern segment, sample 3, Figure 2), yielded an age of 2768 ± 3 Ma (Appendix 1, Table 1).

Châtelain Suite (Achl)

The Châtelain Suite (Achl) is introduced in this report to describe a granodiorite unit encountered in the northwestern corner of the map area, which is intruded by the porphyritic monzogranite, granodiorite and quartz monzonite unit of the La Chevrotière Suite (Alcv1).

Granodiorites of the Châtelain Suite (Achl) are reddish grey to whitish, homogeneous and leucocratic. They are massive to foliated, medium to coarse-grained and weakly magnetic. They contain cm-scale enclaves of diorite and amphibolite, elongated and stretched parallel to the foliation. Biotite schlieren are often observed. Plagioclase grains exhibit a very distinctive burgundy colour, and black hornblende commonly contains bottle green clinopyroxene cores. Under the microscope, the granodiorites appear to consist of a heterogranular assemblage of quartz, plagioclase, porphyroclastic microcline, green hornblende, biotite locally altered to chlorite, and magnetite. Accessory phases include apatite, zircon, sphene, allanite, epidote and muscovite. Hematized and epidotized granodiorites also contain traces of disseminated pyrite.

La Chevrotière Suite (Alcv)

The La Chevrotière Suite (Alcv), introduced by Parent *et al.* (2000) in map area 34H, designates a series of elongate, lenticular sheets or plutons, covering a surface area greater than 10 km^2 , outlined by positive magnetic anomalies. This suite was expanded in this report, to include porphyritic monzogranites, granodiorites to quartz monzonites (Alcv1), granites (Alcv2), granodiorites (Alcv3) and hornblende-biotite diatexites (Alcv4).

Porphyritic Monzogranite, Granodiorite to Quartz Monzonite (Alcv1)

These *monzogranites, granodiorites to monzonites (Alcv1)* are grey-pink to reddish in fresh surface, and yellowish pink in weathered surface. They are characterized by the presence of microcline or orthoclase megaphenocrysts reaching up to 10 cm in length, that define a foliation that sometimes appears to be igneous, sometimes tectonic. Rocks in this unit may be heterogeneous, changing from a leucocratic to a melanocratic variety, or homogeneous and present only one of the two varieties. The leucocratic variety (Appendix 2; Photo 5) is weakly to non-magnetic, whereas the melanocratic variety is strongly magnetic. Diorite and gabbro xenoliths are common in the homogeneous varieties, or reduced to schlieren in heterogeneous and deformed varieties. Xenoliths are rounded and their contacts with the enclosing rocks are sharp. In thin section, coarse K-feldspar and plagioclase grains are observed, as well as abundant microcline or orthoclase phenocrysts. Myrmekite commonly appears in plagioclase grains in contact with K-feldspar. Both K-feldspar and plagioclase show a well-developed mortar texture, defined by the développement of small granoblastic polygonal grains. Quartz, fine to coarse-grained, forms interstitial pods between feldspar grains, or bands in mylonitic rocks. Mafic minerals are dominated by biotite, accompanied by highly variable proportions of hornblende, clinopyroxene, allanite and magnetite. These minerals are clustered in aggregates composed of: 1) fine and coarse brownish green, orange-brown or reddish brown biotite, 2) coarse grains of pale green or green hornblende, which may be poikilitic and contain quartz globules, 3) coarse magnetite and sphene, and 4) fine to coarse, hypidiomorphic to allotriomorphic epidote (pistacite) grains. Epidote cuts all other mafic mineral phases, as well as plagioclase. Magnetite is surrounded by a sphene corona. Accessory minerals include apatite, sulphides and zoned zircon. Secondary chlorite and muscovite locally replace biotite and hornblende. A porphyritic monzogranite sample collected in the Lac La Potherie area (NTS 34I) yielded an age of crystallization of $2732 \pm 4/-2$ Ma (David, in preparation; Leclair *et al.*, 2001).

Granite (Alcv2)

In the Lac du Pélican area (NTS 34P), the granitic unit of the La Chevrotière Suite (Alcv2) corresponds to the type of granite assigned to the La Potherie Batholith (Alpo) defined by Leclair *et al.* (2001) in the Lac La Potherie area (NTS 34I) to the south. These granites (Alcv2) were integrated to the La Chevrotière Suite (Alcv) since they occur in gradual contact or intercalated with units Alcv1 and Alcv3. Furthermore, their age of crystallization (2723 ± 2 Ma; David, in preparation; Leclair *et al.*, 2001) suggests they are associated with the same tectono-magmatic event.

These *granites (Alcv2)* form, with the granodiorites (Alcv3), a series of intrusions randomly distributed throughout the map area, with local clusters in the north-western corner, the east-central part and the southern part of the map area. They are homogeneous, massive to foliated, pinkish white and equigranular, with a typically coarse grain size. Much like the porphyritic monzogranite unit (Alcv1), they host diorite and amphibolite xenoliths, which are reduced to biotite or hornblende schlieren in certain locations. Microcline and plagioclase commonly form porphyroclastic aggregates surrounded by small polygonized and granoblastic grains. Quartz occurs as monocrystalline lenses and bands parallel to the foliation. Brown biotite forms fine flakes, magnetite is common, allanite and zircon are very fine-grained. Carbonate, sericite and muscovite, derived from the plagioclase, are the main alteration products. Where transected by late fault zones, granites of the La Chevrotière Suite (Alcv2) are hematitized, epidotized and chloritized.

Granodiorite (Alcv3)

The *granodiorite unit (Alcv3)* encompasses non-porphyritic equivalents of porphyritic granodiorites of unit Alcv1. These granodiorites show gradual contacts and hybrid facies with the porphyritic unit (Alcv1) and the granitic unit (Alcv2). They are homogeneous, massive to foliated, leucocratic, pale grey-pink and medium-grained. They host rounded gabbro, diorite and amphibolite xenoliths stretched parallel to the foliation. They typically contain coarse to locally porphyroclastic crystals of plagioclase and microcline. Weak sericitization and epidotization of plagioclase grains has led to the development of fine and coarse crystals of muscovite and epidote. More deformed samples exhibit grounded, recrystallized or polygonized feldspars. A mortar texture, with finer-grained feldspar crystals bordering coarser-grained crystals, is locally observed. Quartz occurs either as coarse grains between feldspars or as lenses parallel to the foliation in deformed rocks. Brownish green or brown biotite is the dominant mafic mineral. Olive green hornblende often contains clinopyroxene relics in the core of crystals or in pods. A few muscovite grains are associated with biotite, which is affected by minor chloritization and epidotization. Sphene, magnetite, allanite, apatite, zoned zircon and rare sulphides constitute the accessory phases observed in this unit. These rocks are often altered to hematite, epidote, chlorite and carbonate.

Hornblende-Biotite Diatexite (Alcv4)

Hornblende-biotite diatexites (Alcv4) are medium to coarse-grained and locally porphyritic (granodioritic to monzogranitic facies). They represent a diatexitic equivalent of previous units. These diatexites have a heterogeneous aspect; they exhibit an irregular foliation and are moderately

to strongly magnetic. A tonalitic, granodioritic to monzogranitic leucosome phase forms up to 60% of the volume of this unit. The rock also contains schlieren and enclaves from 1 cm to 10 m in size, of fine to medium-grained amphibolite, paragneiss and melanocratic tonalite, stretched parallel to the foliation.

MacMahon Suite (Acmm)

The MacMahon Suite (Acmm) encompasses all orthopyroxene-bearing rocks that form a series of igneous complexes outlined by strong N-S-trending positive magnetic anomalies. This suite mainly consists of enderbites (Acmm4, Acmm5) that are, for the most part, homogeneous and foliated, medium to coarse-grained, and that contain biotite and magnetite as well as K-feldspar phenocrysts. The proportion of orthopyroxene relative to clinopyroxene and hornblende is used to distinguish an orthopyroxene-biotite-rich enderbite (Acmm4) from an orthopyroxene-poor but clinopyroxene-rich unit (Acmm5), identified in the field by their respectively brownish and greenish weathered surfaces. These two units laterally grade into a unit of opdalite, mangerite and charnockite (Acmm6). An ultramafic rock unit (Acmm1: pyroxenite, peridotite, dunite, hornblendite, serpentinite), a gabbro and leuconorite unit (Acmm2), an orthopyroxene-bearing diorite and monzodiorite unit (Acmm3) and an orthopyroxene-bearing diatexite unit (Acmm7) complete the MacMahon Suite. This suite generally exhibits sharp intrusive contacts with other granitoid suites.

Ultramafic Plutonic Rocks (Acmm1)

Ultramafic rocks (Acmm1) range from a black to very dark green colour, with a buff brown weathered surface. They form homogeneous lenticular bodies generally less than 1 km² in size. They mainly consist of pyroxenite, peridotite, dunite, hornblendite and serpentinite.

Pyroxenites (Appendix 2; Photo 6) exhibit a wide range of facies, mainly clinopyroxenites and wehrlites, and less commonly, websterites or orthopyroxenites as well as their plagioclase-bearing counterparts. Clinopyroxenites are generally medium-grained, homogeneous and massive. They are composed of clinopyroxene, chlorite, biotite and amphibole. Accessory minerals include magnetite and ilmenite. *Peridotites* are banded or gneissic, medium to coarse-grained and homogeneous. They are composed of serpentine, iddingsite, chlorite (clinochlore), amphibole (actinolite or tremolite) and brownish green to green spinel. They possibly represent ultramafic cumulates of olivine (now transformed into serpentine), spinel and clinopyroxene (now amphibole). *Dunites* form m-scale massive heterogranular layers. They are composed of olivine, iddingsite and serpentine. Magnetite, sulphides, very dark green spinel and amphibole are accessory and evenly disseminated throughout the rock. *Hornblendites* are charac-

terized by the presence of green hornblende poikiloblasts up to a few centimetres in size, surrounding clinopyroxene, orthopyroxene and plagioclase grains. All ultramafic intrusions show variable degrees of alteration, to talc - chlorite - carbonate - magnetite for orthopyroxene, actinolite (tremolite) - chlorite for clinopyroxene, serpentine - iddingsite - magnetite for olivine and sericite - chlorite - epidote for plagioclase. *Serpentinites* are also observed on a local scale. They are homogeneous, with serpentine as the dominant mineral phase. They contain abundant magnetite, in stringers, thin layers and disseminations. Chlorite and carbonates also form long stringers and thin bands. Magnetite and chlorite define a good foliation. Iddingsite occurs as brownish patches, and sulphides are rare. Tremolite is accessory, and phlogopite, rimmed with magnetite, is locally observed.

Gabbro and Leuconorite (Acmm2)

Gabbros and leuconorites (Acmm2; Appendix 2; Photo 7) form bands less than 1 km wide, of massive to well foliated melanocratic to leucocratic rocks. These fine to coarse-grained and generally strongly magnetic rocks exhibit a subophitic texture. They are often cut by quartzofeldspathic injections, enderbite rocks or pegmatitic granites. In thin section, rocks of this unit are characterized by the presence of plagioclase-rich horizons, either coarse-grained porphyroclastic or fine-grained granoblastic, alternating with pyroxene-hornblende-rich horizons. Pyroxenes are coarse-grained, primary and oriented parallel to the foliation. A few grains have undergone polygonization, leading to a grain size reduction. Pyroxene grains occasionally appear unstable: weakly altered crystals show large relics of orthopyroxene in clinopyroxene, whereas more intensely altered crystals contain very small orthopyroxene relics or none at all. Alteration products of orthopyroxene are: talc, carbonate, magnetite, iddingsite, amphibole and chlorite. The pyroxenes may also be replaced by olive green to brownish green hornblende; some crystals may be cored by clinopyroxene or orthopyroxene relics. Biotite is reddish and lepidoblastic, and cuts across both hornblende and pyroxene. Accessory minerals include magnetite, zircon, sulphides and carbonates. A leucocratic gabbro sampled west of Lac Tasiallujjuaq (eastern part of the map area, sample 4; Figure 2) yielded an age of crystallization of 2723±2 Ma (Appendix 1, Table 1).

Orthopyroxene Diorite to Monzodiorite (Acmm3)

Orthopyroxene diorites are greenish grey to dark grey-blue, homogeneous, massive to foliated, and often inter-layered with enderbite. Frequently, enderbite "rafts" wedged in the diorite may contain pyroxene, hornblende and magnetite phenocrysts. They are most often moderately to strongly magnetic. They are fine to medium-grained, and locally exhibit a porphyritic texture, with mm-scale to cm-scale plagioclase phenocrysts. In addition to pyroxene

(clinopyroxene and orthopyroxene), orthopyroxene diorites also contain hornblende, biotite and magnetite as ferromagnesian minerals. They generally exhibit a granoblastic texture, and the clinopyroxene content is greater than the orthopyroxene content. They locally display coarse-grained assemblages of primary (igneous) porphyroclastic plagioclase and pyroxene, with some finer granoblastic (metamorphic) grains. Plagioclase are twinned, and a few coarse-grained porphyroclastic relics exhibit deformed twins. Red lepidoblastic biotite defines the foliation. Hornblende is olive green to brownish green. Pyroxenes, plagioclase and hornblende may also be polygonal. Fine to coarse-grained quartz is generally common, but may be rare in certain samples. Magnetite crystals are abundant and disseminated throughout the rock. Sulphides, apatite and coarse-grained zircon are accessory phases.

Orthopyroxene monzodiorites are yellowish brown (golden brown) and medium to coarse-grained. They are leucocratic to mesocratic, massive to weakly foliated. They contain orthopyroxene, clinopyroxene, biotite, and locally hornblende and K-feldspar phenocrysts (up to 2 cm long).

Orthopyroxene-Rich Enderbite (Acmm4)

Orthopyroxene-rich enderbites (Acmm4) are yellowish brown (golden brown), moderately to strongly magnetic, generally homogeneous but locally heterogeneous. They are massive to strongly foliated and banded. These rocks are most often medium to coarse-grained, and may locally be fine-grained or even porphyritic (minor amounts of plagioclase or K-feldspar phenocrysts). These enderbites contain up to 30% coarse-grained orthopyroxene-bearing leucosome. They often host enclaves of diorite, and locally of amphibolite, gabbro or ultramafic rock, stretched parallel to the foliation. These leucocratic to mesocratic enderbites contain 5 to 25% mafic minerals; the proportion of orthopyroxene outweighs that of clinopyroxene; red biotite is abundant whereas hornblende is a minor phase. Magnetite generally forms an important proportion of the mafic mineral content, making the rock strongly magnetic. In thin section, enderbites are heterogranular and homogeneous to banded. Accessory minerals include apatite and zircon. Alteration minerals such as muscovite, carbonate, talc and sericite, mainly affect orthopyroxene grains. Overall, these enderbites appear to be moderately recrystallized.

Clinopyroxene-Rich Enderbite (Acmm5)

Clinopyroxene-rich enderbites (Acmm5) are composed of greenish plagioclase, hornblende and clinopyroxene, which give this type of enderbite its typical light greenish brown colour in fresh surface, and grey with brown-green spots in weathered surface. These enderbites are massive to foliated, heterogeneous, heterogranular, ranging from coarse to fine-grained, and moderately magnetic. They generally host enclaves of orthopyroxene-bearing diorite,

and locally, of gabbro or clinopyroxenite. These enclaves are most often stretched and elongated parallel to the foliation. Whitish, occasionally pegmatitic, mobilized with clinopyroxene-orthopyroxene±hornblende is often observed around the enclaves. Clinopyroxene-rich enderbites are generally mesocratic, and contain 15 to 35% mafic minerals. Among these, the clinopyroxene content, locally occurring as mm-scale to cm-scale phenocrysts, is greater than the orthopyroxene content. Red biotite and magnetite are nearly always present, whereas green or brown hornblende is frequently observed, as replacement rims around orthopyroxene or as mm-scale to cm-scale phenocrysts. The K-feldspar phenocrysts content ranges from 2 to 10%. Magnetite, sulphides, apatite and zoned zircon are accessory minerals.

In deformed facies, plagioclase, clinopyroxene and orthopyroxene occur as coarse-grained porphyroclasts and finer-grained, fractured, granoblastic or polygonal grains. The porphyroclastic plagioclase crystals may display bent or broken twins. Quartz occurs as pods or stretched ribbons that define the foliation. In altered facies, orthopyroxene is partially to almost completely replaced by its alteration products: talc, carbonate, chlorite, biotite, iddingsite and magnetite. Clinopyroxene is coarse-grained and weakly altered to muscovite and sericite. Biotite is dark red to brownish red, altered to chlorite and overgrown by epidote (pistacite). Plagioclase may be altered to sericite, muscovite and epidote (pistacite).

Opdalite, Mangerite and Charnockite (Acmm6)

Unit Acmm6 encompasses all pyroxene-bearing units that also contain more than 10% K-feldspar. This unit is dominated by opdalites, which laterally grade into minor mangeritic and charnockitic components.

Opdalites and *charnockites* are yellowish brown (golden brown) with a slightly pinkish hue in fresh surface. They are massive, foliated or banded, with leucocratic quartzofeldspathic layers alternating with melanocratic biotite-rich layers. The grain size is generally medium to coarse, and K-feldspar phenocrysts (1 to 10 cm) are locally present. Mafic minerals observed in these opdalites include orthopyroxene, clinopyroxene and biotite, with local hornblende. They are generally heterogeneous, with irregularly distributed leucocratic and melanocratic phases. They contain abundant enclaves from 10 cm to 1 m in size, of diorite and hornblende-biotite enderbite, or amphibolite and orthopyroxene and/or hornblende-bearing ultramafic rock, stretched parallel to the foliation. Overall, these rocks are moderately magnetic. From a petrographic standpoint, the opdalites appear to be heterogranular, with coarse grains of primary antiperthitic plagioclase and microcline, as well as finer-grained, broken or recrystallized grains. Orthopyroxenes are coarse or fine-grained, fractured and partially polygonized. They exhibit a yellowish alteration, composed of iddingsite, talc, magnetite and carbonates. Clinopyroxene,

occasionally absent, is associated with orthopyroxene, and may partially surround it. Orthopyroxene and clinopyroxene grains still clearly preserve their magmatic shapes, when they are intergrown and in optical continuity. Biotite is red, brownish red or orange red, lepidoblastic and locally poikilitic. It overgrows pyroxene phases and defines the foliation. Quartz is interstitial relative to the other phases, and occurs in highly variable proportions. Magnetite is common, whereas zircon (zoned or occasionally clear), apatite and sulphides are accessory minerals. Alteration minerals (chlorite, hematite, epidote) are occasionally observed.

A massive opdalite sampled southwest of Lac du Pélican (sample 5, Figure 2) yielded an age of crystallization of 2717 ± 10 Ma, and an inherited age of 2758 ± 7 Ma (Appendix 1, Table 1).

Mangerites are yellowish brown (golden brown), medium-grained and foliated. They are leucocratic to melanocratic, and contain 5 to 10% plagioclase phenocrysts reaching up to 5 cm in size. K-feldspar (microcline or orthoclase) and quartz complete the felsic component of these rocks. Mafic minerals are orthopyroxene, biotite and magnetite, with occasional clinopyroxene and hornblende. In thin section, mangerites exhibit coarse-grained magmatic pyroxenes, intergrown and in optical continuity. Red lepidoblastic biotite overgrows pyroxene grains, which are themselves fractured and recrystallized in certain locations. Magnetite, apatite and zoned and clear zircon are accessory minerals.

Orthopyroxene Diatexite (Acmm7)

Orthopyroxene diatexites (Acmm7) are the most common. This unit is heterogeneous, both on the scale of the outcrop and in hand sample. Enderbitic to charnockitic material forms up to 60% of the volume of the rock, which also contains 40 to 70% enclaves of diorite (with or without orthopyroxene), amphibolite and paragneiss. These enclaves are most often stretched, locally boudinaged and may define a planar alignment parallel to the foliation. Orthopyroxene diatexites are generally yellowish brown, medium-grained, locally porphyritic, and affected by an irregular weak to mylonitic foliation. They are weakly to strongly magnetic. In thin section, plagioclase and orthopyroxene porphyroclasts were observed. Orthopyroxene also occurs as polygonal grains. Brown lepidoblastic biotite is common, whereas magnetite, sulphides and zircon (zoned and clear) are accessory phases.

Lepelle Suite (Alep)

The Lepelle Suite (Alep) is composed of two units occurring in the northern part of the map area: diorites and gabbros to leucogabbros (Alep1) and tonalites to granodiorites (Alep2).

Diorite, Gabbro to Leucogabbro (Alep1)

Diorites, gabbros and leucogabbros (Alep1; un subdivided facies) are charcoal grey or medium to dark green, moderately to strongly magnetic, and generally form voluminous bodies (> 100 m) interlayered with tonalites and granodiorites, or occur as very homogeneous fine to medium-grained enclaves up to m-scale in size, with a massive to foliated texture. Locally, these enclaves are reduced to cm-scale schlieren. These rocks contain the same mafic minerals as the tonalites (biotite \pm clinopyroxene \pm hornblende), but in greater proportions, and exhibit an equigranular granoblastic texture.

Tonalite to Granodiorite (Alep2)

Tonalites and granodiorites (Alep2) are generally light grey, greenish grey to pinkish, homogeneous, massive, locally banded to foliated. They are weakly to moderately magnetic, medium to coarse-grained and locally porphyritic. They contain intermediate and mafic to ultramafic enclaves. Plagioclase occurs as large porphyroclasts, as well as granoblastic grains. Quartz occurs as pods in between the plagioclase crystals. Biotite and rare clinopyroxene, often accompanied by hornblende, form the mafic component of tonalites and define the foliation. Lepidoblastic biotite is brown or orange to reddish. Clinopyroxene is coarse or fine-grained and granoblastic. It may be partially replaced by amphibole and biotite. Epidote and allanite locally cross-cut the biotite, amphibole and clinopyroxene. Magnetite is common, and accessory minerals include sulphides, apatite, zoned zircon and sphene. A granodiorite sampled east of Lac du Pélican (sample 6, Figure 2) yielded an age of crystallization of 2714 ± 10 Ma, and an inherited age of 2731 ± 5 Ma (Appendix 2, Table 1).

Late Dykes (Paleoproterozoic)

All Archean units in the area are intruded by Paleoproterozoic dyke swarms, associated with brittle faults or fractures that postdate the Archean regional deformation and metamorphism. These dykes correspond to the Klotz dykes (pPktz) and the Payne River dykes (pPpay), terms respectively introduced by Buchan *et al.* (1998) and Fahrig *et al.* (1985), and recognized by Madore *et al.* (1999) and Madore and Larbi (2000).

Klotz dykes (pPktz)

Klotz dykes (pPktz), gabbroic in composition (coarse-grained diabase), are preferentially oriented WNW. These dykes are associated with fault zones, and are commonly several tens of metres wide, even exceeding 100 metres in certain cases. They occur in positive relief over much greater distances (up to 50 km) and in a more continuous fashion

than diabase dykes. The gabbro dykes are homogeneous, massive and strongly magnetic. They range from medium to coarse-grained, and exhibit a subophitic to ophitic texture. They display aphanitic chilled margins from one to ten centimetres wide. They are generally mesocratic, but locally leucocratic. The rock is mainly composed of clinopyroxene phenocrysts, idiomorphic tabular plagioclase and amphibole ranging from green or khaki green hornblende to bluish green amphibole (actinolite). Clinopyroxene grains are uralitized, and surrounded by an amphibole rim. Accessory minerals include red-brown biotite, interstitial quartz, sericite, muscovite, apatite, Fe-Ti oxides, zircon, leucoxene and sphene. In conjunction with the fault zones that control their emplacement, these gabbro dykes are generally altered to actinolite, chlorite, epidote and sericite.

Klotz dykes were dated at *ca.* 2209 Ma (U-Pb), according to a paleomagnetic and geochronology study conducted by Buchan *et al.* (1998) in this part of the Superior Province.

Payne River dykes (pPpay)

Payne River dykes (pPpay) are diabase dykes preferentially oriented NW. These dykes display an isotropic texture with well-developed chilled margins. Most dykes are discontinuous, and 10 to 50 cm thick on average, although they may reach up to 65 m in thickness. They are homogeneous, massive, and generally very magnetic. They show a greenish brown to blackish brown weathered surface, and a bluish grey fresh surface. Contacts with country rocks are sharp, but may occasionally be lobate, and cross-cut the foliation in the country rock. The rock, generally fresh, commonly exhibits an ophitic, even trachytoid texture. In the latter case, the flow texture is defined by the planar orientation of plagioclase + clinopyroxene ± olivine ± orthopyroxene phenocrysts in an aphanitic or microlitic matrix made up of plagioclase + clinopyroxene ± brown hornblende, with abundant disseminated magnetite grains. The magnetite is fine-grained, and surrounded by brown biotite or leucoxene. Clinopyroxene is often uralitized and cut by green hornblende. Orthopyroxene and olivine are cut by orange-red lepidoblastic biotite. Accessory phases include apatite, muscovite, sericite, epidote, chlorite, leucoxene and pyrite. Disseminated pyrite forms up to 1% of the mineral assemblage.

Fahrig *et al.* (1985) dated two samples collected from chilled margins, which yielded K-Ar ages of *ca.* 1875 and 1790 Ma for the Payne River dykes.

STRUCTURAL ANALYSIS

The Lac du Pélican area has undergone several phases of deformation, which are largely reflected in the structural

trend and the various aeromagnetic signatures that characterize lithological assemblages in the NE Superior Province. The central and southwestern parts of the Lac du Pélican area are characterized by a weak aeromagnetic gradient oriented NW-SE, intersected by a set of N-S-trending positive aeromagnetic anomalies (Figure 3). These two aeromagnetic patterns are characterized by ductile structures (D_1 to D_3), and are disturbed by folds or cross-cut by different networks of lineaments oriented N-S (D_4), and by brittle-ductile structures oriented WNW-ESE (D_5) to NW-SE (D_6). Lin *et al.* (1996) suggested that the preferential NNW orientation of the structural and magnetic trend, as well as the regional amphibolite and granulite-grade metamorphism recorded in volcano-sedimentary belts are the result of the lateral accretion (collision) of the Utsalik, Goudalie and Lac Minto domains (Figure 1), between 2.693 and 2.675 Ga. This regional tectono-metamorphic event was later reinterpreted as the result of the burial of the Lac Minto and Goudalie domains, brought on by thrusting of an arc formed between 2.71-2.70 Ga (Tikkerutuk Domain; Percival and Skulski, 2000).

The structural analysis of the Lac du Pélican area is based on attitude variations and cross-cutting relationships observed for different ductile to brittle-ductile structural elements present in all lithodemic units. It takes into account the fact that primary volcanic or sedimentary structures (S_0 : bedding, differential lamination) in supracrustal rocks, grouped in the Faribault-Thury (A_{fth}) and Pélican-Nantais (A_{pn}) complexes, were penetratively deformed and transposed by the different episodes of ductile deformation (D_1 to D_3), and also considerably modified by metamorphic recrystallization. Planar structural elements include: a foliation defined by the preferential orientation of mafic (biotite, hornblende, pyroxene) or felsic (plagioclase, K-feldspar) minerals of magmatic or tectonic origin; a tectonic to mylonitic banding resulting from an increase in the rate of deformation; a gneissosity, foliation or migmatitic layering defined by the presence of alternating "leucosomes" and "restites", most often occurring as mafic schlieren, and derived from *in situ* partial melting of the rock; shear zones; folds, and a local crenulation cleavage. Linear structural elements include stretching lineations, tectono-metamorphic lineations, and rare primary (magmatic) lineations, fold axes, quartz-feldspar rods and fault striations.

Phases of Ductile Deformation D_1 to D_3

Domains 1a, 1b and 1c group structures that particularly overprint the oldest lithodemic units in the map area, and that are characterized by a generally weak aeromagnetic gradient: the Faribault-Thury Complex (A_{fth}), the Pélican-Nantais Complex (A_{pn}), the tonalitic Rochefort (A_{rot}; 2768±9/-6 Ma; David, in preparation; Leclair *et al.*, 2001) and Bottequin (A_{btq}; 2768±3 Ma; Sample 3, Figure 2, Table 1) suites. These three domains are affected by three phases

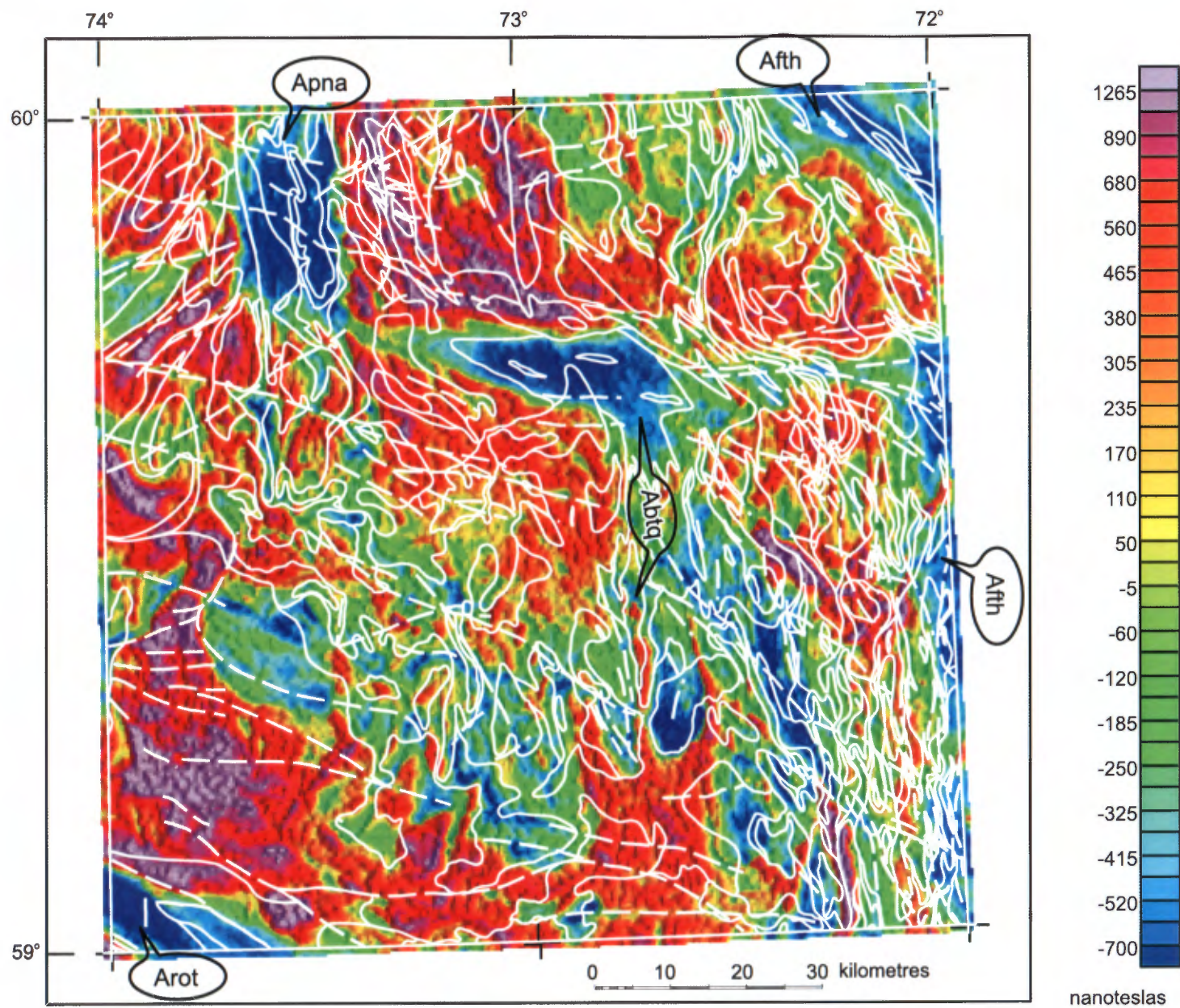


FIGURE 3 – Total residual magnetic field map of the Lac du Pélican area (34P). Aeromagnetic data taken from Dion and Lefebvre (2000). Apna = Pélican-Nantais Complex; Aftth = Faribault-Thury Complex; Abtq = Bottequin Suite; Arot = Rochefort Suite.

of deformation (D_1 , D_2 and D_3), which form complex interference patterns. Planar structures associated with D_1 are characterized by a tectonic foliation outlined by mylonitic banding, gneissosity and migmatitic layering (S_1), as well as isoclinal folds (F_1) that affect S_0 and are all oriented NW-SE (figures 4 and 5). These NW-SE-trending structures (D_1) are successively affected by: (i) subvertical planar structures (S_2) oriented E-W (D_2) and (ii) planar structures (S_3) and folds (F_2) oriented N-S (D_3). A dome-and-basin-type interference pattern (Figure 4) is defined in units of structural domains 1a, 1b and 1c, and particularly in volcano-sedimentary units of the Faribault-Thury (A_{fth}) and Pélican-Nantais (A_{pn}) complexes. This interference pattern is the result of a reorientation of S_1 planar structures along S_3 planar structures, and the refolding of F_1 folds by F_2 folds. Lineations ($L_{1,3}$) associated with planar structures ($S_{1,3}$) are subvertical to steeply plunging, whereas $F_{1,2}$ fold axes show moderate plunges towards the northwest or east (Figure 5).

Domain 2, restricted to the southwest corner of NTS sheet 34P (Figure 4), extends further south into the Lac La Potherie area (34I) and corresponds to Domain 5 defined by Leclair *et al.* (2001). The structural style in Domain 2 is markedly different from that in domains 1a, 1b and 1c. Domain 2 is characterized by a vertical E-W-striking S_2 foliation (Figure 5). This S_2 foliation is mainly defined by the preferential orientation of weakly deformed to undeformed K-feldspar crystals, indicating a magmatic origin. This magmatic foliation locally alternates with a tectonic to mylonitic foliation or banding (S_2), and parallel isoclinal microfolds. No regional-scale folds were recognized in Domain 2.

Domains 3a, 3b and 3c contain lithodemic units characterized by strongly positive aeromagnetic anomalies oriented N-S. Phase of deformation D_3 is very homogeneous. Planar structures are defined by a primary (magmatic) and tectonic foliation outlined by tectonic to mylonitic banding, gneissosity and migmatitic layering (S_3) (Figure 5). All these structures are coplanar, subvertical and oriented N-S. The attitude of S_0 bedding and S_3 foliation forms numerous isoclinal F_2 folds (Figure 4). Linear elements (L_3) associated with these vertical planes and F_2 fold axes are coaxial, and steeply plunging (mainly to the SW) to vertical. The effect of D_3 deformation is essentially manifested in domain 1b by a tectonic foliation, gneissosity and migmatitic layering oriented N-S, *i.e.* at an angle relative to D_1 planar structures oriented NW-SE (Figure 5).

D_1 structures observed in domains 1a, 1b and 1c are dominated by tectonic or metamorphic structures oriented NW-SE. These D_1 structures are rarely preserved in domains 2 and 3, where deformation zones or tectonites (S_2 and S_3), with amphibolite and granulite-grade metamorphic textures, laterally grade into zones of predominantly undeformed rocks with well-preserved magmatic textures. Both D_2 and D_3 deformation episodes are consequently interpreted as synmagmatic.

Since Domain 2 is almost exclusively underlain by the various granites and granodiorites of the La Chevrotière Suite (Alcv; 2732+4/-2 Ma and 2723±2 Ma; David, in preparation; Leclair *et al.*, 2001), D_2 deformation is interpreted as being coeval with the emplacement of this suite. This synmagmatic deformation is also coeval with metamorphism recorded in a diatexite from the Pélican volcano-sedimentary belt dated at 2733±3 Ma (sample 1; Figure 2, Table 1). The *ca.* 2735 Ma age therefore also represents a minimum age for phase of deformation D_1 .

Tectono-metamorphic D_3 structures affect D_1 structures preserved in domains 1a, 1b and 1c, however magmatic and tectono-metamorphic D_3 structures are for the most part restricted to rocks of the MacMahon Suite (Acmm; 2723±2 Ma, sample 4 and 2717±10 Ma, sample 5; Figure 2, Table 1) and the Lepelle Suite (Alep; 2714±10 Ma, sample 6; Figure 2, Table 1). Consequently, the synmagmatic phase of deformation D_3 is interpreted as having controlled the emplacement of these suites, and therefore as being younger than *ca.* 2725 Ma.

Phase of Deformation D_4

D_3 structures are also truncated by brittle-ductile to locally protomylonitic shear zones, pseudotachylites and faults (D_4), also oriented N-S to locally NNE-SSW, with vertical to moderate dips to the west (figures 4 and 5). Furthermore, D_4 deformation is probably responsible for the overturn of F_2 folds towards the east (Figure 4). These structures penetratively affect all lithodemic suites, with increasing intensity eastward. In the northwestern part of the map area, near Lac du Pélican, biotite leucotonalites and trondhjemitic (units A_{pn}3 and A_{pn}3a) are injected within shear zones (Pélican structure; Figure 4). One of these leucotonalites was dated to constrain the age of deformation D_4 ; it yielded an age of 2691±6 Ma (sample 2; Figure 2, Table 1). These faults were retrograded to the greenschist facies, as a result of late hydrothermal fluid circulation. This hydrothermal event may be responsible for a secondary age of 2659±9 Ma obtained in the same leucotonalite injected in the Pélican structure (Appendix 1; Table 1).

Phases of Deformation D_5 and D_6

All D_1 to D_4 structures are cut by late brittle-ductile shear zones and faults (D_5 to D_6). These structures which contain greenschist facies metamorphic assemblages resulting from hydrothermal activity are oriented WNW-ESE to E-W (D_5) and NW-SE (D_6). These D_5 and D_6 deformation zones are respectively parallel to the Klotz dyke network (pPktz; *ca.* 2209 Ma; Buchan *et al.*, 1998) and the Payne River dyke swarm (pPpay; *ca.* 1875-1790 Ma; Fahrig *et al.*, 1985), and may have controlled their emplacement.

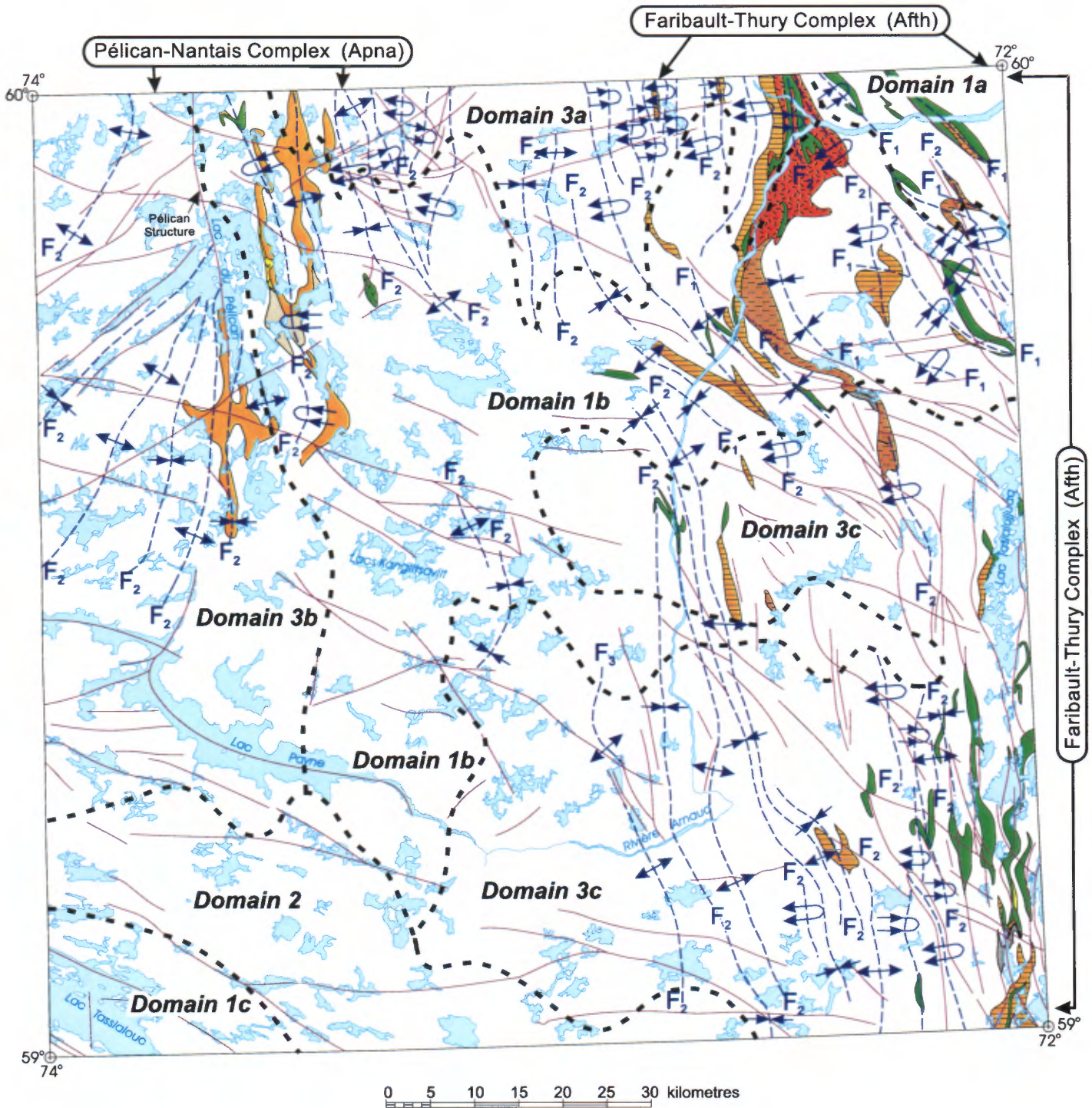


FIGURE 4 – Structural map of the Lac du Pélican area (34P), showing the location of structural domains (1a, 1b, 1c, 2, 3a, 3b, 3c), folds (F1, F2), and faults, with volcano-sedimentary units of the Faribault-Thury (Aftth) and Pélican-Nantais (Apna) complexes, and major lakes in the background.

LITHOGEOCHEMISTRY

In order to define the lithogeochemical characteristics of the main lithodemic units mapped in the Lac du Pélican area, 97 samples were analyzed for major elements and a few trace elements (Nb, Rb, Sr, Y and Zr) by X-ray fluorescence at the Centre de recherche minérale du Québec (COREM). Among these, 39 samples were selected for trace element and rare earth element (REE) analysis by ICP-MS at Geolabs (Ontario). All analytical results are available in the SIGÉOM database, and are summarized in tables 2 and 3 (Appendix 1).

Volcano-Sedimentary Complexes

Based on their major and trace element compositions, volcanic rocks of the Faribault-Thury Complex (Afh) and the Pélican-Nantais Complex (Apna) were subdivided into four groups: mafic, ultramafic, intermediate and felsic rocks. Analytical data collected on these volcanic rocks are plotted on diagrams in figures 6 and 7 and listed in Table 2 (Appendix 1). Their principal geochemical characteristics indicate that they form two different magmatic suites: a tholeiitic suite (TS) and a calc-alkaline suite (CAS).

The *tholeiitic suite* (TS) is characterized by higher TiO_2 , Fe_2O_3 , MgO, CaO and MnO contents, and lower SiO_2 , Al_2O_3 and $\text{K}_2\text{O}+\text{Na}_2\text{O}$ contents than the *calc-alkaline suite* (CAS). Relative to a fractionation index (FeO^*/MgO or Mg#), rocks of the TS are marked by a sharp enrichment in FeO and TiO_2 , weak to strong $\text{Na}_2\text{O}+\text{K}_2\text{O}$ enrichment, weak to nil $\text{Al}_2\text{O}_3/\text{TiO}_2$ and $\text{CaO}/\text{Al}_2\text{O}_3$, and SiO_2 and Al_2O_3 depletion. Variations in these element contents allow to define three magmatic evolution trends for the tholeiitic suite (TS_1 , TS_2 , TS_3). In contrast, rocks of the CAS are marked by a sharp enrichment in SiO_2 , $\text{Al}_2\text{O}_3/\text{TiO}_2$ and $\text{Na}_2\text{O}+\text{K}_2\text{O}$, and a depletion in FeO, TiO_2 , MnO and $\text{CaO}/\text{Al}_2\text{O}_3$ as a function of fractionation. The rate of evolution of these elements, and the behaviour of Al_2O_3 allows to define two magmatic evolution trends for the calc-alkaline suite (CAS_1 and CAS_2) (Figure 6).

Mafic volcanic rocks

Mafic rocks of the Faribault-Thury Complex (Afh3; TS_1 series; Mg# = 53.8-36.75) and the Pélican-Nantais Complex (Apna2a; TS_2 series; Mg# = 56.6-42.2) have subalkaline basalt compositions, ranging from high-Mg to high-Fe tholeiites (Figure 6a to 6c). Basaltic rocks of unit Afh3 exhibit a stronger enrichment in TiO_2 , $\text{Na}_2\text{O}+\text{K}_2\text{O}$, Ba, Zr and Y, but weaker in FeO^* and Al_2O_3 relative to unit Apna2a (Table 2; Figure 6c to 6f). This translates, for basaltic rocks of unit Afh3, into lower $\text{Al}_2\text{O}_3/\text{TiO}_2$ (9-15) and Ti/Zr (81-134) ratios, and higher Zr/Y ratios (1.0-3.3) than those for rocks of unit Apna2a ($\text{Al}_2\text{O}_3/\text{TiO}_2 = 15-29$; Ti/Zr = 166-365; Zr/Y = 0.7-1.4). Mafic volcanic rocks of unit Afh3 (TS_1) show flat rare earth element (REE) patterns ($[\text{La}/\text{Yb}]_{\text{NCH}} = 0.7-2.0$) at

less than 10 times chondrite (Figure 7a). The absence of Nb and Ti anomalies (Figure 7b), and the close to primitive mantle (0.11) Th/Nb concentrations (0.08-0.12) indicate that basaltic rocks of unit Afh3 have compositions similar to those of mantle-plume-derived plateau basalts. On the other hand, basalts of unit Apna2a follow a different evolutionary trend, essentially controlled by FeO enrichment (Figure 6b to 6f); the absence of accurate REE data makes it impossible to constrain the source of this tholeiitic magma.

Intermediate volcanic rocks

Intermediate gneisses of the Faribault-Thury Complex (Afh3b) have subalkaline tholeiitic basaltic andesite compositions ($\text{TS}_{1,3}$), whereas intermediate gneisses of the Pélican-Nantais Complex (Apna2b) are subalkaline and show tholeiitic andesite (TS_2) or calc-alkaline basaltic andesite to andesite (CAS_2) compositions (Figure 6a to 6c).

Tholeiitic basaltic andesites of unit Afh3b ($\text{TS}_{1,3}$; Mg# = 41.8-21.8), compared to tholeiitic andesites of unit Apna2b (TS_2 ; Mg# = 36.8-17.5), display higher values for $\text{Na}_2\text{O}+\text{K}_2\text{O}$, Ba, Sr and Zr/Y but lower SiO_2 , Fe_2O_3 , $\text{Al}_2\text{O}_3/\text{TiO}_2$, $\text{CaO}/\text{Al}_2\text{O}_3$, Zr/Ti and Sc (Table 2; Figure 6c to 6f). No REE patterns are available to characterize these two different tholeiitic suites.

On the other hand, calc-alkaline basaltic andesites and andesites (CAS_2 ; Mg# = 52.7-44.2) of unit Apna2b contrast with tholeiitic andesites (TS_2) of unit Apna2b by their higher values of SiO_2 , $\text{Na}_2\text{O}+\text{K}_2\text{O}$, Rb, Ba, Sr, Sc, Y, and Zr/Y, but lower TiO_2 , Fe_2O_3 , $\text{CaO}/\text{Al}_2\text{O}_3$ values (Table 2; Figure 6c to 6f). A sample of calc-alkaline basaltic andesite (CAS_2) shows a steep REE pattern ($[\text{La}/\text{Yb}]_{\text{NCH}} = 12.3$) with strongly enriched light REE ($[\text{La}/\text{Sm}]_{\text{NCH}} = 3.0$) relative to middle or heavy REE ($[\text{Gd}/\text{Yb}]_{\text{NCH}} = 2$ to 3 times chondrite) (Figure 7a), and a spiderdiagram with negative Th+U, Hf+Zr and Ti anomalies (Figure 7b).

Felsic volcanic rocks

Felsic volcanic rocks of the Faribault-Thury Complex (Afh3c) and the Pélican-Nantais Complex (Apna2c) are subalkaline with calc-alkaline dacitic, rhyodacitic and rhyolitic compositions (Figure 6a to 6c), and all follow the CAS_2 -type evolutionary trend (Figure 6c to 6f).

Dacites/rhyodacites of unit Afh3c (Mg# = 50.4-43.9) have higher MgO, $\text{CaO}/\text{Al}_2\text{O}_3$ and Ti/Zr values and lower P_2O_5 , Ba, Sr and Th contents than dacites/rhyodacites/rhyolites of unit Apna2c (Mg# = 47.3-29.2) (Table 2).

Dacites/rhyodacites of unit Afh3c show patterns enriched in large ion lithophile elements (Cs to K) (Figure 7b) and moderately steep REE patterns ($[\text{La}/\text{Yb}]_{\text{NCH}} = 3.5-5.0$) marked by a depletion in middle ($[\text{La}/\text{Sm}]_{\text{NCH}} = 1.4-3.0$) and heavy elements ($[\text{Gd}/\text{Yb}]_{\text{NCH}} = 0.9-1.7$ to 3 times chondrite) relative to tholeiitic basalts of unit Afh3 (Figure 7a). The fact that felsic volcanic rocks of unit Afh3c show less evolved patterns than calc-alkaline andesites of unit Apna2b for a similar Mg# or FeO^*/MgO index suggests the two calc-alkaline

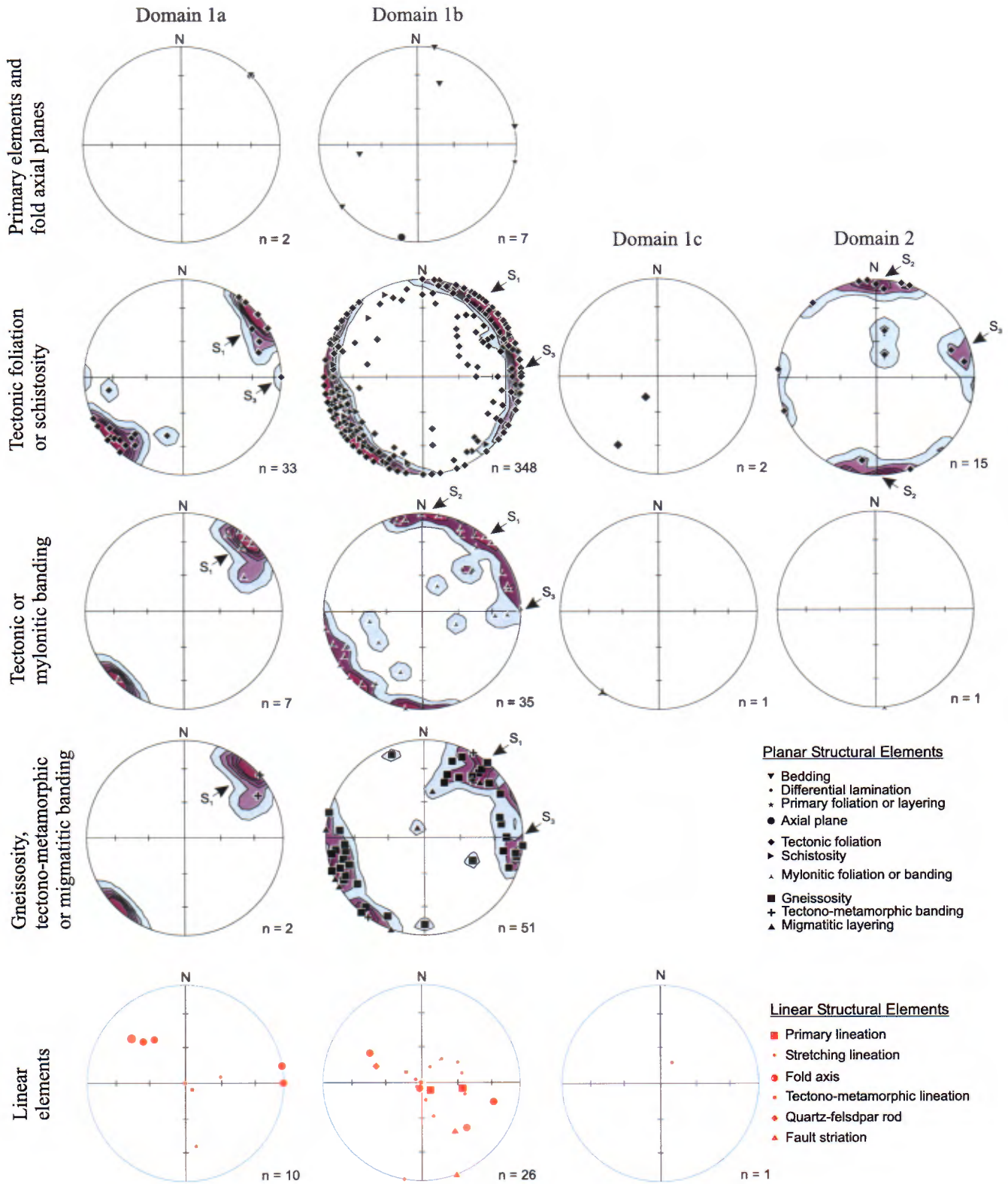


FIGURE 5 – Stereographic projections of structural elements (planar and linear) for all structural domains (1a, 1b, 1c, 2, 3a, 3b, 3c) and dykes in the Lac du Pélican area (34P).

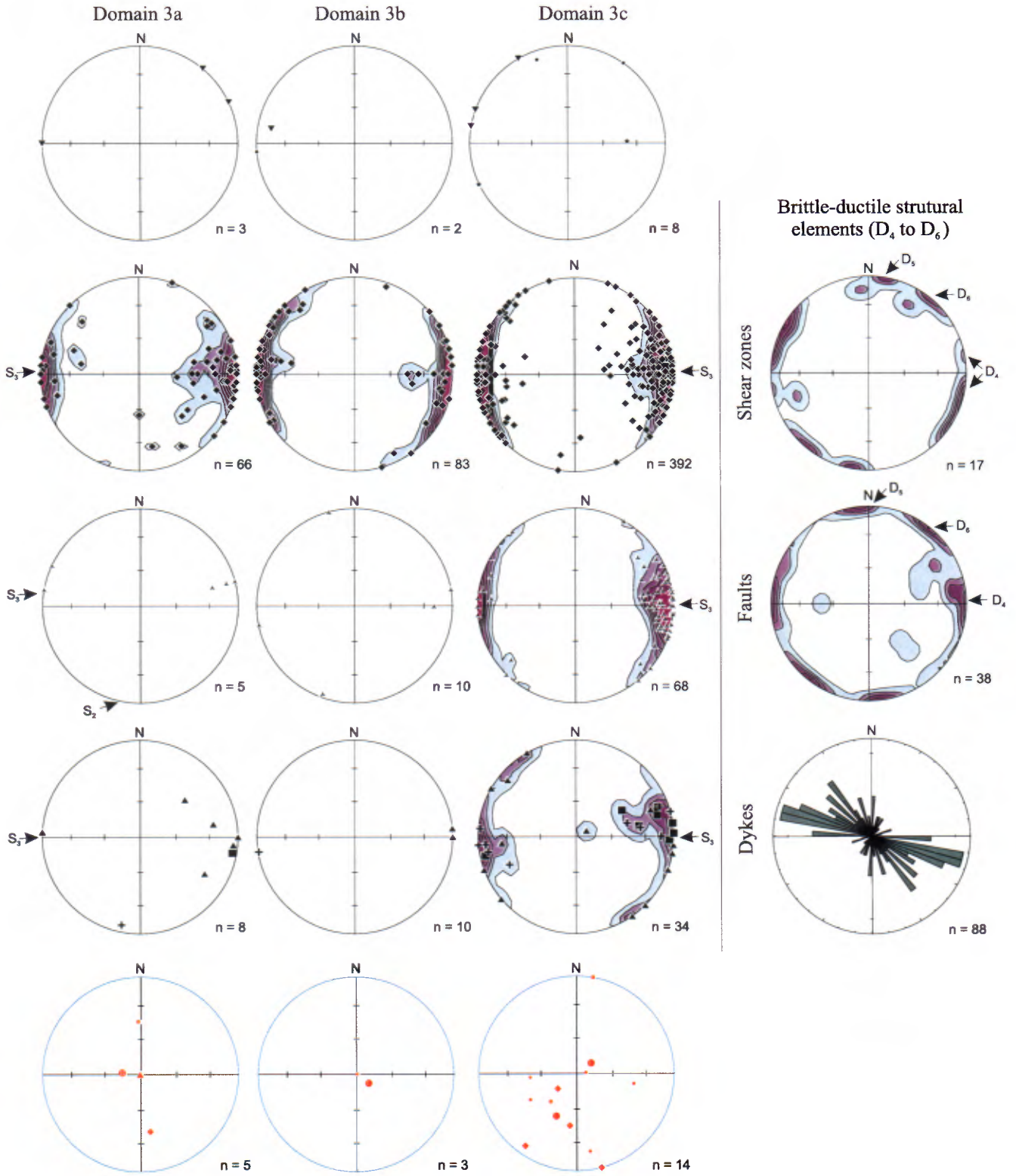


FIGURE 5 - Continued

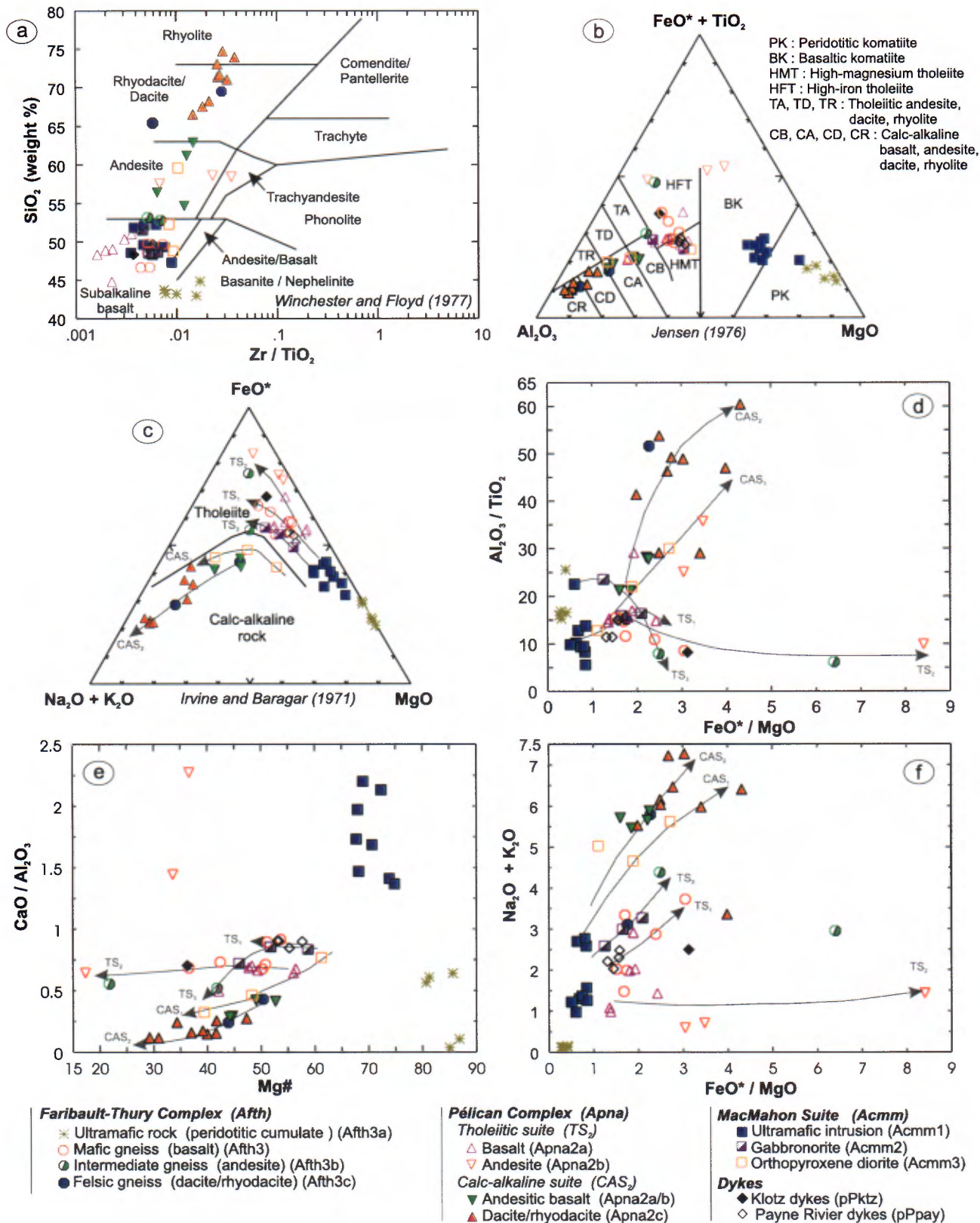


FIGURE 6 – Geochemical diagrams illustrating the results of major and trace element analyses of volcanic rocks from volcano-sedimentary complexes and ultramafic and mafic plutonic rocks of the MacMahon Suite in the Lac du Pélican area (34P) : a) SiO_2 versus Zr/TiO_2 binary classification diagram (Winchester and Floyd, 1977); b) AFM diagram (Jensen, 1976); c) AFM diagram (Irvine and Baragar, 1971); d) $\text{Al}_2\text{O}_3/\text{TiO}_2$ versus FeO^*/MgO binary diagram; e) $\text{CaO}/\text{Al}_2\text{O}_3$ versus Mg\# binary diagram; f) $\text{Na}_2\text{O}+\text{K}_2\text{O}$ versus FeO^*/MgO binary diagram.

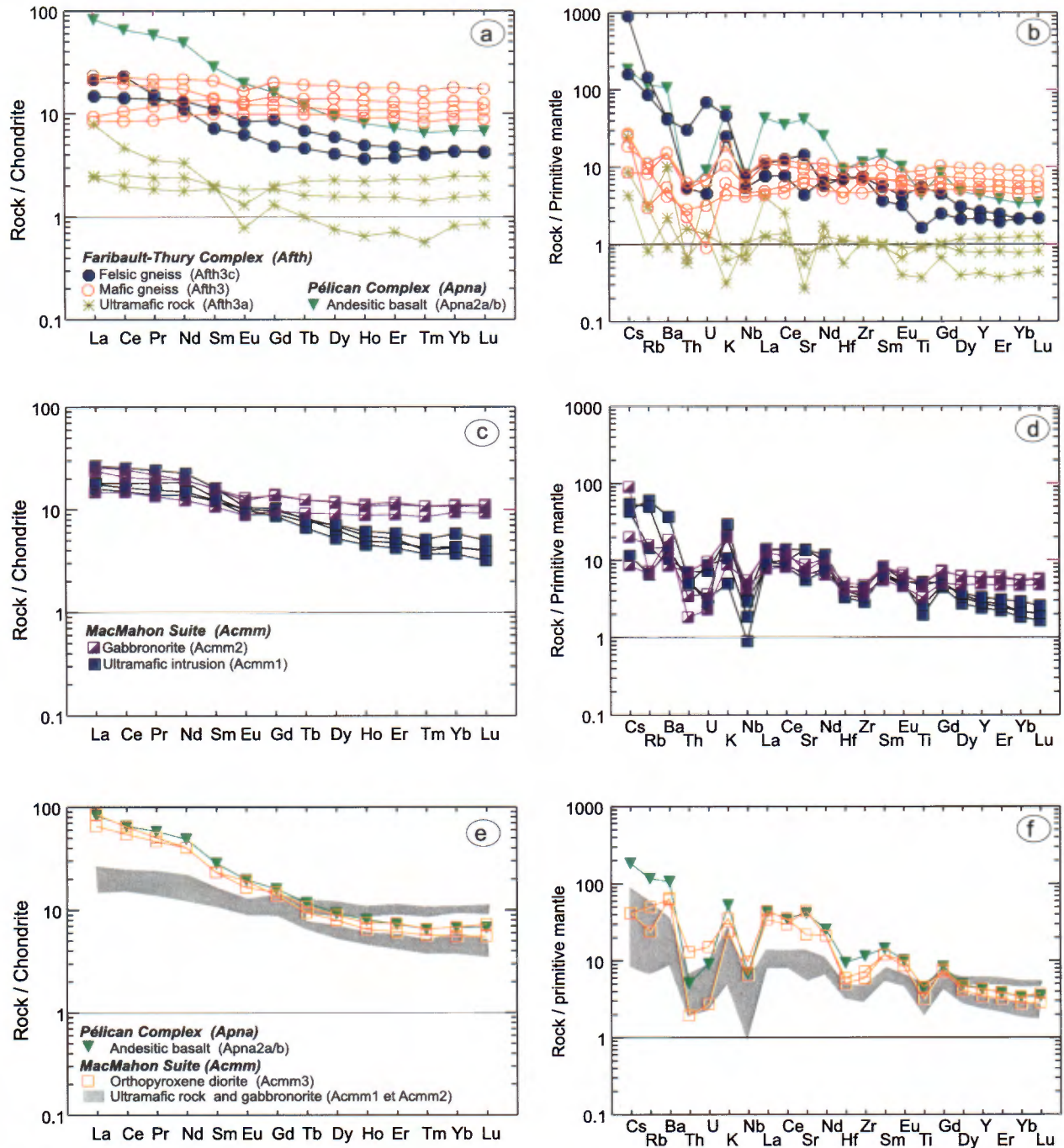


Figure 7 – Geochemical diagrams of rare earth elements normalized to chondrites (a,c,e) and multi-element spiderdiagrams normalized to the primitive mantle (b,d,f) illustrating the results of trace and rare earth element analyses of volcanic rocks from volcano-sedimentary complexes and ultramafic and mafic plutonic rocks of the MacMahon Suite in the Lac du Pélican area (34P).

suites are probably not derived from the same source, or else underwent different evolutionary processes.

Ultramafic volcanic rocks of the Faribault-Thury Complex

Ultramafic rocks of the Faribault-Thury Complex (AftH3a) show subalkaline to weakly alkaline peridotitic cumulate compositions (Table 2; Figure 6a and 6b). They exhibit high

MgO (30.3-36.6%), Cr (2,600-5,400 ppm) and Ni (930-1,800 ppm) contents, and low SiO₂ (37.8-39.6%), Al₂O₃ (1.1-4.6%) and TiO₂ (0.07-0.018%).

Ultramafic cumulates with less magnesium content (TS₁; Mg# = 80.7-85.7; Al₂O₃/TiO₂ = 16.5-25.6; CaO/Al₂O₃ = 0.56-0.64; Ti/Zr = 60-80; Zr/Y = 2.2-3.3) show flat REE patterns ([La/Yb]_{NCH} = 1.0-1.6 to 2 times chondrite), with weak Sr and Eu anomalies (Figure 7a and 7b). Th/Nb concentrations (0.15-0.21) markedly enriched relative to the primitive mantle

(0.11), and patterns parallel to those of tholeiitic basalts (TS,) indicate that these ultramafic rocks represent cumulates related to plateau basalts of unit Afth3.

The more magnesian cumulates (CAS₂₇; Mg# = 86.9-85.1) are depleted in Al, Ca and Ti (Al₂O₃/TiO₂ = 15.3-16.0; CaO/Al₂O₃ = 0.04-0.11; Ti/Zr = 35-38; Zr/Y = 3.6). They exhibit REE patterns slightly enriched in light REE ([La/Yb]_{n_{CH}} = 10) and depleted in middle ([La/Sm]_{n_{CH}} = 4.1) and heavy REE ([Gd/Yb]_{n_{CH}} = 1.4 to <1 times chondrite), with negative anomalies in Sr, Eu, Ti, Hf and Tm (Figure 7a and 7b).

Granitoid Suites

Analytical results for the various granitoid suites are plotted on diagrams in figures 8 and 9, and listed in Table 3 (Appendix 1).

Diorites and tonalites

Two diorite samples were analyzed, one from the *Faribault-Thury Complex (Afh4b)* and the second from the *Bottequin Suite (Abtq1)*; both show tholeiitic and metaluminous compositions, whereas the various tonalite samples from the *Faribault-Thury Complex (Afh4)*, the *Rochefort (Arot)*, *Bottequin (Abtq2 and Abtq2a)*, *Lepelle (Alep2)* suites and the *Pélican-Nantais Complex (Apna3)*, on the whole show calc-alkaline and more peraluminous compositions than the diorites (Figure 8a to 8c). The various tonalites cover a very wide compositional spectrum (Table 3; Figure 9a and 9b).

A clinopyroxene melatonalite of the Bottequin Suite (Abtq2a; Mg# = 51.1) has a normative composition akin to a metaluminous quartz monzogabbro, which contrasts with biotite ± hornblende tonalites *sensu stricto* of the

LEGENDE

- Faribault-Thury Complex (Afh)**
 - Diorite (Afh4b)
 - Tonalite (Afh4)
- Rochefort Suite (Arot)**
 - ▣ Tonalite (Arot)
- Bottequin Suite (Abtq)**
 - Diorite (Abtq1)
 - ◆ Tonalite (Abtq2)
 - Clinopyroxene melatonalite (Abtq2a)
- Châtelain Suite (Achl)**
 - + Granodiorite (Achl)
- La Chevrotière Suite (Aicv)**
 - ✱ Porphyritic monzogranite (Aicv1)
 - ✕ Granite (Aicv2)
- MacMahon Suite (Acmm)**
 - ⊙ Orthopyroxene diorite (Acmm3)
 - △ Orthopyroxene-rich enderbite (Acmm4)
 - ▲ Clinopyroxene-rich enderbite (Acmm5)
 - ▽ Mangerite (Acmm6)
 - ▽ Opdalite/Charnockite (Acmm6)
- Lepelle Suite (Alep)**
 - ◆ Porphyritic tonalite with clinopyroxene (Alep2)
- Pélican-Nantais Complex (Apna)**
 - ◇ Tonalite (Apna3)

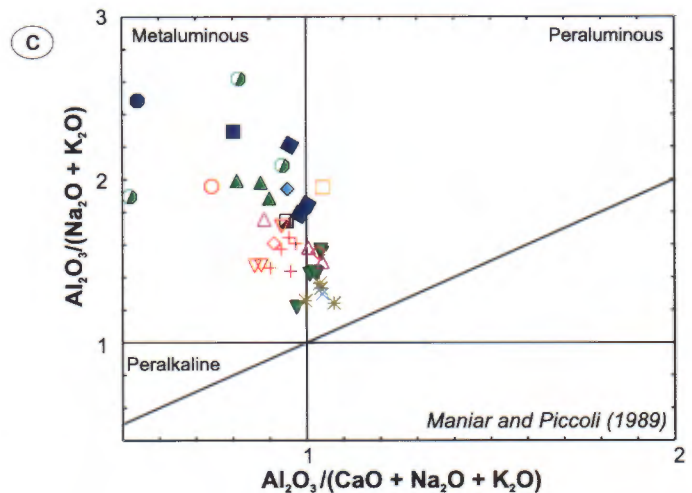
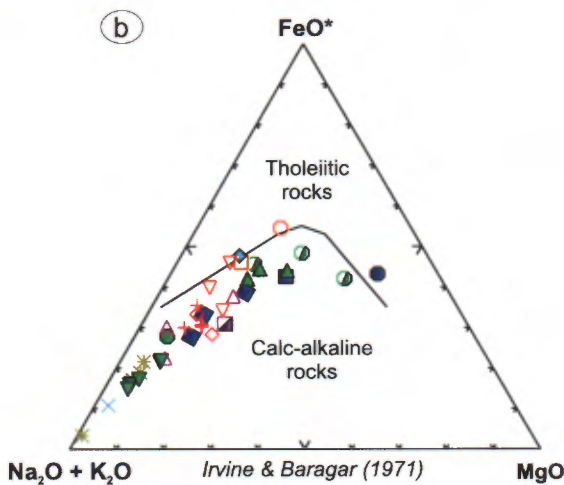
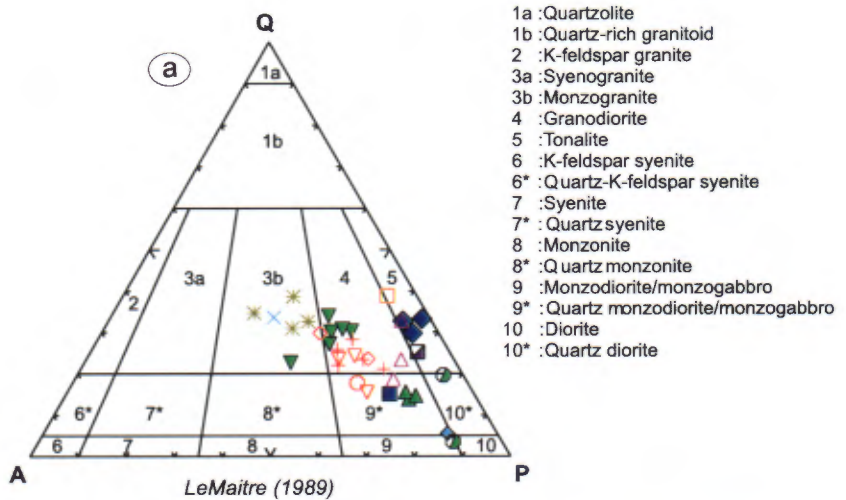


FIGURE 8 – Geochemical diagrams illustrating the results of major and trace element analyses of granitoid units in the Lac du Pélican area (34P) : a) Normative quartz-alkali feldspar-plagioclase classification diagram (LeMaitre, 1989); b) AFM diagram (Irvine and Baragar, 1971); c) A/NK versus A/CNK discrimination diagram (Maniar and Piccoli, 1989).

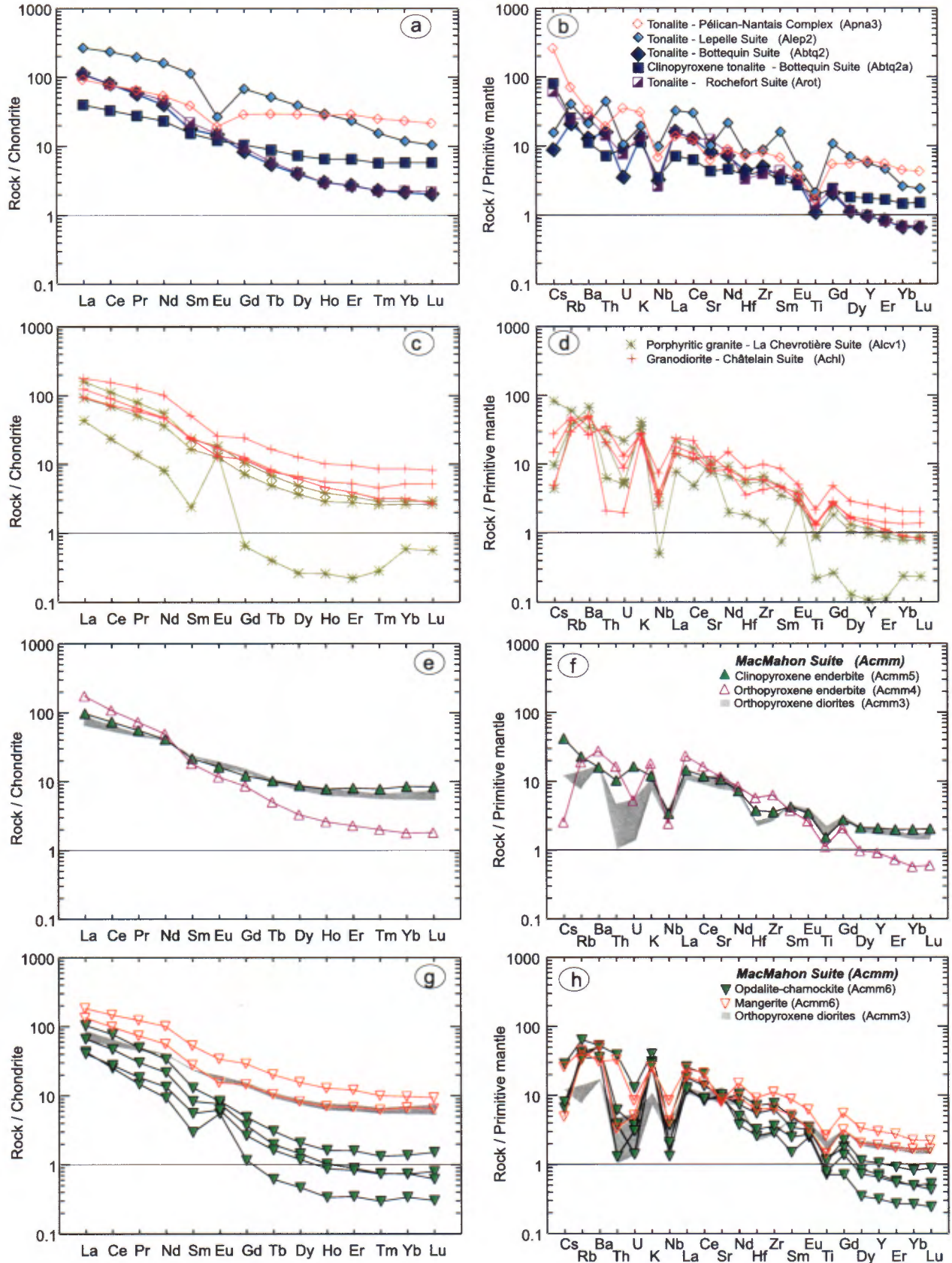


FIGURE 9 – Geochemical diagrams showing rare earth elements normalized to chondrites (a,c,e,g) and spiderdiagrams normalized to the primitive mantle (b, d, f, h) illustrating the results of trace and rare earth element analyses of granitoid units in the Lac du Pélican area (34P).

Faribault-Thury Complex (Aft4; Mg# = 34.9), the Rochefort Suite (Arot; Mg# = 50.6) and the Bottequin Suite (Abtq2; Mg# = 45.6-39.2). The clinopyroxene melatonite (Abtq2a) shows a slightly inclined REE pattern ($[La/Yb]_{n_{CH}} = 7$), weakly enriched in light and middle REE ($[La/Sm]_{n_{CH}} = 2.7$) relative to heavy REE ($[Gd/Yb]_{n_{CH}} = 1.5$ to 5 times chondrite), and a spiderdiagram with negative anomalies in Ba+Th, Nb and Ti. Biotite±hornblende tonalites of the Rochefort (Arot) and Bottequin (Abtq2) suites show similar REE patterns and spiderdiagrams. These rocks have steeper REE patterns ($[La/Yb]_{n_{CH}} = 48-52$), due to light REE enrichment ($[La/Sm]_{n_{CH}} = 5.0-6.4$) and heavy REE depletion ($[Gd/Yb]_{n_{CH}} = 3.3-3.6$ to <5 times chondrite), and also show negative anomalies in U, Nb, Sr and Ti (Figure 9a and 9b).

Younger tonalites exhibit very different multi-element patterns. The clinopyroxene bearing porphyritic tonalite of the Lepelle Suite (Alep2; Mg# = 31.8) has a normative monzogabbro composition (Figure 8a), and shows a steep REE pattern ($[La/Yb]_{n_{CH}} = 22.5$) characterized by heavy REE markedly more fractionated ($[Gd/Yb]_{n_{CH}} = 4.8$) than light REE ($[La/Sm]_{n_{CH}} = 2.7$). The spiderdiagram shows strong negative Cs+Ba anomalies relative to Rb, in U+Nb relative to K, and in Sr, Hf+Zr and Eu+Ti. On the other hand, a tonalite from the Pélican-Nantais Complex (Apna3; Mg# = 50.9-36.4) shows a weakly inclined REE pattern ($[La/Yb]_{n_{CH}} = 4.0$) marked by an enrichment in light REE ($[La/Sm]_{n_{CH}} = 2.4$) and a flat heavy REE pattern ($[Gd/Yb]_{n_{CH}} = 1.0$ to <5 times chondrite). The spiderdiagram is marked by a strong enrichment in large ion lithophile elements (Cs-Nb) and strong negative anomalies in Th, Nb, Sr and Eu+Ti (Figure 9a and 9b).

Granodiorites and Granites

Hornblende±clinopyroxene granodiorites of the Châtelain Suite (Ach1; Mg# = 44.4-32.8) show very homogeneous and weakly metaluminous compositions ($A/CNK < 1$; Figure 8c). The different types of granites of the La Chevrotière Suite (Alcv; Mg# = 36.2-29.8) also show very homogeneous, weakly peraluminous compositions ($A/CNK = 1.0-1.1$; Figure 8c). These granites are enriched in SiO_2 , K_2O and Na_2O+K_2O but depleted in TiO_2 , CaO, Fe_2O_3 , MgO and P_2O_5 relative to granodiorites of the Châtelain Suite (Table 3; Appendix 1).

Except for one sample of porphyritic granite (Alcv1), REE diagrams and spiderdiagrams show fairly parallel patterns for the two suites (Figure 9c and 9d). Granodiorites of the Châtelain Suite (Ach1) have very steep REE patterns ($[La/Yb]_{n_{CH}} = 21-30$) marked by a greater fractionation of light REE ($[La/Sm]_{n_{CH}} = 3.5-5.4$) relative to heavy REE ($[Gd/Yb]_{n_{CH}} = 1.9-3.4$). Spiderdiagrams are characterized by strong negative Cs, Th+U, Nb and Ti anomalies, and weaker Sr and Eu anomalies. On the other hand, porphyritic granites

of the La Chevrotière Suite (Alcv1) exhibit steeper REE patterns ($[La/Yb]_{n_{CH}} = 35-56$) more depleted in middle ($[La/Sm]_{n_{CH}} = 5.7-7.0$) and heavy REE ($[Gd/Yb]_{n_{CH}} = 2.3-3.1$). However, a porphyritic granite sample (Alcv1) stands out due to its multi-element pattern enriched in large ion lithophile elements (Cs to K), but severely depleted in all other elements except Sr and Eu. Its light and middle REE pattern is steeply inclined ($[La/Yb]_{n_{CH}} = 75$; $[La/Sm]_{n_{CH}} = 19$) and is marked by a U-shaped pattern for heavy REE ($[Gd/Yb]_{n_{CH}} = 0.9$).

Enderbitic to charnockitic rocks and associated ultramafic to mafic rocks

Ultramafic plutonic rocks of the MacMahon Suite (Acmm1; Mg# = 78-68) show subalkaline compositions akin to those of basaltic komatiites and peridotitic komatiites (Figure 6a and 6b). They have moderate SiO_2 and MgO contents, high Fe_2O_3 and low Cr and Ni values (Table 2, Appendix 1). Ultramafic plutonic rocks are characterized by moderately inclined REE patterns ($[La/Yb]_{n_{CH}} = 3.1-6.3$) with enriched light REE ($[La/Sm]_{n_{CH}} = 1.3-1.7$) and middle REE ($[Gd/Yb]_{n_{CH}} = 1.3-2.0$) (Figure 7c). Spiderdiagrams exhibit negative Th+U, Nb, Hf+Zr and Ti anomalies (Figure 7d). Among these rocks, three analyses show Na_2O+K_2O enrichment (Figure 6c and 6f), which translates, on spiderdiagrams, into an enrichment in large ion lithophile elements (Cs+Ba+Th and K), caused by more substantial crustal contamination.

Gabbronorites of the MacMahon Suite (Acmm2; Mg# = 59-46) show subalkaline high-Mg and high-Fe tholeiitic basalt compositions (Figure 6a and 6b) that plot along a TS_3 -type evolutionary trend (Figure 6c to 6f). Compared to ultramafic rocks (Acmm1), they display higher Al_2O_3 and Na_2O , and lower MgO, Cr and Ni values (Table 2). Gabbronorites have weakly inclined REE patterns ($[La/Yb]_{n_{CH}} = 1.6-2.4$) characterized by weakly enriched light and middle REE ($[La/Sm]_{n_{CH}} = 1.4-1.7$) and a flat heavy REE pattern ($[Gd/Yb]_{n_{CH}} = 0.9-1.1$ to 5 times chondrite; Figure 7c). As for ultramafic rocks, spiderdiagrams for gabbronorites show negative anomalies in Th+U, Nb, Hf+Zr and Ti, and occasional positive Cs and K anomalies (Figure 7d).

Orthopyroxene diorites of the MacMahon suite (Acmm3; Mg# = 61.4-39.5) have subalkaline and calc-alkaline compositions that contrast with ultramafic rock and gabbronorite compositions (Figure 6a and 6b). They exhibit even higher Al_2O_3 , Na_2O and K_2O contents, and lower Fe_2O_3 , MnO, MgO, CaO, Cr, Co and Ni (Table 2). These variations translate into higher Al_2O_3/TiO_2 ratios, and lower CaO/Al_2O_3 ratios that define a CAS_1 -type evolution patterns (Figure 6c and 6f). These diorites (Acmm3) are represented by steeply inclined REE patterns ($[La/Yb]_{n_{CH}} = 12-13$) characterized by strongly enriched light and middle REE ($[La/Sm]_{n_{CH}} = 2.9-3.7$) relative to heavy REE ($[Gd/Yb]_{n_{CH}} = 1.9-2.1$ to 5-7 times chondrite; Figure 9e). Spiderdiagrams for diorite

samples show negative anomalies in Th+U, Nb, Hf+Zr and Ti (Figure 9f).

Felsic rocks assigned to the MacMahon Suite form a calc-alkaline evolution suite ranging from clinopyroxene enderbites (Acmm5; Mg# = 50-42) through mangerites (Acmm6; Mg# = 45-31), orthopyroxene enderbites (Acmm4; Mg# = 43-26), up to opdalites-charnockites (Acmm6; Mg# = 41.5-36) (Figure 8a and 8b; Table 3, Appendix 1). This evolution, marked by a transition from metaluminous to weakly peraluminous compositions (Figure 8c), is typical of CAS₂-type rocks. Clinopyroxene enderbites (Acmm5) and mangerites (Acmm6) have very steep REE patterns ($[La/Yb]_{n_{CH}} = 11.5$ and $19-20$, respectively) parallel to those of orthopyroxene diorites (Acmm3) (Figures 9e and 9g). The only distinction lies in their greater concentrations of large ion lithophile elements (Cs-K) (Figures 9f and 9h). The orthopyroxene enderbite sample shows a more steeply inclined REE pattern ($[La/Yb]_{n_{CH}} = 99$) marked by weakly enriched light REE ($[La/Sm]_{n_{CH}} = 9.7$) and particularly strongly depleted heavy REE ($[Gd/Yb]_{n_{CH}} = 4.1$) (Figure 9g and 9h). The same trends, albeit somewhat stronger, of large ion lithophile element and light REE enrichment and middle and heavy REE depletion, are observed for opdalites-charnockites ($[La/Yb]_{n_{CH}} = 52-123$; $[La/Sm]_{n_{CH}} = 7.2-14.6$; $[Gd/Yb]_{n_{CH}} = 2.8-4.1$) (Figure 9g and 9h).

At this point, it is important to note that the major element, trace element and REE compositions of orthopyroxene diorites (Acmm3) and opdalites-charnockites (Acmm6) of the MacMahon Suite are respectively similar to those of calc-alkaline (CAS₂) andesites (Apna2b) and dacites-rhyodacites (Apna2c) of the Pélican-Nantais Complex. Andesitic lavas and rhyodacitic to rhyolitic felsic tuffs of the Pélican-Nantais Complex may represent extrusive equivalents of dioritic and opdalitic to charnockitic plutonic rocks of the MacMahon Suite. All these rocks are interpreted as being derived from a common source of tholeiitic composition, represented by the gabbronorites of the MacMahon Suite. The calc-alkaline signature, marked by a progressive enrichment in SiO₂, Na₂O+K₂O, Al₂O₃/TiO₂, Zr/Y and in light REE, as well as depletion in FeO, TiO₂, MnO, CaO/Al₂O₃, Ti/Zr and in heavy REE, is not perceived as the result of arc-type magmatism (Stern *et al.*, 1994). It may be interpreted as the result of a combination of: (i) magma mixing between a tholeiitic source (gabbronorite of the MacMahon Suite) and a granitic magma (La Chevroitière Suite), and (ii) progressive fractionation, followed by volcanic extrusion of this mixture. However, this relation is somewhat contradicted by obtained ages of *ca.* 2742 Ma for tuffs of the Pélican-Nantais Complex (Percival *et al.*, 1997), versus ages of *ca.* 2723-2717 Ma obtained for the different plutonic rocks of the MacMahon Suite, and of *ca.* 2732-2723 Ma obtained for the different granites of the La Chevroitière Suite.

Proterozoic Gabbro and Diabase Dykes

Klotz gabbro dykes (pPktz) and Payne River diabase dykes (pPpay) respectively yield subalkaline high-Fe and high-Mg tholeiitic compositions (Figure 6a and 6b). Payne River diabases (pPpay; Mg# = 58-53) are markedly enriched in MgO, CaO, K₂O, Cr, Ni and Rb, and depleted in TiO₂, Al₂O₃, Fe₂O₃t and Na₂O relative to Klotz gabbros (pPktz; Mg# = 36; Table 2). The two types of dykes are enriched in Fe₂O₃t, and depleted in Cr and Ni. Their respective compositions lie along the TS₂ and TS₁ trends (Figure 6c to 6f), which is similar to those of plateau basalts formed in an intraplate setting.

ECONOMIC GEOLOGY

Very little mineral exploration was conducted in the Lac du Pélican area prior to our mapping survey in the summer 2000. Other than lake sediment geochemistry anomalies, exploration conducted by SOQUEM in 1999 had identified a few lithochemical anomalies in gold, silver, copper and zinc in the Pélican belt.

Our work in the summer 2000 uncovered two showings (Tukimurtuk and Tasiaalujuaq showings) and eighteen anomalous occurrences of various elements, which may be grouped into three types of ore deposit settings: 1) iron formations with Cu ± Au ± Ag ± Zn mineralization; 2) ultramafic to mafic intrusions with Cu ± Zn mineralization, and 3) fault zones and quartz veins with Cu ± Zn ± Au ± Ag ± Mo ± U mineralization (Table 4 and Figure 10). Polished thin sections were prepared for all showings and occurrences with anomalous metal grades (Table 4). Furthermore, a detailed study on the volcanogenic sulphide potential of volcanic rocks in the Pélican belt was conducted, in the NW part of the map area (NTS 34P/13; Figure 10). A summary of results from this study is provided below (see Figure 11).

Lithochemical anomalies clearly outline the distribution of volcanic and sedimentary rocks, as well as fault zones, in an environment dominated by granitoids. Lake sediment geochemistry anomalies (for Cu, Ni, Cr and Zn, 95th percentile) are plotted in the background on Figure 10. They are derived from a survey conducted in 1997 by the MRN (1998) within the scope of the Far North project. Five multi-element anomalies (Cr-Ba-Ce), which may indicate remobilization of kimberlitic till, are shown on Figure 10. They correspond to "kimberlite targets", as proposed by Moorhead *et al.* (2000). Most lithochemical anomalies overlap with multi-element lake sediment geochemistry anomalies. Copper shows the best correlation. In fact, copper-rich

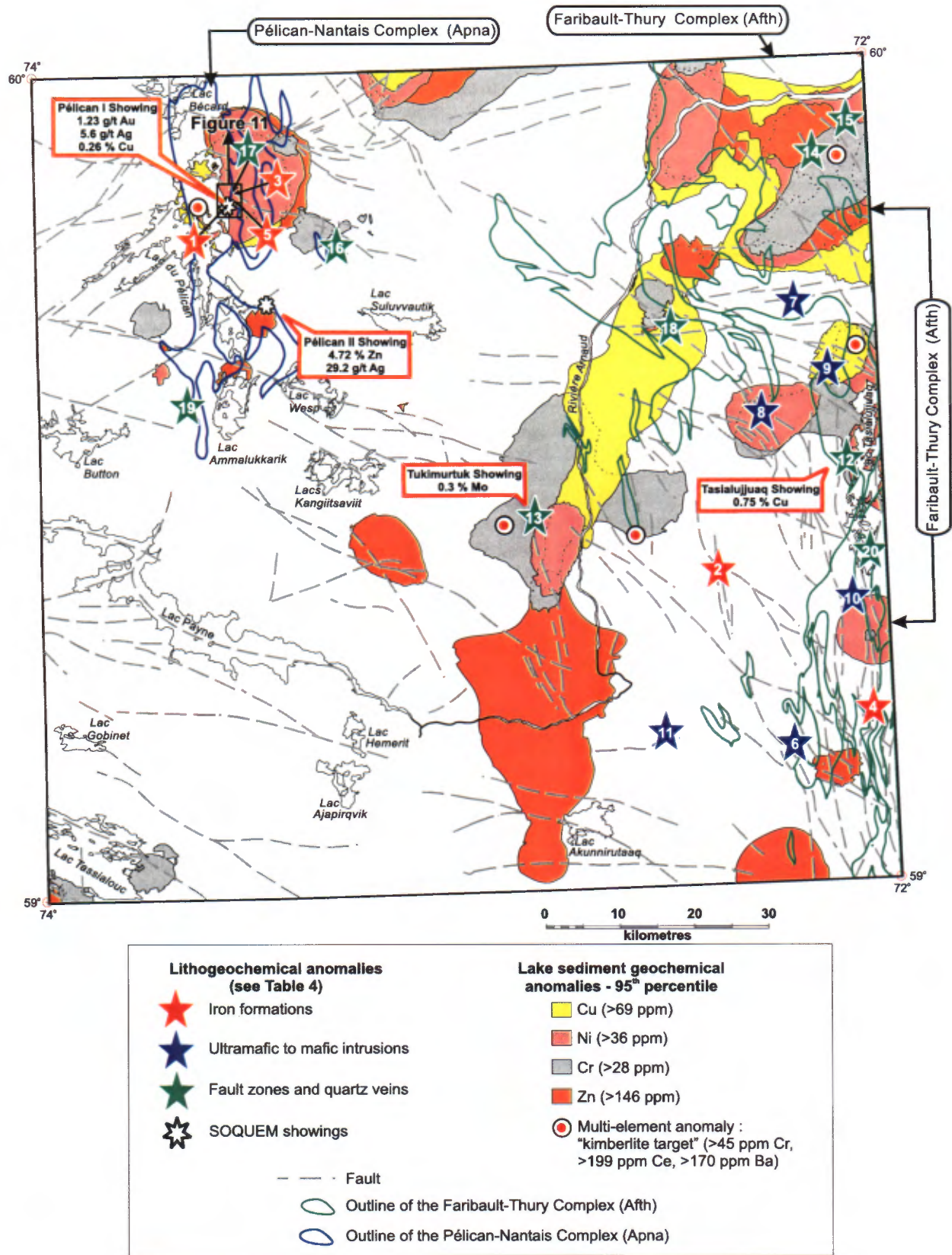


FIGURE 10 – Location map of the main sites of economic interest in the Lac du Pélican area (34P) which yielded anomalous lithochemical result. In the background, lake sediment geochemical anomalies are shown, along with the main fault and lakes in the area, as well as the limits of the Faribault-Thury and Pélican-Nantais complexes. See also Table 4.

lithogeochemical anomalies are all correlated with Cu anomalies in lake sediments. This is the case for sites 1, 3, 9, 14, 15, 17 and 18, which contain up to 0.35% Cu. However, several geochemistry anomalies derived from lake sediments could not be reproduced by lithogeochemistry of surface rocks; this is particularly the case for an elongate series of anomalies located along the Rivière Arnaud, which most likely represent a concentration of elements produced by regional drainage patterns.

Mineralization Associated with Iron Formations

Volcano-sedimentary belts (one to several kilometres in size, up to 20 km in length and 5 km in width) host most occurrences found in the area. Iron formations, occurring as dismembered horizons from one to ten metres in width, are generally located in volcanic sequences in belts of the Pélican-Nantais Complex (*Apna*) and the Faribault-Thury Complex (*Afth*). These iron formations, generally banded, exhibit both oxide and silicate facies, with an occasional hybrid facies. Paragneisses associated with these iron formations host disseminated sulphides (pyrite, pyrrhotite and chalcopyrite). The best grades obtained in iron formations mapped during the summer 2000 are: 901 ppm Cu, 2 g/t Ag and 210 ppb Au in the Pélican belt (site 1; Figure 10, Table 4), and 389 ppm Cu, 280 ppb Au and 243 ppm Zn in the Faribault-Thury Complex (site 2; Figure 10, Table 4).

In the Pélican belt, several iron formation horizons host mineral occurrences (sites 1, 3 and 5; Figure 10, Table 4). Oxide-facies iron formations (sites 1 and 5) predominate, whereas silicate-facies iron formations are rare (site 3). The former occur either as massive magnetite horizons within paragneiss or mafic volcanic units, or at the contact between mafic and felsic volcanic rocks. The latter are rare, highly siliceous, and contain very little magnetite. They are enclosed in mafic rock sequences. Pyrite, pyrrhotite and chalcopyrite mineralization occurs disseminated between magnetite crystals or in mm-scale laminae parallel to banding.

Similar iron formation horizons were encountered in belts of the Faribault-Thury Complex, in the eastern part of the map area (sites 2 and 4; Figure 10, Table 4). Silicate-facies iron formations (ex: site 4) are however more common. These rocks are composed of thin laminations of grunerite, hornblende, clinopyroxene, orthopyroxene, garnet, quartz, feldspar, magnetite and locally cordierite. Disseminated pyrite, pyrrhotite and chalcopyrite mineralization is associated with magnetite.

Mineralization Associated with Ultramafic to Mafic Intrusions

Bands from 10 m to 1 km in size, and m-scale enclaves of ultramafic (pyroxenite, hornblende pyroxenite and pyroxene

hornblende) and mafic rocks (gabbro, diorite and their orthopyroxene-bearing counterparts), enclosed in enderbite, opdalite and charnockite units of the MacMahon Suite, locally host copper mineralization associated with minor zinc. These occurrences (sites 6 to 11; Figure 10, Table 4) consist of disseminated or cm-scale pods of sulphides. The best grade obtained in this type of setting is 875 ppm Cu (site 6).

Sulphides observed in decreasing order are: pyrite, chalcopyrite, pyrrhotite and pentlandite. They occur in mm-scale aggregates. Coarse-grained hypidiomorphic pyrite contains inclusions of all other sulphides (it appears to be a late phase). Chalcopyrite is fine-grained, occurring as inclusions in pyrite or pyrrhotite, or intergrown with pyrrhotite. Pyrrhotite is coarse-grained, disseminated or in pods with chalcopyrite and/or pyrite. Pentlandite was observed in only a few samples; it is fine-grained and mainly occurs as flame-like exsolutions in pyrrhotite and in irregular aggregates with other sulphides.

In these ultramafic rocks, magnetite forms up to 1% of the mineral assemblage. It is generally allotriomorphic, disseminated, and also forms lamellar and vermicular inclusions in pyroxene grains.

Mineralization Associated with Fault Zones and Quartz Veins

Deformation zones and faults are characterized by brittle-ductile deformation generally accompanied by a red to orange-coloured alteration, with a variety of disseminated sulphides and iron oxides and hydroxides. These zones locally contain quartz and epidote veins, as well as diabase and gabbro dykes. They represent a favourable setting for the remobilization of precious metals, base metals and uranium. Two showings were discovered in this type of setting, with grades of 0.75% Cu, 3.9 g/t Ag and 140 ppb Au (Tasiaalujuaq showing, site 12; Figure 10, Table 4), and 0.3% Mo (Tukimurtuk showing, site 13; Figure 10, Table 4).

Pyrrhotite is the dominant sulphide in this environment of deformation, and constitutes up to 10% of the mineral assemblage. It generally occurs as disseminated allotriomorphic grains, or as mm-scale aggregates. Pyrrhotite is most often surrounded by an oxidation rim composed of magnetite and/or hematite and/or goethite. It often occurs intergrown with chalcopyrite, and locally, as inclusions in pyrite. Chalcopyrite is often observed; it may form up to 3% of the mineral assemblage. It occurs intergrown with pyrrhotite, disseminated, locally infilling microfractures in ilmenite, or as small globular inclusions in pyrite. Pyrite is also common and forms 1 to 2% of the mineral assemblage. It is fine-grained, hypidiomorphic, disseminated or in mm-scale pods. Certain samples contain pentlandite, occurring as flame-like exsolutions in pyrrhotite. Molybdenite is locally observed, but only one sample yielded anomalous molybdenum grades (Tukimurtuk showing, site 13,

with 0.3% Mo; Figure 10, Table 4). At the Tukimurtuk showing, molybdenite forms 3% of the mineral assemblage, occurring as veinlets and disseminations concentrated in fine fractures. Molybdenite crystals are idiomorphic to hypidiomorphic and fine-grained.

Magnetite is abundant, as magnetite_{ss} or titaniferous magnetite. It generally occurs as coarse, allotriomorphic grains, disseminated and in mm-scale to cm-scale aggregates, locally intergrown with coarse allotriomorphic ilmenite. It sometimes contains lamellar exsolutions of hematite and/or ilmenite. These oxides also form alteration coronas around sulphide phases (pyrite, chalcopyrite and pyrrhotite) and infill late microfractures.

Mineral Potential of the Pélican Belt

Volcanic rocks of the Pélican belt represent a particularly interesting setting from an economic standpoint. However, very little exploration has been conducted to date. Following the lake sediment geochemistry survey conducted in 1997 (MRN, 1998), a multi-element anomaly was identified east of Lac du Pélican (Figure 10), and an exploration licence was acquired. An airborne magnetic and electromagnetic survey, commissioned by SOQUEM and Cambior, was conducted in June 1999 (Venter *et al.*, 1999). Two parallel conductors, nearly two kilometres long and spaced roughly 200 metres apart, were identified in the northeastern part of Lac du Pélican (Figure 11; Figure 10, Pélican I showing). Rocks in this area correspond to a contact zone between mafic and felsic volcanic rocks. An isolated conductor was also detected about 15 km to the SSE (Figure 10, Pélican II showing). Reconnaissance work was then carried out on these conductors (Cuerrier, 1999). Anomalous grades were obtained in the northeastern part of Lac du Pélican, with the best grades found on the Pélican I showing (Figure 10): 1.23 g/t Au, 5.6 g/t Ag and 0.26% Cu. A tuff sample with 4.72% Zn and 29.2 g/t Ag was collected in the southern sector corresponding to the isolated conductor (Pélican II showing, Figure 10).

Detailed work was carried out during the summer 2000, in order to define the potential for volcanogenic sulphide deposits in the northeastern part of Lac du Pélican. This work consisted of detailed mapping (1:20,000 scale) and bedrock sampling for petrographic and geochemical studies of alteration zones. The resulting geological map is shown in Figure 11. The map also shows the two conductors and the two samples with anomalous Au and Ag grades. The eastern part of the belt consists of biotite-garnet paragneiss, with a few magnetite iron formation horizons. These paragneisses are in contact with a thin (< 100 m) horizon of mafic volcanic rocks. This contact is generally rusty, and hosts several bands of disseminated sulphides. Anomalous metal grades are scattered along the contact, which corresponds to the westernmost conductor (Figure 11). The other

conductor appears to correspond to an iron formation horizon. The western part of the belt consists of felsic volcanic rocks, mainly highly siliceous fine-grained tuffs, with local lapilli and block tuffs. These felsic rocks are not mineralized, and do not appear to have undergone volcanogenic alteration. They are in contact, to the west, with intensely deformed tonalites. Mafic and felsic rocks are also observed in the southeastern part of the paragneiss-dominated area, where they form a circular structure characterized by substantial variations in the attitude of the main foliation. This may represent a dome or basin structure. Magnetite iron formation horizons roughly 10 cm thick are also associated with these mafic rocks.

Overall, there is very little evidence of volcanogenic hydrothermal activity in the volcanic rocks of the northeastern part of Lac du Pélican, except in the SE, where rocks in the circular structure locally contain mineral assemblages which may reflect this type of activity. The presence of garnet in metabasalts and of biotite and sillimanite in certain felsic tuff horizons may be related to a metamorphosed volcanogenic alteration zone. A felsic tuff sample with sillimanite (SM) and biotite (BO) is chemically similar to a sericitic volcanogenic alteration zone (Labbé and Lacoste, 2001).

A traverse across the isolated electromagnetic anomaly area (15 km south; Pélican II showing, Figure 10) was unsuccessful in identifying the Zn-Ag-rich tuff, since rocks in this area scarcely outcrop.

CONCLUSIONS

The Lac du Pélican area (34P) was subdivided into two lithodemic complexes and six intrusive suites, which were emplaced between *ca.* 2.77 and 2.69 Ga. These Archean units are intruded by two Paleoproterozoic dyke swarms: the Klotz gabbro dykes (pPktz; *ca.* 2209 Ma; Buchan *et al.*, 1998) and the Payne River diabase dykes (pPpay; *ca.* 1875-1790 Ma; Fahrig *et al.*, 1985).

The oldest elements in the area correspond to the Rochefort Suite in the southwesternmost part of the map area, the Bottequin Suite in the centre, and the Faribault-Thury Complex in the east. All three consist of strongly foliated to gneissic biotite±hornblende tonalites and trondhjemites, dated at *ca.* 2.78-2.77 Ga. In the Faribault-Thury Complex, remnants of volcano-sedimentary belts are abundant, and form discontinuous bands reaching up to 20 km in length and 5 km in width. They are mainly composed of metabasalts, but also contain ultramafic, intermediate and felsic volcanic rocks, as well as paragneisses and iron formations.

In the northwestern part of the map area, the Pélican volcano-sedimentary belt, assigned to the Pélican-Nantais

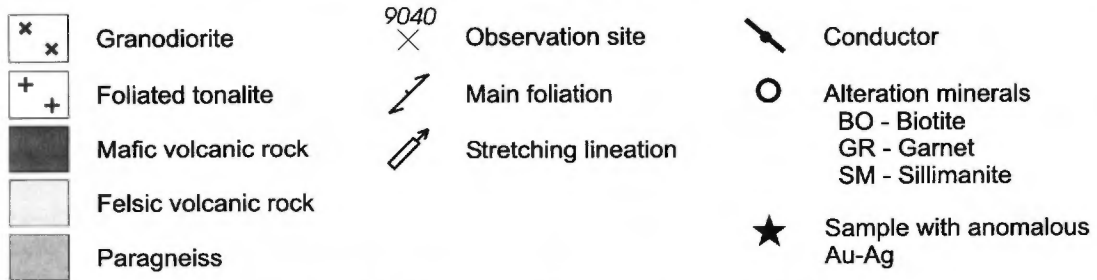
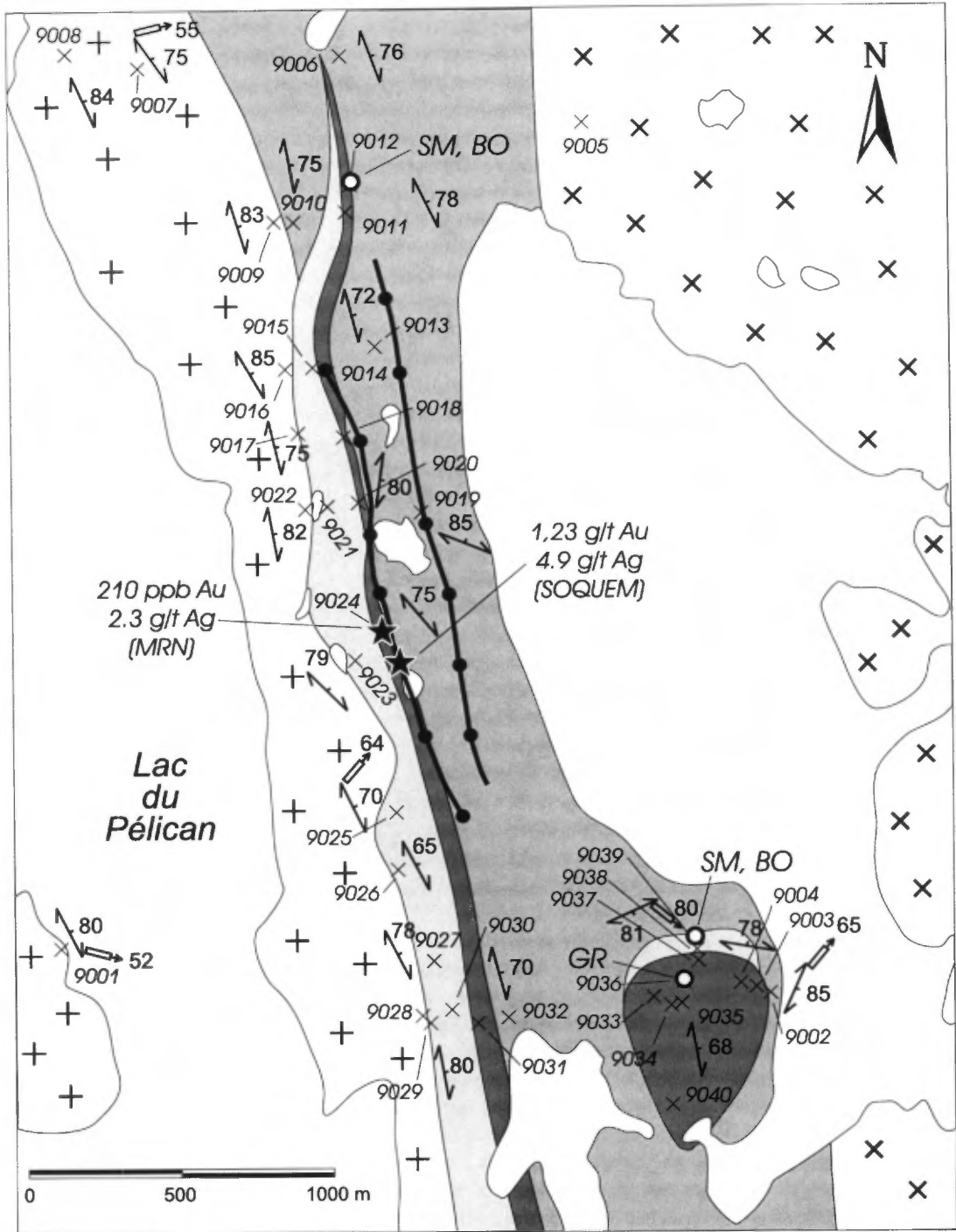


FIGURE 11 – Detailed geology of the NE part of the Pélican belt (34P/13) and location of mapped outcrops (figure location shown in figures 2 and 10).

Complex, extends along a N-S axis less than 10 km in width. It is dominated by migmatitic paragneisses (from which an age of *ca.* 2733 Ma was obtained) and contains a series of volcanic rocks, composed of felsic tuffs (*ca.* 2.74 Ga?), andesites and basalts (*ca.* 2.77 Ga; David, in preparation).

The southwestern part of the map area is dominated by biotite bearing porphyritic granodiorite to monzogranite intrusions that laterally grade into leucogranites and homogeneous biotite-hornblende granodiorites. These units are assigned to the La Chevrotière Suite (*ca.* 2.72-2.73 Ga), also recognized southward in the Lac La Potherie area (34I). Granodiorites of the Châtelain Suite, of unknown age and concentrated in the northwestern corner of the map area, are intruded by granites of the La Chevrotière Suite.

All of these units are in turn injected by a suite of orthopyroxene-bearing rocks (MacMahon Suite; *ca.* 2.725-2.715 Ga) dominated by biotite + orthopyroxene ± clinopyroxene ± hornblende enderbites and opdalites, with minor proportions of pyroxenite, gabbro-norite, orthopyroxene diorite and diatexite. This enderbitic to charnockitic suite forms intrusive complexes, outlined by a positive magnetic signature and granulite-facies metamorphism. Laterally, enderbitic to charnockitic units grade into hornblende + biotite ± clinopyroxene granodiorites – tonalites (Lepelle Suite; *ca.* 2.715 Ga) and white granitic pegmatites.

All lithologies in the Lac du Pélican area underwent complex polyphase deformation. Primary volcanic or sedimentary structures in supracrustal rocks were deformed in a penetrative fashion, transposed by a series of deformation events, and considerably modified by metamorphic recrystallization. The central and southwesternmost parts of the Lac du Pélican area are characterized by a weak aeromagnetic gradient, oriented NW-SE, and cut by a prominent set of N-S-trending positive aeromagnetic anomalies. These two patterns are characterized by ductile structures (D₁ to D₃), and are cross-cut by different networks of lineaments oriented N-S (D₄) and WNW-ESE (D₅) to NW-SE (D₆), characterized by brittle-ductile structures.

The 2000 mapping campaign led to the discovery of two mineral occurrences (Tukimurtuk and Tasiaalujjuaq showings), and eighteen litho-geochemical anomalies. These sites fall into one of three types of ore deposit settings: 1) iron formations (with Cu ± Au ± Ag ± Zn mineralization), 2) ultramafic to mafic intrusions (with Cu ± Zn mineralization), and 3) fault zones and quartz veins (with Cu ± Zn ± Au ± Ag ± Mo ± U mineralization). The two showings were discovered in fault and quartz vein settings: a mylonitized amphibolite injected with quartz veins yielded grades of 0.75% Cu, 3.9 g/t Ag, 140 ppb Au (Tasiaalujjuaq showing), and a strongly mylonitized granite with pyrite-molybdenite veinlets yielded 0.3% Mo (Tukimurtuk showing).

REFERENCES

- BERCLAZ, A. - CADIEUX, A.-M. - SHARMA, K.N.M. - DAVID, J. - PARENT, M. - LECLAIR, A., 2001 - Geology of the Lac Aigneau area (24E and 24F/04). Ministère des Ressources naturelles, Québec; RG 2001-05, 44 pages.
- BUCHAN, K.L. - MORTENSEN, J.K. - CARD, K.D. - PERCIVAL, J.A., 1998 - Paleomagnetism and U-Pb geochronology of diabase dyke swarms of Minto Block, Superior Province, Quebec, Canada. *Canadian Journal of Earth Sciences*; volume 35, pages 1054-1069.
- CARD, K.D. - CIESIELSKI, A., 1986 - Subdivisions for the Superior Province of the Canadian Shield. *Geoscience Canada*; volume 13, pages 5-13.
- CARD, K.D. - POULSEN, K.H., 1998 - Geology and mineral deposits of the Superior Province of the Canadian Shield: Chapter 2 *In*: Geology of the Precambrian Superior and Grenville Provinces and Precambrian Fossils in North America (S.B. Lucas and M.R. St-Onge, coordinators); *Geology of Canada*, volume 7; pages 13-194.
- CUERRIER, G., 1999 - Propriété Pélican (1244) : travaux de reconnaissance. Ministère des Ressources naturelles, Québec; GM 57515.
- DAVID, J., in preparation - Géochronologie U-Pb du Projet Grand-Nord. Les régions des lacs Maricourt, des Loups Marins, Aigneau, La Potherie, du Pélican, Vernon et Minto, Klotz, et de la rivière Arnaud. Ministère des Ressources naturelles, Québec.
- DAVIS, D.W., 1982 - Optimum linear regression and error estimation applied to U-Pb data. *Canadian Journal of Earth Sciences*; volume 19, pages 2141-2149.
- DION, D.J. - LEFEBVRE, D.L., 2000 - Données numériques (profils) des levés aéromagnétiques du Québec. Ministère des Ressources naturelles, Québec; DP 99-01.
- FAHRIG, W.F. - CHRISTIE, K.W. - CHOWN, E.H. - MACHADO, N., 1985 - The tectonic significance of some basic dyke swarms in the Canadian Superior Province with special reference to the geochemistry and paleomagnetism of the Mistassini swarm, Quebec, Canada. *Canadian Journal of Earth Sciences*; volume 23, pages 238-253.
- GOSELIN, C. - SIMARD, M., 2000 - Geology of the Lac Gayot Area (NTS 23M). Ministère des Ressources naturelles, Québec; RG 2000-03, 30 pages.
- HOFFMAN, P.F., 1988 - United plates of America, the birth of a craton: Early Proterozoic assembly and growth of Laurentia. *Annual Reviews of Earth and Planetary Sciences*; volume 16, pages 543-603.
- HOFFMAN, P.F., 1989 - Precambrian geology and tectonic history of North America - An Overview (A.W. Balby and A.R. Palmer, editors); Boulder, Colorado. Geological Society of America; *The Geology of North America*; volume A.
- IRVINE, T.N. - BARAGAR, W.R.A., 1971 - A guide to the chemical classification of the common volcanic rocks. *Canadian Journal of Earth Sciences*; volume 8, pages 523-548.
- JENSEN, L.S., 1976 - A new cation plot for classifying subalkalic volcanic rocks. Ontario Division of Mines; *Miscellaneous Paper* 66.

- LABBÉ, J.-Y. - LACOSTE, P., 2001 - Environnements propices aux minéralisations polymétalliques de type volcanogène dans le Grand-Nord québécois. Ministère des Ressources naturelles, Québec; MB 2001-07, 82 pages.
- LAMOTHE, D., 1997 - Géologie de la région du lac Dupire (34H/03). Ministère des Ressources naturelles, Québec; RG 96-01, 17 pages.
- LECLAIR, A. - PARENT, M. - DAVID, J. - SHARMA, K.N.M. - DION, D.-J., 2001 - Geology of the Lac La Potherie Area (34I). Ministère des Ressources naturelles, Québec; RG 2001-04, 43 pages.
- LEMAÎTRE, R.W., 1989 - A classification of igneous rocks and glossary of terms. Blackwell, Oxford, 193 pages.
- LIN, S. - PERCIVAL, J.A. - SKULSKI, T., 1996 - Structural constraints on the tectonic evolution of a late Archean greenstone belt in the northeastern Superior Province, northern Quebec (Canada). *Tectonophysics*; volume 265, pages 151-167.
- LUDWIG, K.R., 2000 - Isoplot/Ex v.2.32: A geochronological toolkit for Microsoft Excel. Berkeley Geochronology Center; Special Publication 1a.
- MACHADO, N. - GOULET, N. - GARIÉPY, C., 1989 - U-Pb geochronology of reactivated Archean basement and of Hudsonian metamorphism in the northern Labrador Trough. *Canadian Journal of Earth Sciences*; volume 26, pages 1-15.
- MADORE, L. - BANDYAYERA, D. - BÉDARD, J.H. - BROUILLETTE, P. - SHARMA, K.N.M. - BEAUMIER, M. - DAVID, J., 1999 - Geology of the Lac Peters Area (NTS 24 M). Ministère des Ressources naturelles, Québec; RG 99-16, 43 pages.
- MADORE, L. - LARBI, Y., 2000 - Geology of the Rivière Arnaud area (25D) and adjacent coastal areas (25C, 25E and 25F). Ministère des Ressources naturelles, Québec; RG 2001-06, 35 pages.
- MADORE, L. - LARBI, Y. - SHARMA, K.N.M., 2001 - Geology of the Lac Klotz (35A) and the Cratère du Nouveau-Québec (southern half of 35H) areas. Ministère des Ressources naturelles, Québec; RG 2002-05, 45 pages.
- MANIAR, P.D. - PICCOLI, P.M., 1989 - Tectonic discrimination of granitoids. *Geological Society of America Bulletin*; volume 101, pages 635-643.
- MOORHEAD, J. - PERREAULT, S. - BERCLAZ, A. - SHARMA, K.N.M. - CADIEUX, A.-M., 2000 - Kimberlites and Diamonds in Northern Québec. Ministère des Ressources naturelles, Québec; PRO 99-09, 10 pages.
- MRN, 1998 - Résultats d'analyses de sédiments de fond de lacs, Grand Nord du Québec. Ministère des Ressources naturelles, Québec; DP 98-01 (digital data).
- PARENT, M. - LECLAIR, A. - DAVID, J. - SHARMA, K.N.M., 2000 - Geology of the Lac Nedluc Area (NTS 34H and 24E). Ministère des Ressources naturelles, Québec; RG 2000-09, 41 pages.
- PARENT, M. - LECLAIR, A. - DAVID, J. - SHARMA, K.N.M. - LACOSTE, P., 2001 - Geology of the Lac Vernon area (34J). Ministère des Ressources naturelles, Québec; RG 2002-07, 40 pages.
- PERCIVAL, J.A. - CARD, K.D. - STERN, R.A. - BÉGIN, N.J., 1991 - A geologic transect of the Leaf River area, northeastern Superior Province, Ungava Peninsula, Québec. In: *Current Research, Part C*; Geological Survey of Canada; Paper 91-1C, pages 55-63.
- PERCIVAL, J.A. - MORTENSEN, J.K. - STERN, R.A. - CARD, K.D. - BEGIN, N.J., 1992 - Giant granulite terranes of northeastern Superior Province: the Ashuanipi Complex and Minto Block. *Canadian Journal of Earth Sciences*; volume 29, pages 2287-2308.
- PERCIVAL, J. - CARD, K.D., 1994 - Geology, Lac Minto - Rivière aux Feuilles. Geological Survey of Canada; Map 1854A, scale 1:500,000.
- PERCIVAL, J. - SKULSKI, T. - CARD, K.D., 1995 - Geology, Rivière Kogaluc - Lac Qalluviartuuq region (parts of 34J and 34O). Geological Survey of Canada; Open File 3112.
- PERCIVAL, J. - SKULSKI, T. - NADEAU, L., 1996 - Granite-greenstone terranes of the northern Minto Block, northeastern Superior Province, Quebec. In: *Current Research 1996-C*; Geological Survey of Canada; pages 157-167.
- PERCIVAL, J. - SKULSKI, T. - NADEAU, L., 1997a - Reconnaissance geology of the Pelican - Nantais Belt, northeastern Superior Province, Québec. Geological Survey of Canada; Open File 3525.
- PERCIVAL, J.A. - SKULSKI, T. - NADEAU, L., 1997b - Granite-greenstone terranes of the Northern Minto Block, northeastern Québec: Pélican-Nantais, Faribault-Leridon and Duquet Belts. In: *Current Research, 1997-C*; Geological Survey of Canada; pages 211-221.
- PERCIVAL, J.A. - SKULSKI, T., 2000 - Tectonothermal evolution of the Northern Minto Block, Superior Province, Québec, Canada. *The Canadian Mineralogist*; volume 38, pages 345-378.
- SIMARD, M. - GOSSELIN, C. - DAVID, J., 2001 - Geology of the Maricourt Area (24D). Ministère des Ressources naturelles, Québec; RG 2001-07, 44 pages.
- SKULSKI, T. - ORR, P. - TAYLOR, B., 1997 - Archean carbonate in the Minto Block, NE Superior Province. *GAC-MAC Ottawa 1997; Program with Abstracts*, pages A-138 and A-139.
- STERN, R.A. - PERCIVAL, J.A. - MORTENSEN, J.K., 1994 - Geochemical evolution of the Minto Block: a 2.7 Ga continental magmatic arc built on the Superior protocraton. *Precambrian Research*; volume 65, no 1-4, pages 115-153.
- STEVENSON, I.M., 1968 - Geology, Leaf River, Quebec. Geological Survey of Canada; map 1229A, scale 1:1,000,000.
- VENTER, N. - ANDREWS, O.E.G. - CUERRIER, G., 1999 - Logistics and final interpretation report for a combined helicopterborne magnetic and electromagnetic survey over the Ungava Bay. Ministère des Ressources naturelles, Québec; GM 57515.
- VERPAELST, P. - BRISEBOIS, D. - PERREAULT, S. - SHARMA, K.N.M. - DAVID, J., 2000 - Geology of the Koroc River area and part of the Hébron area (NTS 24I and 14L). Ministère des Ressources naturelles, Québec; RG 2000-02, 59 pages.
- WINCHESTER, J.A. - FLOYD, P.A., 1977 - Geochemical discrimination of different magma series and their differentiation products using immobile elements. *Chemical Geology*; volume 20, pages 325-343.

TABLE 1 – U/Pb age dating results from samples collected in the Lac du Pélican area (34P).

Site no. (see location in Figure 2)	Stratigraphy	Lithology	Analytical technique	Age of crystallization	Inherited age	Secondary age	UTM coordinates	
							Northing	Easting
1	Pélican-Nantais Complex	Paragneiss mobilizate (Apna1)	I	2733 ±3 (18/*1.8)			588 846	6 640 201
2	Pélican-Nantais Complex	BO leucotonalite (Apna3)	I	2691 ±6 (14/*3.7)		2659 ±9 (5/*1.6)	584 205	6 634 333
3	Bottequin Suite	Banded tonalite (Abtq2)	T	2768 ±3 (2/59%)			622 985	6 618 594
4	MacMahon Suite	Leucogabbronorite (Acmm2)	T	2723 ±2 (4/91%)			661 228	6 598 460
5	MacMahon Suite	Opdalite (Acmm6)	I	2717 ±10 (5/*3.3)	2758 ±7 (14/*7.4)		565 891	6 605 592
6	Lepelle Suite	CX tonalite (Alep2)	I	2714 ±10 (5/*0.3)	2731 ±5 (10/*0.6)		595 935	6 629 033

Analytical technique:

T : U-Pb analysis by isotopic dilution and thermal ionization mass spectrometry (TIMS).

I : U-Pb analysis by in situ laser ablation and multi-collection inductively coupled plasma mass spectrometry (LA-MC-ICP-MS).

Age :

In million years (Ma) with uncertainty (\pm) representing a confidence interval of 2 standard deviations (95%).

Results for dilution analyses are derived from linear regression analysis by Davis (1982), and by Ludwig (2000) for ablation analyses.

In parentheses : number of analyses, and probability % or MSWD (mean standard weight deviation) respectively obtained for each regression type.

TABLE 2 – Compositional range of volcanic rocks of the Faribault-Thury (Afh) and Pélican-Nantais (Apna) complexes, ultramafic and mafic plutonic rocks of the MacMahon Suite (Acmm) and Klotz (pPktz) and Payne River (pPpay) dykes in the Lac du Pélican area (34P).

Stratigraphy	Faribault-Thury Complex (Afh)					Pélican-Nantais Complex (Apna)		
	Afh3	Afh3	Afh3c	Afh3a	Afh3a	Apna2a	Apna2b	Apna2a/b
Stratigraphic unit	M16-V3	M3-V2	V1D/V1C	I4/V4	I4/V4	V3	V2	V3-V2
Lithology (SIGÉOM)								
Geochemical suite ^(a)	TS ₁	TS ₁₋₃	CAS ₂	TS ₁	CAS ₂₇	TS ₂	TS ₂	CAS ₂
Number (n = x / y) ^(b)	n = 6 / 4	n = 2 / 0	n = 2 / 2	n = 3 / 1	n = 2 / 1	n = 6 / 0	n = 3 / 0	n = 2 / 1
Major elements (% oxides)								
SiO₂	46.6-49.6	53.0-53.3	64.8-69.3	37.8-39.6	38.2-39.8	43.5-50.9	57.0-57.6	54.6-55.7
TiO₂	0.92-1.69	1.94	0.31-1.04	0.16-0.18	0.07	0.67-1.07	0.15-1.10	0.77-0.83
Al₂O₃	14.1-15.1	12.0-15.4	15.8-16.0	2.7-4.6	1.07-1.12	14.1-19.4	3.9-10.9	16.4-17.6
Cr₂O₃	0.01-0.04	0.01-0.02	0.01-0.04	0.38-0.67	0.72-0.76	0.04-0.07	0.01-0.03	0.01
Fe₂O₃*	12.4-16.5	12.1-20.7	3.1-4.9	10.9-14.6	10.9-12.7	9.5-21.8	19.0-20.6	8.3-9.1
MnO	0.20-0.25	0.27	0.06-0.12	0.14-0.18	0.13-0.14	0.15-0.28	0.15-0.31	0.14-0.15
MgO	5.3-8.3	2.9-4.4	1.2-2.5	30.3-32.9	36.5-36.6	4.4-9.7	2.0-6.1	4.4-4.7
CaO	9.9-13.5	6.7-8.0	3.8-6.8	1.6-2.8	0.04-0.12	7.0-13.3	7.0-8.8	6.8-7.4
K₂O	0.12-0.61	0.43-0.48	0.80-1.50	0.01-0.03	0.01-0.02	0.15-0.51	0.24-0.58	1.25-1.70
Na₂O	1.36-3.11	2.55-3.89	2.28-4.28	0.10-0.12	0.10	0.80-2.54	0.37-0.84	3.76-4.39
P₂O₅	0.03-0.09	0.16-0.19	0.06-0.07	<0.01	<0.01	0.04-0.09	0.15-0.36	0.23-0.25
LOI	0.1-0.9	-0.3-0.C229	0.5-0.9	8.6-13.2	10.4-10.7	0.3-0.65	0.4-2.9	0.6-0.9
Total	100.0-100.6	100.55-100.6	100.0-100.2	100.3-100.5	100.1-100.2	99.3-100.4	99.7-100.4	99.3-100.8
Trace elements (ppm)								
Cr	44-280	20-140	20-240	2600-4500	4900-5400	163-285	78-149	20-74
Co	51-61	43-48	7-36	100-130	120-170	n.a.	n.a.	n.a.
Ni	<140	<100	<100	930-1800	1600	n.a.	n.a.	n.a.
Sb	<0.1	<0.1-0.3	<0.1	<0.1	<0.1	11-21	<5-13	0.1-12
Rb	1.66-6.29	16-24	46-79	0.45-1.71	1.72	3-36	4-48	61-70
Sr	98-199	64-155	75-257	10.55-14.4	5.1	114-228	22-122	719-788
Ba	26-97	<50-210	260-268	5.7-13.9	63.4	9-78	10-73	470-644
Ga	16-22	20-21	18-19	3-5	3	n.a.	n.a.	n.a.
Sc	43-49	42-46	5.9-40	13-21	8.0-8.2	33.7-45.1	3.0-19.4	22.0-22.5
Nb	2.70-5.01	6	3.5-5.2	0.41-0.76	0.49	2-4	2-10	4-6
Zr	28-100	100-134	61-88	14-17	11-12	16-35	36-76	50-99
Th	0.05-0.56	0.8-1.1	0.5-2.7	0.06-0.14	0.05	n.a.	n.a.	n.a.
Y	18.9-27.3	26-57	8-10	3.04-4.63	1.65	15-28	9-94	18-20
Br	0.8-1.3	0.5-0.9	0.5-2.7	0.5-2.8	2.1-7.5	n.a.	n.a.	n.a.
Element ratios								
Al₂O₃/TiO₂	8.5-15.4	6.2-7.9	15.2-51.6	16.5-25.6	15.3-16.0	14.5-29.1	9.9-35.7	21.2
CaO/Al₂O₃	0.68-0.92	0.52-0.56	0.24-0.43	0.56-0.64	0.04-0.11	0.50-0.70	0.64-2.27	0.41-0.42
Mg#	53.8-36.75	41.8-21.8	50.4-43.9	85.7-80.7	86.9-85.1	56.6-42.2	36.8-17.5	52.7-49.1
Zr/Hf	25-37	n.a.	36-37	31-33	38	n.a.	n.a.	43
Th/Nb	0.09-0.15	0.13-0.18	0.13-0.51	0.15-0.21	0.10	n.a.	n.a.	0.43
Th/La	0.06-0.09	n.a.	0.10-0.38	0.08-0.12	0.02	n.a.	n.a.	0.02
Ti/Zr	81-134	87-116	21-102	60-80	35-38	166-365	17-87	50-93
Zr/Y	1.0-3.3	2.4-3.8	6.9-8.8	2.2-3.3	3.6	0.7-1.4	0.8-4.2	2.5-5.5
(La/Yb)_{nCH}	0.7-2.0	n.a.	3.5-5.0	1.0-1.6	9.8	n.a.	n.a.	12.3
(La/Sm)_{nCH}	0.7-1.5	n.a.	1.4-3.0	1.3	4.1	n.a.	n.a.	3.0
(Gd/Yb)_{nCH}	0.9-1.0	n.a.	0.9-1.7	0.7-1.0	1.4	n.a.	n.a.	2.0

a : TS designates the tholeiitic magmatic suite; CAS the calc-alkaline magmatic suite; numbers 1 to 3 in subscript refer to sub-trends (described in the text) for each of these magmatic suites. See Figure 6.

b : (n = x / y) number of analyses performed by X-ray fluorescence (x) and the number of analyses reprocessed by ICP-MS (y).

n.a. : not analyzed

TABLE 2 – (continued)

Stratigraphy	Pélican-Nantais Complex (Apna)			MacMahon Suite (Acmm)			Dykes	
	Apna2b	Apna2c	Apna2c	Acmm1	Acmm2	Acmm3	pPktz	pPpay
Stratigraphic unit	V2	V1C/V1D	V1B	I4	I3Q	I2Q	I3A	I3B
Lithology (SIGÉOM)	CAS ₂	CAS ₂	CAS ₂	TS _{1,3}	TS ₃	CAS ₁	TS ₂	TS ₁
Geochemical suite ^(a)	CAS ₂	CAS ₂	CAS ₂	TS _{1,3}	TS ₃	CAS ₁	TS ₂	TS ₁
Number (n = x / y) ^(b)	n = 2 / 0	n = 3 / 0	n = 6 / 0	n = 9 / 3	n = 3 / 3	n = 3 / 2	n = 1 / 0	n = 4 / 0
Major elements (% oxides)								
SiO₂	60.1-62.0	66.3-67.4	70.3-74.1	46.8-52.4	48.8-51.7	48.2-59.8	48.2	48.0-49.0
TiO₂	0.58-0.63	0.39-0.54	0.24-0.33	0.37-0.98	0.62-0.94	0.60-1.04	1.77	0.90-1.25
Al₂O₃	16.1-17.6	15.6-16.0	14.5-15.6	3.2-8.3	14.5-15.4	13.3-18.9	14.5	13.5-14.3
Cr₂O₃	0.01-0.02	0.02	0.01-0.03	0.08-0.25	0.04-0.06	<0.01-0.07	0.01	0.03-0.05
Fe₂O₃*	6.3-6.6	3.4-4.9	2.1-3.3	10.1-14.7	12.3-13.4	7.6-11.4	17.3	12.2-13.4
MnO	0.09-0.11	0.02-0.07	0.03-0.04	0.18-0.24	0.22-0.23	0.16-0.17	0.22	0.20-0.23
MgO	2.57-2.63	1.26-1.78	0.49-0.85	13.4-18.6	5.3-8.9	2.5-9.14	5.0	7.6-8.4
CaO	4.6-5.2	3.8-4.0	1.7-2.7	10.8-14.3	11.1-12.4	5.8-10.2	10.2	12.1-12.3
K₂O	2.4-2.9	1.17-1.69	3.14-3.55	0.16-1.58	0.28-0.66	0.76-2.03	0.17	0.45-0.54
Na₂O	2.89-3.13	3.77-4.96	0.48-3.64	0.81-1.66	1.94-3.00	2.93-4.50	2.32	1.46-1.96
P₂O₅	0.18-0.19	0.07-0.16	0.07-0.11	<0.01-0.05	0.02-0.03	0.20-0.32	0.05	0.02-0.05
LOI	0.8-1.0	0.35-1.1	0.6-1.0	0.4-2.2	<0.05-0.4	0.25-0.9	0.4	0.4-1.6
Total	99.2-99.4	99.3-99.98	99.8-100.0	99.1-100.8	100.5-100.7	99.69-100.7	100.1	100.0-100.4
Trace elements (ppm)								
Cr	74-91	61-78	31-67	320-1800	270-420	20-450	28	180-340
Co	n.a.	n.a.	n.a.	52-90	53-66	17-49	59	52-56
Ni	n.a.	n.a.	n.a.	<100-440	<100-120	<100	<100	<100-130
Sb	9-13	8-14	<5-12	<0.1	<0.1-0.4	<0.1	<0.1	<0.1
Rb	115-168	64-87	117-208	6-73	4-9	12-146	7	30-54
Sr	660-671	642-924	176-499	46-235	115-235	403-835	100	88-150
Ba	800-834	427-597	318-817	<50-230	63-84	389-530	50	50-69
Ga	n.a.	n.a.	n.a.	7-14	17-19	18-23	21	16-19
Sc	9.9-11.0	4.6-7.7	2.8-5.6	38-64	45-50	14-36	46	42-53
Nb	5-7	4-6	5-11	2-6	4-5	4-6	6	4-7
Zr	79-85	79-98	72-107	22-46	40-48	63-97	66	51-69
Th	n.a.	0.39-0.54	n.a.	0.2-7.2	0.2-0.8	0.4-1.2	0.5	0.3-0.4
Y	11-19	10-13	9-22	11-22	23-28	16-20	22	18-23
Br	n.a.	n.a.	n.a.	<0.5-1.1	<0.5	<0.5-1	1.6	<0.5-1.1
Element ratios								
Al₂O₃/TiO₂	27.8-28.2	29.0-41.3	46.2-60.4	5.6-22.5	15.9-23.5	12.8-30.0	8.2	11.4-15.0
CaO/Al₂O₃	0.29	0.24-0.27	0.12-0.17	1.37-2.20	0.72-0.86	0.32-0.77	0.7	0.85-0.90
Mg#	44.7-44.2	47.3-34.4	41.6-29.2	78.0-67.8	58.8-45.9	61.4-39.5	36.3	57.7-53.0
Zr/Hf	n.a.	n.a.	n.a.	29-34	31-34	41-42	n.a.	n.a.
Th/Nb	n.a.	n.a.	n.a.	0.24-0.79	0.04-0.22	0.04-0.18	n.a.	n.a.
Th/La	n.a.	n.a.	n.a.	0.05-0.12	0.03-0.13	0.01-0.04	n.a.	n.a.
Ti/Zr	41-47	28-41	16-23	67-171	93-131	57-71	161	104-114
Zr/Y	4.2-7.7	7.6-8.2	4.9-10.2	1.6-2.8	1.6-1.7	3.9-4.9	3.0	2.3-3.5
(La/Yb)_{nCH}	n.a.	n.a.	n.a.	3.1-6.3	1.6-2.4	11.9-12.6	n.a.	n.a.
(La/Sm)_{nCH}	n.a.	n.a.	n.a.	1.3-1.7	1.4-1.7	2.9-3.7	n.a.	n.a.
(Gd/Yb)_{nCH}	n.a.	n.a.	n.a.	1.3-2.0	0.9-1.1	1.9-2.1	n.a.	n.a.

a : TS designates the tholeiitic magmatic suite; CAS the calc-alkaline magmatic suite; numbers 1 to 3 in subscript refer to sub-trends (described in the text) for each of these magmatic suites. See Figure 6.

b : (n = x / y) number of analyses performed by X-ray fluorescence (x) and the number of analyses reprocessed by ICP-MS (y).

n.a. : not analyzed

TABLE 3 – Compositional range of granitoid units in the various complexes and suites in the Lac du Pélican area (34P).

Stratigraphy	Faribault-Thury (AftH)		Rochefort (Arot)	Botteguin (Abtq)			Lepelle (Alep)	Pélican-Nantais (Apna)
	AftH4b	AftH4	Arot	Abtq1	Abtq2	Abtq2a	Alep2	Apna3
Stratigraphic unit	I3A/I2J	I1D-Bo	I1D-Hb	I2J	I1D-Bo-Hb	I1D-Cx	I1D/I1C-Cx	I1D-Bo
Lithology (SIGÉOM)	I3A/I2J	I1D-Bo	I1D-Hb	I2J	I1D-Bo-Hb	I1D-Cx	I1D/I1C-Cx	I1D-Bo
Number (n = x / y) ^(b)	n = 1 / 0	n = 1 / 0	n = 1 / 1	n = 1 / 0	n = 3 / 1	n = 1 / 1	n = 1 / 1	n = 2 / 1
Major elements (% oxides)								
SiO₂	56.7	66.8	65.2	45.6	66.6-68.9	58.6	52	66.2-65.7
TiO₂	1.73	0.74	0.53	1.5	0.37-0.50	0.76	0.86	0.45-0.65
Al₂O₃	14.5	14.8	16.6	12.6	16.0-16.3	16.7	20.5	15.7-16.0
Fe₂O₃*	11.2	6.6	4.22	13	2.96-4.66	7	9.6	3.96-4.99
MnO	0.15	0.14	0.06	0.16	0.04-0.11	0.11	0.09	0.07-0.08
MgO	3.33	1.79	2.18	11.9	1.15-1.97	3.69	2.26	1.44-2.07
CaO	6.62	3.6	4.42	10	4.01-5.26	7.44	6.08	2.79-4.15
K₂O	1.71	1.65	1.53	1.16	0.70-1.42	1.18	2.34	2.66-4.22
Na₂O	3.38	3.53	4.78	2.32	3.97-4.62	3.65	4.88	3.37-4.30
P₂O₅	0.54	0.18	0.17	0.06	0.06-0.15	0.1	0.96	0.14-0.44
LOI	0.58	0.35	0.55	1.77	0.36-0.68	0.8	0.69	0.39-0.56
Total	100.45	100.19	100.25	100.08	100.2-100.6	100.04	100.27	99.9-100.5
Trace elements (ppm)								
Cr	52	20	33	46	<20-37	92	41	32
Co	28	9	13	68	6-15	28	16	8-12
Rb	49	82	52	24	14-57	55	97	102-184
Sr	352	115	800	305	189-569	198	605	318-680
Ba	590	270	660	360	240-260	190	470	690-780
Ga	20	19	20	18	19-20	19	31	19-21
Sc	21	12	6.8	63	4.2-11.0	18	14	9-11
Nb	14	9	2	4	5-7	6	17	5-10
Zr	313	212	98	52	106-134	106	302	119-218
Th	5	4.1	4.7	0.8	1.8-9.8	1.5	18	6.3-6.9
Y	35	24	5	20	9-11	16	59	8-59
Element ratios								
Al₂O₃/TiO₂	8	20	31	8	33-43	22	24	24-36
CaO/Al₂O₃	0.46	0.24	0.27	0.79	0.25-0.33	0.45	0.30	0.18-0.26
Mg#	37.1	34.9	50.6	64.5	45.6-39.2	51.1	31.8	50.9-36.4
K/Rb	289	167	244	401	205-415	178	200	190-216
Zr/Hf	n.a.	n.a.	43	n.a.	41	41	41	41
Th/Nb	0.36	0.40	2.35	0.20	0.25-1.06	0.25	1.06	0.69-1.26
Th/La	n.a.	n.a.	0.12	n.a.	0.13	0.14	0.21	0.21
Ti/Zr	33	21	32	173	17-25	13	17	18-23
Zr/Y	8.9	8.8	19.6	2.6	9.6-14.9	6.6	5.1	3.7-14.9
(La/Yb)_{nCH}	n.a.	n.a.	48.0	n.a.	52.3	7.0	22.5	4.0
(La/Sm)_{nCH}	n.a.	n.a.	5.0	n.a.	6.4	2.7	2.4	2.4
(Gd/Yb)_{nCH}	n.a.	n.a.	3.6	n.a.	3.3	1.5	4.8	1.0

b : (n = x / y) number of analyses performed by X-ray fluorescence (x) and the number of analyses reprocessed by ICP-MS (y).

n.a. : not analysed

TABLE 3 – (Continued)

Stratigraphy	Châtelain (AchI)	La Chevrotière (Alcv)			Mac Mahon (Acmm)			
	Achl	Alcv1	Alcv2	Alcv4	Acmm4	Acmm5	Acmm6	Acmm6
Stratigraphic unit								
Lithology (SIGÉOM)	I1C-Hb,Cx	I1M-I2F[PO]	I1B[LX]-BO	I1B/M21b	I1T-Ox	I1T-Cx	I2O	I1S/I1P
Number (n = x / y) ^(b)	n = 5 / 3	n = 4 / 3	n = 1 / 0	n = 1 / 0	n = 3 / 1	n = 3 / 1	n = 3 / 2	n = 6 / 4
Major elements (% oxides)								
SiO₂	63.9-67.2	71.5-76.1	72.9	68.3	61.6-70.5	57.7-58.8	58.3-64.5	67.6-72.2
TiO₂	0.46-0.88	0.05-0.28	0.26	0.63	0.37-0.56	0.56-1.05	0.53-1.39	0.22-0.41
Al₂O₃	15.5-17.0	12.6-14.7	13.9	14.6	14.9-17.3	16.3-17.5	14.9-16.3	14.5-16.3
Fe₂O₃*	4.20-5.53	0.35-2.05	1.16	3.91	2.70-5.83	7.23-8.38	5.24-9.02	1.61-2.73
MnO	0.05-0.08	0.01-0.04	0.02	0.05	0.03-0.08	0.11-0.14	0.10-0.13	0.02-0.04
MgO	1.36-1.70	0.10-0.61	0.29	0.88	0.59-2.26	2.63-4.18	2.03-2.18	0.47-0.89
CaO	3.03-4.10	0.96-1.84	1.43	1.98	2.36-5.08	5.59-6.54	3.75-4.36	1.74-2.84
K₂O	2.77-3.65	4.35-6.04	5.34	4.9	1.22-2.13	1.26-2.11	3.16-3.33	3.20-5.72
Na₂O	3.71-4.47	2.88-3.61	3.00	3.36	4.48-5.26	4.1-4.5	3.62-4.38	3.69-4.25
P₂O₅	0.10-0.34	0.01-0.12	0.01	0.14	0.01-0.19	0.02-0.25	0.15-0.62	0.02-0.14
LOI	0.30-1.11	0.36-0.60	0.47	0.88	0.47-0.95	0.29-1.40	0.3-1.2	0.08-1.07
Total	99.7-100.8	99.8-100.9	98.79	99.64	99.5-100.2	99.7-100.2	99.9-100.6	99.7-100.5
Trace elements (ppm)								
Cr	<20	<20	20	20	<20	<20-54	<20	<20
Co	7-11	<5	5	5	6-14	17-33	14-16	<5-6
Rb	62-117	90-152	139	136	10-36	46-74	57-112	77-167
Sr	449-815	386-674	170	304	703-747	512-678	449-653	313-619
Ba	650-1300	800-2000	1400	1600	650-1100	340-540	760-1500	910-1400
Ga	18-23	13-17	16	20	21-22	22-24	18-22	16-19
Sc	8-10	0.2-2.4	2.2	7.9	1.6-13.0	13-17	7-15	1.0-1.7
Nb	4-11	2-8	4	9	2-4	7-9	6-34	2-5
Zr	83-321	33-194	183	510	126-164	61-138	119-291	58-194
Th	0.5-10	2-11	14	10	0.2-5.7	1.2-4.1	0.9-13.0	0.4-16
Y	6-25	3-13	3	42	3-10	18-23	14-28	3-9
Element ratios								
Al₂O₃/TiO₂	18-35	51-280	53	23	30-46	16-31	11-31	39-70
CaO/Al₂O₃	0.19-0.24	0.07-0.13	0.10	0.15	0.16-0.31	0.32-0.40	0.15-0.27	0.11-0.18
Mg#	44.4-32.8	36.2-29.8	33.1	30.8	43.4-25.6	49.7-41.9	45.2-30.8	41.5-35.9
K/Rb	251-370	273-563	318.9132518	299	471-1012	227-236	243-460	284
Zr/Hf	35-43	26-41	n.a.	n.a.	39	33	37-45	38-41
Th/Nb	0.12-2.16	2.75-1.00	3.50	1.11	0.10-1.43	0.15-0.49	0.05-2.17	3.2
Th/La	0.01-0.33	0.11-0.36	n.a.	n.a.	0.09	0.09	0.01-0.28	0.01-0.23
Ti/Zr	12-35	9-16	9	7	14-27	32-55	26-29	12-20
Zr/Y	6.9-16.9	11.0-25.0	61.0	12.1	12.6-54.7	3.4-6.4	8.5-11.6	12.5-36.0
(La/Yb)_{nCH}	20.8-30.3	35.5-74.7	n.a.	n.a.	99.0	11.5	19.1-20.1	52.4-123.4
(La/Sm)_{nCH}	3.5-5.4	5.7-18.9	n.a.	n.a.	9.7	4.6	3.6-4.9	7.2-14.6
(Gd/Yb)_{nCH}	1.9-3.4	0.9-3.1	n.a.	n.a.	4.1	1.2	1.8-2.5	2.8-4.1

b : (n = x / y) number of analyses performed by X-ray fluorescence (x) and the number of analyses reprocessed by ICP-MS (y).

n.a. : not analysed

TABLE 4 – Characteristics of showings and lithogeochemical sample sites of interest which yielded anomalous analytical results in the Lac du Pélican area (34P). The locations of showings and sample sites are shown in Figure 10.

IRON FORMATIONS					
<i>Site or showing</i>	<i>Location (UTM Nad 83)</i>	<i>Sample</i>	<i>Metal content</i>	<i>Setting</i>	<i>Opaque minerals (thin section)</i>
1	581974E 6635360N	9024-B	901 ppm Cu 2 g/t Ag 210 ppb Au	Oxide-facies iron formation horizon with chert and sulphides (5-15% pyrite-chalcocopyrite) in a mafic volcanic unit (Pélican-Nantais Complex)	<5% PY-MG, tr. PO, tr. CP
2	647984E 6584966N	3264-F and G	389 ppm Cu 280 ppb Au 243 ppm Zn	Oxide-facies iron formation, with paragneiss enclaves, in a metatexitic enderbite (Faribault-Thury Complex)	Sample F: 15% MG, <1% HM, tr. PY Sample G: 2% PY, 2% PO, <1% CP, <1% MG
3	581900E 6635790N	9020-B	331 ppm Cu	Silicate-facies iron formation, with oxides and sulphides, at the contact between felsic and mafic volcanic rocks and a paragneiss unit (Pélican-Nantais Complex)	5-10% PO-PY, 5% MG
4	668403E 6565827N	1153-D	238 ppm Cu 1.3 g/t Ag	Silicate-facies iron formation, with pyrite-pyrrhotite, within a paragneiss unit in contact with a basalt (Faribault-Thury Complex)	5% PY, 2% MG, 1% PO, <1% HM, tr. CP
5	582105E 6636755N	9019-B	110 ppb Au	Oxide-facies iron formation horizon (massive magnetite with 1-2% arsenopyrite) in a paragneiss unit (Pélican-Nantais Complex)	—
ULTRAMAFIC TO MAFIC INTRUSIONS					
6	658138E 6561767N	7055-C	875 ppm Cu 167 ppm Zn	Clinopyroxenite enclaves in a mylonitized tonalite (Faribault-Thury Complex)	—
7	657694E 6621970N	7099-C	794 ppm Cu 112 ppm Zn	Clinopyroxenite – mylonitized amphibolite, with disseminated pyrrhotite (Faribault-Thury Complex)	7% PO, 2% PY, 1% CP
8	653965E 6606449N	7043-B	369 ppm Cu 239 ppm Zn	Clinopyroxenite with disseminated pyrrhotite and chalcocopyrite (MacMahon Suite)	—
9	663743E 6612744N	5123-A	274 ppm Cu 177 ppm Zn	Rusty zone in a hornblendite (MacMahon Suite)	—
10	666666E 6581338N	5228-A	319 ppm Cu	Hornblendite with disseminated pyrite (MacMahon Suite)	—
11	640615E 6563309N	5261-B	361 ppm Zn	Gabbro with disseminated sulphides in a biotite-orthopyroxene enderbite (MacMahon Suite)	—

TABLE 4 – (Continued)

FAULT ZONES AND QUARTZ VEINS					
<i>Site or showing</i>	<i>Location (UTM Nad 83)</i>	<i>Sample</i>	<i>Metal grades</i>	<i>Setting</i>	<i>Opaque minerals (this section)</i>
12 (Tasia-lujjuaq showing)	665296E 6600171N	7091-B	0.75% Cu 3.9 g/t Ag 140 ppb Au	Mylonitized amphibolite injected by quartz veins hosting 3-5% chalcopyrite (Faribault-Thury Complex)	3% CP, 2% PO, 1% PY, <1% MG, tr. PD
13 (Tuki-muntut showing)	624279E 6592650N	4234-B	0.3% Mo	Fine-grained, hematitized and strongly mylonitized granite with pyrite-molybdenite veinlets (La Chevrotière Suite)	3% MO, <1% PY
14	660913E 6642026N	3265-G	0.35% Cu	Contact between a basalt and a schistose ultramafic rock, with pyrite and pyrrhotite disseminated and in veinlets (Faribault-Thury Complex)	2% CP, tr. oxides
15	664946E 6645312N	7112-B	289 ppm Cu 243 ppm Zn	Silicified and mylonitized trondhjemite injected with quartz veins and pyrrhotite veinlets at the contact with a basalt (Faribault-Thury Complex)	10% PO
16	596637E 6628919N	147-C	293 ppm Cu	Shear zone with quartz veins containing pyrite and chalcopyrite (2-5%) in an opdalite (MacMahon Suite)	—
17	581804E 6636234N	9014-A	516 ppm Cu	Strongly silicified mafic volcanic rock with trace sulphides (Pélican-Nantais Complex)	10% PO, 5% MG, tr. PY, tr. CP
18	641256E 6618108N	1106-C	216 ppm Cu 1.8 g/t Ag	Brittle fault zone hosting up to 20% pyrite in dioritic bands alternating with tonalite (Faribault-Thury Complex)	1% PY, tr. CP
19	577411E 6607216N	4221-A	205 ppm Zn 181 ppm Cu	Alteration zone with quartz-biotite in a garnet paragneiss (Pélican-Nantais Complex)	—
20	668271E 6587568N	4249-C	13 ppm U	Hematitized pegmatite in a fault zone (La Chevrotière Suite)	—

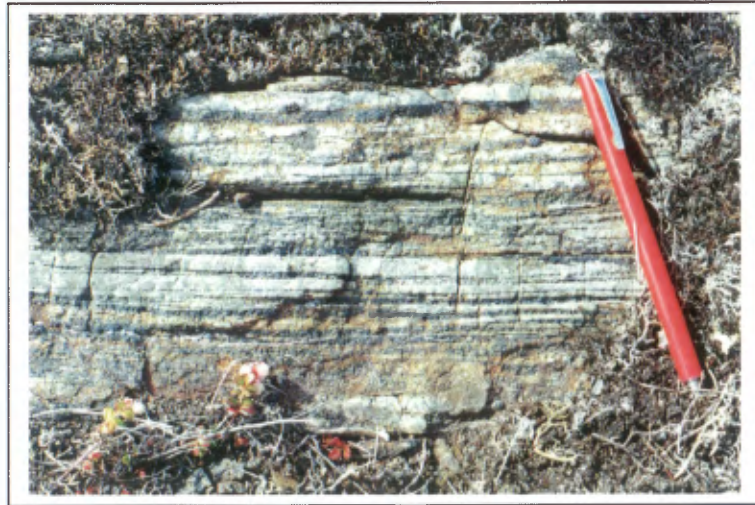


PHOTO 1 – Hybrid-facies (iron formation (*Afih1*) between silicate and oxide facies) in the Faribault-Thury Complex (*Afth*).

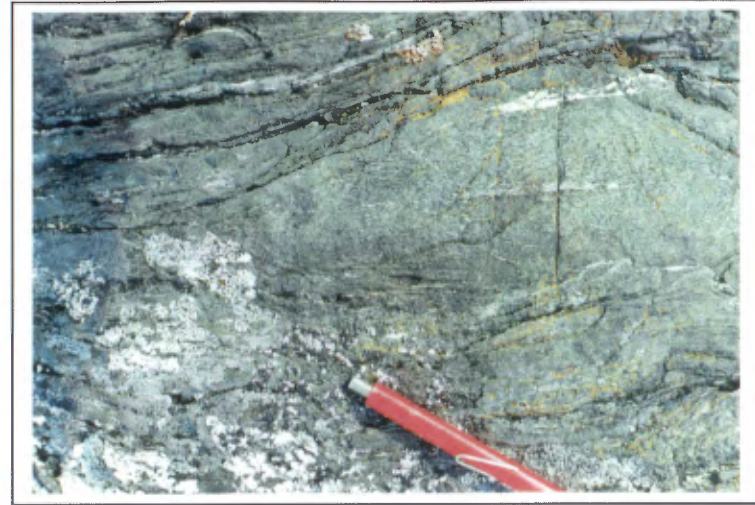


PHOTO 2 – Mafic metavolcanic rock : HB-PG-CX basalt (*Afth3*) in the Faribault-Thury Complex (*Afth*).



PHOTO 3 – Migmatitic paragneiss (*Apna1*) in the Pélican belt.



PHOTO 4 – Rhyodacite (*Apna2c*) with texture suggesting a block or lapilli tuff.

APPENDIX 2 : PHOTOGRAPHS



PHOTO 5 – Leucocratic variety of the porphyritic granodiorite unit *Alc1*.

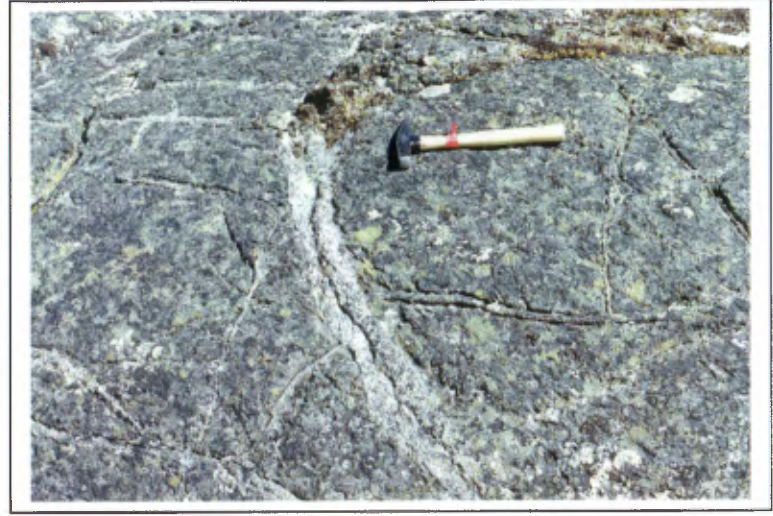


PHOTO 6 – Pyroxenite in the ultramafic plutonic rock unit (*Acmm1*) of the MacMahon Suite (*Acmm*).



PHOTO 7 – Leuconorite in unit *Acmm2* of the MacMahon Suite (*Acmm*).

Abstract

The rocks in the Lac du Pélican area (NTS 34P), mapped at 1:250,000 scale during the summer of 2000, were subdivided into two lithodemic complexes and six intrusive suites, which formed between 2.77 and 2.69 Ga. The Faribault-Thury Complex and the Pélican-Nantais Complex contain a variety of mafic, intermediate to felsic metavolcanic rocks and metasedimentary rocks that form volcano-sedimentary belts within the different granitoid suites. From the oldest to the youngest, these suites are: the Rochefort Suite (tonalite), the Bottequin Suite (tonalite, trondhjemite, quartz diorite), the Châtelain Suite (granodiorite), the La Chevrotière Suite (porphyritic monzogranite to quartz monzonite, granodiorite, granite), the MacMahon Suite (enderbite, opdalite, gabbro, orthopyroxene diorite, pyroxenite), and the Lepelle Suite (tonalite to granodiorite). All these Archean units are cut by two sets of Paleoproterozoic dykes: the Klotz gabbro dykes (2209 Ma), and the Payne River diabase dykes (1875-1790 Ma).

All lithologies in the Lac du Pélican area underwent several phases of deformation. Primary volcanic or sedimentary structures in supracrustal rocks were deformed in a penetrative fashion, transposed by a series of deformational events and considerably

modified by metamorphic recrystallization. The central and southwesternmost parts of the area are characterized by a weak aeromagnetic gradient. The latter is oriented NW-SE and cut by a prominent set of N-S-trending positive aeromagnetic anomalies. These two patterns are characterized by ductile structures (D1 to D3), and are transected by various networks of lineaments oriented N-S (D4) and WNW-ESE (D5) to NW-SE (D6), which outline brittle structures at the brittle-ductile transition.

Our work has outlined three types of settings which yielded anomalous analytical results: 1) iron formations with $\text{Cu} \pm \text{Au} \pm \text{Ag} \pm \text{Zn}$ mineralization, 2) ultramafic and mafic intrusions with $\text{Cu} \pm \text{Zn}$ mineralization, and 3) fault zones and quartz veins with $\text{Cu} \pm \text{Zn} \pm \text{Au} \pm \text{Ag} \pm \text{Mo} \pm \text{U}$ mineralization. Two showings discovered in fault zones respectively yielded concentrations of 0.75% Cu and 0.3% Mo.

